

ANNUAL TECHNICAL REPORT

**Urban and Regional Seismic Monitoring—Wasatch Front Area, Utah,
and Adjacent Intermountain Seismic Belt**

Year Three: January 1 – December 31, 2003

U.S. Geological Survey Cooperative Agreement No. 01HQAG0014

Dr. Walter J. Arabasz, Principal Investigator
Dr. Robert B. Smith, Co-Principal Investigator
Susan J. Nava, Co-Investigator
Dr. James C. Pechmann, Co-Investigator
Dr. Kristine L. Pankow, Co-Investigator

University of Utah
Department of Geology and Geophysics
135 South 1460 East, Room 705 WBB
Salt Lake City, UT 84112-0111
Tel: (801) 581-6274 Fax: (801) 585-5585
E-mail: arabasz@seis.utah.edu
URL: www.seis.utah.edu

USGS Project Officer: Dr. John Unger
USGS Administrative Contracting Officer: Sherry Ly Newman

Program Element: Seismic Networks
Key Words: Regional Seismic Hazards, Real-time Earthquake Information,
Seismotectonics, Engineering Seismology

March 30, 2004

Research supported by the U.S. Geological Survey (USGS), Department of the Interior, under USGS award number 01HQAG0014. The views and conclusions contained in this document are those of the authors and should not be interpreted as necessarily representing the official policies, either expressed or implied, of the U.S. Government.

**Urban and Regional Seismic Monitoring—Wasatch Front Area, Utah,
and Adjacent Intermountain Seismic Belt
01HQAG0014**

W. J. Arabasz, R. B. Smith, S. J. Nava , J. C. Pechmann, and K. L. Pankow

University of Utah
Department of Geology and Geophysics

135 South 1460 East, Room 705 WBB
Salt Lake City, UT 84112-0111
Tel: (801) 581-6274 Fax: (801) 585-5585
E-mail: arabasz@seis.utah.edu
URL: www.seis.utah.edu

Program Element: Seismic Networks

Key Words: Regional Seismic Hazards, Real-time Earthquake Information,
Seismotectonics, Engineering Seismology

Non-technical Summary

January 1 – December 31, 2003

This cooperative agreement provides major support for urban and regional seismic monitoring in the study area. During 2003 we added ten new strong-motion stations to our real-time earthquake information system in the Wasatch Front area as part of the Advanced National Seismic System (ANSS). At the end of 2003 our newly developed urban network included 75 ANSS-funded stations, and our regional/urban network recorded data from a total of 202 stations. We located 1,084 earthquakes in our Utah study region during 2003; nineteen had a magnitude of 3.0 or larger, and thirteen were reported felt. The largest local earthquakes, all in central Utah, were shocks of magnitude 4.3 on April 16 and a triplet of earthquakes with magnitudes of 3.6, 3.6, and 3.7 on December 27. One important investigation completed during the report period was a study of increased seismicity in Utah remotely triggered by the magnitude 7.9 Denali Fault, Alaska, earthquake that occurred on November 3, 2002.

**Urban and Regional Seismic Monitoring—Wasatch Front Area, Utah,
and Adjacent Intermountain Seismic Belt
01HQAG0014**

W. J. Arabasz, R. B. Smith, S. J. Nava , J. C. Pechmann, and K. L. Pankow

University of Utah
Department of Geology and Geophysics
135 South 1460 East, Room 705 WBB
Salt Lake City, UT 84112-0111
Tel: (801) 581-6274 Fax: (801) 585-5585
E-mail: arabasz@seis.utah.edu
URL: www.seis.utah.edu

Program Element: Seismic Networks

Key Words: Regional Seismic Hazards, Real-time Earthquake Information,
Seismotectonics, Engineering Seismology

Summary

January 1 – December 31, 2003

The cooperative agreement identified here, combined with funding from the State of Utah, provided major support for the operation of (1) the University of Utah Seismograph Stations' (UUSS) regional and urban seismic network and (2) a regional earthquake-recording and information center on the University of Utah campus in Salt Lake City.

At the end of December 2003, UUSS operated 161 stations and recorded 202 stations (~50% short-period, ~35% strong-motion, ~15% broadband, with some stations having multiple sensor types). USGS support is focused on the seismically hazardous Wasatch Front urban corridor of north-central Utah, but also encompasses neighboring areas of the Intermountain Seismic Belt. During the report period, project efforts involved: (a) continued development of a real-time earthquake information system in the Wasatch Front area as an element of an Advanced National Seismic System (ANSS); (b) timely study of new data acquired with our modernized network—including studies of increased seismicity in Utah remotely triggered by the November 3, 2002, Denali Fault, Alaska, earthquake; (c) ongoing network operations; and (d) miscellaneous related activities.

Notable accomplishments during 2003 included: (1) improving the performance of our Earthworm system for real-time earthquake monitoring and automated alerts; (2) using a ShakeMap scenario option to model observed ground-shaking intensity from an M 5.2 earthquake in the Salt Lake Valley in 1962 and to explore sensitivity to the choice of attenuation relation and uncertainty in site amplification; (3) adding ten new stations to Utah's real-time urban strong-motion network and integrating two more strong motion stations operated by the USGS National Strong Motion Program into our real-time system; (4) completing a study of triggered seismicity caused by the M_w 7.9 Denali Fault earthquake (manuscript submitted to the *Bulletin of the Seismological Society of America*); (5) improving methods for determining magnitudes of very small earthquakes and optimizing record lengths for automatic determination of local magnitude (M_L); (6) providing technical assistance to other regional seismic networks in the ANSS Intermountain West Region; (7) and participating in working groups to develop the next generation of ground-shaking hazard maps in Utah.

During the report period, we detected and analyzed approximately 5,100 seismic events, including local earthquakes, teleseismic and regional earthquakes, and blasts. A total of 2,314 earthquakes were located

within and near our regional seismic network—including 1,084 within the Utah region, of which 827 were within the Wasatch Front area. Nineteen earthquakes of magnitude 3.0 and larger occurred in the Utah region during the report period; thirteen were felt. The largest earthquakes were (1) a shock of magnitude (M_L) 4.3 that occurred at 01:04 UTC on April 17, 2003, 6 km (4 mi) SSW of Levan in central Utah and (2) a triplet of earthquakes of magnitude (M_L) 3.6, 3.6, and 3.7 that occurred respectively at 00:39, 00:40, and 00:43 UTC on December 27, 2003. The latter earthquakes also occurred in central Utah, 12 km (8 mi) SW of Nephi and 16 km (10 mi) NNW of the April 17 earthquake.

TABLE OF CONTENTS

NON-TECHNICAL SUMMARY	ii
SUMMARY	iii
INTRODUCTION	1
General Background	1
Earthquake Hazards and Risk in the Study Region	1
Contributions and Benefits to NEHRP	2
Regional/Urban Seismic Network	3
RESULTS AND ACCOMPLISHMENTS	4
Overview of Seismicity	4
Real-Time Earthquake Information System	4
Earthworm	
ShakeMap and attenuation studies	
Ten new strong-motion stations	
Integration of USGS/NSMP strong-motion data	
“Earthquakes in the News”	
Seismicity Remotely Triggered by Denali Fault Earthquake—and Other Studies	6
Triggered seismicity following the Denali Fault earthquake	
Receiver function analysis	
Space Shuttle Columbia	
Coal-mining-induced seismicity	
Accomplishments in Ongoing Network Operations	7
Continued maintenance and operation of short-period stations	
Improved magnitude determination for very small earthquakes	
Analysis of optimal record lengths for automatic determination of local magnitude (M_L)	
Near-real-time data exchange with other networks	
Assistance to other seismic networks	
Archiving waveform data	
Submission of earthquake catalog data to ANSS information outlets	
Miscellaneous	8
ANSS planning activities	
Next-generation ground-shaking hazard maps	
AVAILABILITY OF DATA	9
REFERENCES CITED	9
REPORTS AND PUBLICATIONS	11
TABLES AND FIGURES	12

APPENDIX A

Station information for University of Utah Regional/Urban Seismic Network,
December 31, 2003

A-1

APPENDIX B

Triggered Seismicity in Utah from the November 3, 2002, Denali Fault Earthquake
— by K. L. Pankow, W. J. Arabasz, J. C. Pechmann, and S. J. Nava

B-1

DISTRIBUTION OF ANNUAL TECHNICAL REPORT

INTRODUCTION

This technical report summarizes results and accomplishments under this cooperative agreement during the period January 1–December 31, 2003. During the report period, project efforts involved: (a) continued development of a real-time earthquake information system in the Wasatch Front area as an element of an Advanced National Seismic System (ANSS); (b) timely study of new data acquired with our modernized network—including studies of increased seismicity in Utah remotely triggered by the November 3, 2002, Denali Fault, Alaska, earthquake; (c) ongoing network operations; and (d) miscellaneous related activities.

General Background

This cooperative agreement, combined with funding from the State of Utah, provided major support for the operation of (1) the University of Utah Seismograph Stations' (UUSS) regional and urban seismic network and (2) a regional earthquake-recording and information center on the University of Utah campus in Salt Lake City.

At the end of December 2003, UUSS operated 161 stations and recorded 202 stations (~50% short-period, ~35% strong-motion, ~15% broadband, with some stations having multiple sensor types). USGS support is focused on the seismically hazardous Wasatch Front urban corridor of north-central Utah, but also encompasses neighboring areas of the Intermountain Seismic Belt. State funds contribute significantly to network-operation costs in the Wasatch Front area, and they support network operations in Utah outside this area.

Information products and services produced under this cooperative agreement include rapid earthquake alert, a Web site with near-real-time earthquake information, earthquake catalogs (issued on a quarterly basis in preliminary form and periodically in finalized form), automated transfer of hypocentral, waveform, and arrival-time data to other outlets prescribed by the USGS for broad access, and extensive expert assistance to individuals and groups in earthquake education and awareness, public policymaking, planning and design, and hazard and risk assessment.

Scientific objectives include the characterization of tectonic framework and earthquake potential, surveillance of space-time seismicity and characteristics of small-to-moderate earthquakes (for understanding the nucleation of large earthquakes in the region), improved ground-motion modeling for engineering applications, and the documentation and evaluation of various earthquake-related parameters for accurate hazard and risk analyses. Some scientific results are reported to the USGS under separate research awards.

Earthquake Hazards and Risk in the Study Region

Earthquakes pose the greatest natural threat for destruction of life and property in Utah. On a national level, the relative hazard and risk of Utah's Wasatch Front area led the USGS to target it for an urban strong-motion network of 500 instruments in its 1999 report to Congress for an Advanced National Seismic System (ANSS) (USGS Circular 1188). The Federal Emergency Management Agency (FEMA) ranks Utah seventh in the Nation in absolute risk and sixth in relative risk when one takes the average of the average annualized earthquake loss to the replacement value of the building inventory (FEMA, 2000).

Tectonically, the Wasatch Front area occupies an active segment of the ISB—roughly centered on the 343-km-long Wasatch fault zone. Diffuse shallow seismicity, Holocene normal faulting, and episodic surface-faulting earthquakes of M6.5 to M7.5+ characterize the area. The Wasatch fault is notable as the longest continuous, active normal fault in the United States (10 discrete segments)—with five central segments between Brigham City and Nephi (just off the bottom of the map in Figure 2) having an average length of about 50 km, Holocene slip rates of 1–2 mm/yr, and average recurrence intervals ranging from about 1,300 to 2,800 years (Machette et al., 1991; McCalpin and Nishenko, 1996). One of the most active segments is the Salt Lake City segment, which has produced large, M~7, surface-faulting earthquakes on the average of once every 1,350±200 years during the past 6,000 years, with the last one occurring 1,230±60 years ago (Black et al., 1995; McCalpin and Nishenko, 1996; McCalpin and Nelson, 2000).

The National Seismic Hazard Maps of Frankel et al., (1996, gridded data; 2003 gridded data were inaccessible) indicate relatively high ground-shaking hazard for the Wasatch Front—reflected, for example, by the following values of peak ground acceleration in the Salt Lake Valley for specified probabilities of exceedance: 0.30 g (10% in 50 yr), 0.53 g (5% in 50 yr), 0.87 g (2% in 50 yr).

More than three-quarters of Utah's population and economy are concentrated in the Wasatch Front area, literally astride the five most active segments of the Wasatch fault. Population in the Greater Wasatch Area, most densely concentrated in the Ogden-Salt Lake City-Provo urban corridor, is growing rapidly from a 1995 base of 1.6 million and is projected to reach 2.3 million by 2010 and 3.1 million by 2030 (QGET Work Group, 2003). Based on data for 1997–2001, total new construction in the Greater Wasatch Area has averaged \$3.3 billion per year (Isaacson, 2002). From 2000 to 2030, a billion dollars per year will be spent on new infrastructure for transportation and water (QGET Work Group, 2003).

Estimated direct economic losses to buildings and lifelines for a magnitude 7.5 earthquake in Salt Lake County are approximately \$12 (±3) billion (in 1997 dollars) (Rojahn et al., 1997). If one adds indirect economic and social losses (casualties, displaced households, and short-term shelter needs), total losses could be 20 percent higher, putting the total in the range of \$11 billion to \$18 billion.

Contributions and Benefits to NEHRP

Both NEHRP and the USGS benefit greatly from this project in the form of (1) significant (albeit not formal) sharing of costs by the state of Utah under this state-federal partnership and (2) wide-ranging activities by the University of Utah seismologists, which effectively relieve the USGS from having to meet the same first-order needs in this region. (Unlike other NEHRP focus regions such as southern and northern California, the Pacific Northwest, and New Madrid, there are no collocated USGS earthquake scientists here.) Data and information from our regional/urban network provide essential underpinnings for earthquake engineering, emergency response, and science in our region.

The strength of the combined state-federal funding to our earthquake research group is that it has allowed us to balance the practical necessities of a regional seismological approach along with careful attention to Utah's urban corridor. Federal funding also gives us essential flexibility to study—and to respond to significant earthquakes in—other parts of the ISB outside of Utah, where our state funds can't appropriately be used.

In recent testimony to the U.S. House Committee on Science/Subcommittee on Research, as part of NEHRP reauthorization hearings, Dr. L. D. Reaveley, a prominent structural engineer, described our new urban monitoring as a NEHRP success story: "One of the reasons I call this a success story is because the new urban network and real-time earthquake information system has galvanized interactions among earth

scientists, engineers, emergency managers, the Utah Seismic Safety Commission, and other stakeholders—all concerned with practical steps towards improving earthquake safety in Utah" (Reaveley, 2003).

Two other practical examples, indicative of our success in achieving activism on behalf of earthquake hazard mitigation in Utah, are the following. On May 28, 2003, the governor of Utah, Michael O. Leavitt, wrote the following to all five members of Utah's Congressional delegation: "Continued operation and expansion of [Utah's new real-time earthquake information system] is important for the safety of the public in Utah and for producing data and information that will reduce earthquake losses in the long term. He asked each of them "to consider it a Utah priority to find funding at a higher level [for ANSS]." On June 16, 2003, all three of Utah's House Members signed on to a letter from Representatives Nick Smith and Zoe Lofgren to the House Appropriations Subcommittee on Interior urging an increased funding level of at least \$10 million for ANSS for FY04.

Regional/Urban Seismic Network

Figures 1 and 2 together with Tables 1 and A-1 (Appendix A) summarize essential information for the University of Utah's urban/regional seismic network, which included 202 stations (482 channels) at the end of 2003. The overall distribution of conventional broadband and short-period stations in the Utah region is effectively shown in Figure 1. Larger-scale maps in Figure 2 show better the locations of strong-motion stations installed by the end of 2003 as part of the new urban network in the Wasatch Front area.

The urban/regional network consists of: 130 stations within our traditional Wasatch Front study area (dashed rectangle, Figure 1); an additional 16 stations that provide expanded coverage of the Utah region; and another 56 stations covering neighboring parts of the Intermountain Seismic Belt, mostly from southeastern Idaho to Yellowstone National Park. Separate USGS support is provided for the Yellowstone network. As indicated in Table 1 (see also Table A-1, Appendix A), 42 of the 202 stations were maintained by other institutions—including 14 broadband stations operated by either the USGS, Sandia National Lab, or Lawrence Livermore National Lab as part of the U.S. National Seismic Network. The University of Utah handled the field repair and maintenance of 161 stations, 137 of which were sponsored by the USGS under this award. (One station, DUG, has collocated USGS- and UUSS-maintained equipment.)

During the past three years, the University of Utah's modernized regional/urban seismic network has become a model outside of California for locally implementing the Advanced National Seismic System. This is because of our successes in (1) integrating weak- and strong-motion recording and (2) developing an effective real-time earthquake information system in advance of the 2002 Salt Lake City Winter Olympics. Ours was the first network outside of California to locally customize and produce automatic ShakeMaps, successfully implement the Earthworm Oracle Database for earthquake recording and alarms, engineer point-to-multipoint digital telemetry, and complete the *in-situ* calibration of all broadband and strong-motion stations. Significantly, we are already meeting every ANSS network performance objective listed in Attachment A of the USGS's *Program Announcement 04HQPA0002* for seismic networks, issued in April 2003 (see Table 2).

RESULTS AND ACCOMPLISHMENTS

Overview of Seismicity

During the report period, we detected and analyzed approximately 5,100 seismic events. Of these 45 percent were local earthquakes within or near our regional seismic network, 36 percent were regional earthquakes and teleseisms, and 18 percent were blasts. A total of 2,314 earthquakes were located in the Intermountain Seismic Belt, including 1,084 within the Utah region (Figure 3) and 827 within our standard Wasatch Front region (38° 55'–42° 30' N, 110° 25'–113° 10' W). Nineteen earthquakes of magnitude 3 or larger occurred in the Utah region (Figure 4, Table 3). The largest earthquakes were (1) a shock of magnitude (M_L) 4.3 that occurred at 01:04 UTC on April 17, 2003, 6 km (4 mi) SSW of Levan in central Utah and (2) a triplet of earthquakes of magnitude (M_L) 3.6, 3.6, and 3.7 that occurred respectively at 00:39, 00:40, and 00:43 UTC on December 27, 2003. The latter earthquakes also occurred in central Utah, 12 km (8 mi) SW of Nephi and 16 km (10 mi) NNW of the April 17 earthquake.

Thirteen earthquakes in the Utah region during 2003 were documented as felt (Table 4). During the 2003 report period, the University of Utah Seismograph Stations issued four press releases immediately after earthquakes in the Utah region that were either felt by many or larger than a set threshold magnitude of 3.5. Mining-induced seismicity accounted for about 20 percent of the earthquakes located in the Utah region during 2003. A total of 221 shocks ($M \leq 2.9$) were located in known areas of underground coal-mining within an arcuate zone extending counterclockwise from east of Price to 100 km southwest of it (Figure 3).

Real-Time Earthquake Information System

During the past three years, we have successfully (1) integrated weak- and strong-motion monitoring within a modernized regional/urban seismic network and (2) developed an effective real-time earthquake information system in advance of the 2002 Salt Lake City Winter Olympics. During the 2003 report period we modestly expanded strong-motion instrumentation (ten new stations) in Utah's rapidly-growing Wasatch Front urban corridor for emergency response and long-term risk reduction, and we began efforts to make our real-time information system more robust. Accomplishments in 2003 included the following:

Earthworm — Our Earthworm system (hardware and software) for real-time earthquake monitoring and automated alerts is in a constant state of development and is fragile (Nava et al., 2003). Our Earthworm recording system consists of: (a) four computers (two Suns and two PCs) handling digitizing of incoming analog signals or processing of incoming digital data streams; (b) two sets of independent, redundant systems composed of four computers (two Suns and two PCs) interconnected to handle Earthworm core processing, ShakeMap generation, database storage, short-term waveform storage, and Web-based Rapid Review software; and (c) one Sun dedicated to Earthworm data exchange with other networks typically via import/export modules. A separate PC provides data for the IRIS DMC via a publicly accessible Earthworm waveserver. Efforts were made during 2003 to monitor the Earthworm system performance, fine tune the system to maximize efficiency and minimize false earthquake alarms, transfer some functions from PCs to a smaller number of more powerful SUN workstations, and install Earthworm v6.2 (5/2003). V6.2 is not yet completely operational due to problems with the Oracle database interface. We are working with the USGS Earthworm team to resolve these problems.

Besides our Earthworm system, we are also running a parallel data-acquisition system. We operate a Concurrent Corporation 7200-C computer, which digitizes incoming analog data streams, runs HAWK processing software, and produces triggered event data files in UW1 format.

ShakeMap and attenuation studies — We continued to implement ShakeMap and customize it for use in the Wasatch Front urban corridor. We also worked with the ShakeMap Working Group, contributing code and helping to prepare a ShakeMap Manual. During 2003, seven ShakeMaps were automatically generated and posted to our Web site. They were later reviewed and/or reprocessed for quality assurance purposes. ShakeMap developments involved initiating information transfer directly to a USGS Webserver, which is backed up by Akamai, and to Weathercentral, a private forecast company that specializes in providing TV stations with state of the art graphic capabilities. One new study this year involved using the ShakeMap scenario option to (1) explore the sensitivity to the choice of attenuation relation and uncertainty in site amplification and (2) model the MMI values for an M5.2 shock that occurred on the western edge of the Salt Lake Valley (near the town of Magna, Utah) in 1962 (Pankow, 2003).

Because ShakeMap requires predictive relations for attenuation and site amplification, another part of our ShakeMap development has involved testing the appropriateness of the chosen predictive relations and site amplification. We have used ground-motion data acquired by our new strong-motion network, together with site amplification factors developed for the Wasatch Front region, to validate the appropriateness of using weak-motion attenuation relations developed in southern California. Further, we have used a worldwide strong-motion data set assembled by Spudich et al. (1999) in order to determine a predictive relation for peak horizontal ground velocity (PGV) for earthquakes in extensional tectonic regimes. The details of the PGV regression and a correction we made to account for the 20% bias at rock sites reported by Spudich et al., (1999) are described by Pankow and Pechmann (2004). The new PGV regression has been incorporated into our routine ShakeMap processing. It has also been given to the University of Nevada at Reno for ShakeMap implementation in Nevada.

Ten new strong-motion stations — In FY 2003 we received ANSS equipment and funds for adding ten stations to Utah's real-time urban strong-motion network, bringing the network total to 75 stations (Figure 2). Strong-motion instruments (REF TEK ANSS-130) were received in mid-to-late June. Seven of the stations were installed before September 30, 2003, and the remaining three stations were completed shortly thereafter. The ten new stations include two urban reference stations in small buildings, four urban reference stations on open ground, and four free-field rock stations. Installing and troubleshooting sequential versions of firmware and software provided to us by ANSS instrument vendors for beta testing, both for new and earlier-installed instruments, were greatly time consuming. Major efforts were made to implement point-to-multipoint digital radio telemetry in our Utah network using Time Division Multiple Access (TDMA) technology in order to reduce operational costs. As a cost-savings measure, we started to convert 11 of our FY 2000 and FY 2001 strong-motion stations from frame-relay telephone to spread-spectrum radio (eight stations) and public Internet (3 stations).

Integration of USGS/NSMP strong-motion data — The USGS National Strong-Motion Program (NSMP) operates several digital strong-motion stations in the Wasatch Front area from which data are retrieved by telephone remotely from Menlo Park, CA. During 2003 we began recording continuous data streams from two more of these stations via telemetry links we installed; we now record data from four NSMP stations in real time. We also use an import protocol to automatically receive from NSMP both parametric data (in XML format) and waveform data for all their strong-motion stations in the Wasatch Front area operating with telephone connections. The NSMP data usefully contribute to our ShakeMap database.

“Earthquakes in the News” — In mid-June 2003 our computer professional installed the listening script, "Earthquakes in the News," enabling our UUSS home page to feature "Earthquakes in the News" links. By completing this task, our network staff reached, in advance, full compliance with all of the network-performance expectations (except for standards yet to be developed) set forth by the USGS in Program Announcement 04HQPA0002 for funding seismic networks during FY 2004-2006.

Seismicity Remotely Triggered by Denali Fault Earthquake—and Other Studies

Triggered seismicity following the Denali Fault earthquake — Immediately following the arrival of the surface waves from the M_w 7.9 Denali Fault, Alaska, earthquake on November 3, 2002, the University of Utah's regional seismic network recorded an abrupt increase in local microseismicity throughout most of Utah's main seismic belt. During 2003 we undertook a detailed analysis of the triggered seismicity. The elevated seismicity was most intense during the first 24 hours (> 10 times the average prior rate) but continued above the background level for 25 days (at the 95% confidence level) in most areas. Statistical analyses allow us to reject with $>95\%$ confidence the null hypothesis that the observed increases were due to random occurrence. Data from 37 ANSS strong-motion stations in Utah contributed to the estimation and mapping of peak dynamic stresses that occurred during the passage of surface waves through Utah; the level of the peak dynamic stresses (1.2–3.5 bars) is consistent with the interpretation of remote triggering of local seismicity by the Alaskan earthquake, which occurred more than 3000 km from our study region. Initial results were presented at the 2002 Fall American Geophysical Union meeting (Pankow et al., 2002) and were also reported in the Utah Geological Survey's public outreach bulletin (Pankow et al., 2003). A full manuscript prepared for a forthcoming special issue of the *Bulletin of the Seismological Society of America* on the Denali Fault earthquake is included here as Appendix B.

Receiver-function analysis — In conjunction with a University of Utah graduate student we have been analyzing teleseismic earthquakes recorded by both regional broadband instruments and the ANSS urban strong-motion network. The student has been migrating these data to image crustal/upper-mantle structure. Preliminary results were presented at the 2003 Fall AGU meeting (Sheng et al., 2003).

Space Shuttle Columbia — In response to requests via the USGS from NASA, which was seeking clues to the possible locations of debris from the space shuttle Columbia, we undertook analyses of data from our seismic network stations in southwestern Utah in the vicinity of Columbia's February 1, 2003, ground track. Ultimately, analyses of University of Utah data by J. C. Pechmann and others did not lead to the recognition of any seismic signals that could unambiguously be attributed to falling objects hitting the ground. However, besides Columbia's primary sonic boom, other unidentified signals were recognized which could have been (a) downward-refracted or reflected sonic booms from the shuttle, (b) seismic and/or sonic waves generated by impacts of shuttle debris, or (c) signals of some other origin.

Coal-mining-induced seismicity — We continued studies of seismicity induced by underground coal mining in east-central Utah (Arabasz et al., 2004; McGarr et al., 2004; see also Arabasz et al., 2002a,b) in order to serve the needs of (1) mining engineers and mine operators concerned with mine safety and (2) decision-makers dealing with the potential hazards of mining seismicity to off-site structures and facilities. The studies involved cooperative research with the U.S. Geological Survey and the U.S. Bureau of Reclamation, including accelerographic recording and ground-motion modeling of the mining seismicity in order to evaluate the hazard of surface ground shaking.

During 2003 we developed partnerships with three coal-mining companies to install and operate above-mine seismic stations at three coal mines in the Book Cliffs coal mining region. Each of these three stations has a digital datalogger, a three-component accelerometer, and a vertical-component short-period seismometer.

Continuous data are digitally telemetered to our network operations center in Salt Lake City and are integrated with our regional/urban network recording. These three stations (BCW, DCM, BCE) are shown in Figure 1.

Accomplishments in Ongoing Network Operations

Noteworthy accomplishments during the report period included the following:

Continued maintenance and operation of short-period stations — The short-period stations in our seismic network continue to be fundamentally important for earthquake detection and hypocentral resolution. Forty-five short-period stations in the Wasatch Front area are operated and maintained as part of this cooperative agreement (Appendix A). As the result of a systematic maintenance program, started in the mid-1990s, to upgrade the field electronics and site hardware at every short-period station in our Utah network, these stations perform with exceptional reliability. All stations have a standardized UU-designed VCO, seismometers have systematically been refurbished by the manufacturer, and station polarities have been verified or corrected (only one reversed station currently). Instrument response files are routinely updated for all stations and posted to the IRIS DMC.

Improved magnitude determination for very small earthquakes — We modified our version of the earthquake location program *Hypoinverse* (originally written by F. W. Klein, USGS) to compute and report negative magnitudes instead of discarding them, and we changed the default magnitude from 0.00 to -9.99. These changes were needed because in some areas of our network we are able to locate very small earthquakes for which some or all of the single-station coda magnitude (M_C) estimates are less than zero. Negative magnitudes are set to 0.0 before submission to the Quake Data Distribution System (QDDS) due to limitations in the QDDS software.

Analysis of optimal record lengths for automatic determination of local magnitude (M_L) — We analyzed the times of more than 10,000 maximum peak-to-peak amplitude measurements on synthetic Wood-Anderson records to provide a better basis for selecting the time intervals on such records to be analyzed in automatic local magnitude determinations. We found that 98% of the maximum peak-to-peak amplitudes occurred between the P-wave arrival time and 20 sec after the estimated Sg arrival time. Restricting the search for maximum peak-to-peak amplitudes to these time windows will minimize errors in automatic M_L determinations caused by including maximum amplitude measurements from the wrong seismic events. These errors are sometimes very large.

Near-real-time data exchange with other networks — Throughout the report period, we continued to exchange waveform data in near-real time with the National Earthquake Information Center, the Idaho National Engineering and Environmental Laboratory, the Montana Bureau of Mines and Geology, Brigham Young University (Idaho), the U.S. Bureau of Reclamation, and the University of Nevada, Reno. In March 1993, we began exchanging waveform data with Northern Arizona University. These data exchanges are done via the Internet using Earthworm import/export software modules (see Table 1).

Assistance to other seismic networks — In February 2003 our network staff successfully configured and installed a PC-based (Pentium III) Earthworm system in Flagstaff, Arizona, for the Arizona Earthquake Information Center (AEIC) at Northern Arizona University. Help was provided by Doug Bausch of FEMA (formerly of AEIC) and Dave Brumbaugh, director of AEIC. The Arizona Earthworm system is set up for remote system administration and control at the University of Utah. Continuous data from the 8-station Northern Arizona Seismic Network are exported via Internet to the University of Utah and then relayed to the IRIS DMC. Help to other networks also included the following: (1) we provided to Mike Stickney, the operator of Montana's regional seismograph network, UUSS customized software for calculating Richter local

magnitude (M_L) from broadband waveforms; we also gave him a tutorial on creating dataless SEED volumes (including instrument response information) for submission of his network data to the IRIS DMC; (2) we provided customized ShakeMap modules to the University of Washington seismic network; (3) we provided a ShakeMap module using the new Pankow and Pechmann (2004) ground-motion attenuation relations to the University of Nevada at Reno; (4) in April 2003, two of our group met in San Juan, Puerto Rico, with operators of the Puerto Rico seismic network during SSA2003 to offer technical advice and help on expansion and modernization of that network.

Archiving waveform data — All digital waveform data collected by the University of Utah regional/urban seismic network during the report period were submitted to the IRIS DMC in SEED format. Continuous waveform data from all stations we maintain and operate have been submitted to the IRIS DMC on a daily basis since June 2002. Currently, the IRIS DMC retrieves data from our Earthworm-system wave tanks several times per day. Using a different system, submission of continuous waveform data from our broadband stations began on June 19, 2000, and on April 19, 2001, for continuous waveform data from our strong-motion stations.

Submission of earthquake catalog data to ANSS information outlets — During the report period, Earthworm automatic (non-human-reviewed) hypocenters and magnitudes for earthquakes of magnitude 2.5 and larger in our authoritative regions (Utah and Yellowstone National Park) were automatically submitted to the Quake Data Distribution System (QDDS) of the Advanced National Seismic System. Analyst-determined hypocenters and magnitudes for all earthquakes in our authoritative regions were submitted to QDDS as they were completed. These same data were automatically submitted to the ANSS catalog four times per day during the Monday-Friday work week. Events submitted to QDDS are automatically posted on the ANSS RecentEqs Web pages.

Miscellaneous

ANSS planning activities — During 2003, a 12-member state-level advisory committee continued to guide the development and effective use of urban strong-motion monitoring in Utah. The Utah Advisory Committee for Urban Strong-Motion Monitoring was created in FY 2001, both as part of the ANSS management structure and as part of Utah's state earthquake program. The advisory committee met on January 16, 2003 (for minutes, see < <http://www.seis.utah.edu/urban/011603.shtml> >). The committee identified 23 candidate sites for installing 15 (later reduced to ten) additional ANSS strong-motion stations in Utah's Wasatch Front area during FY 2003. The committee affirmed that the criteria for site selection would continue to be (1) geographic distribution (particularly in uninstrumented areas of rapid development), (2) sampling of different geological site-response units, and (3) proximity to important lifelines and urban infrastructure. In early- to mid-2003, we explored sites and coordinated with Alena Leeds (USGS/Golden) in connection with a new ANSS national backbone station near Cedar City in southwestern Utah.

Next-generation ground-shaking hazard maps — In April 2003 we participated in planning workshops sponsored by the USGS and the Utah Geological Survey for developing the next generation of ground-shaking hazard maps in Utah. Four seismologists in our network group are now serving on a 13-member Utah Ground-Shaking Working Group, and two others are serving on a Utah Quaternary Fault Parameter Working Group, enabling close coordination between our UUSS/ANSS urban strong-motion network and researchers addressing local ground-motion-related issues.

AVAILABILITY OF DATA

All seismic waveform data archived by the University of Utah Seismograph Stations are available upon request directly from our office (typically delivered to the user in SAC ASCII or binary format). Alternatively, waveform data can be retrieved from the IRIS DMC using their SeismiQuery Web tool at <http://www.iris.washington.edu/SeismiQuery> (delivered in a variety of formats). Earthquake catalog data for the Utah region are available (1) via anonymous ftp ftp://seis.utah.edu/pub/UUSS_catalogs, (2) via the Advanced National Seismic System's composite earthquake catalog <http://quake.geo.berkeley.edu/cnss/cnss-catalog.html>, or (3) by e-mail request to webmaster@seis.utah.edu. See also the University of Utah Seismograph Stations homepage at <http://www.seis.utah.edu>. The contact person for data requests is Relu Burlacu, tel: (801) 585-7972; e-mail: burlacu@seis.utah.edu.

REFERENCES CITED

- Arabasz, W. J., S. J. Nava, M. K. McCarter, and K. L. Pankow (2002a). Ground-motion recording and analysis of mining-induced seismicity in the Trail Mountain Area, Emery County, Utah, Technical Report, University of Utah Seismograph Stations, Salt Lake City, Utah, 162 pp. Accessible online at <http://www/seis.utah.edu/Reports/sitla2002a>.
- Arabasz, W. J., J. Ake, M. K. McCarter, and A. McGarr (2002b). Mining-induced seismicity near Joes Valley Dam: Summary of ground-motion studies and assessment of probable maximum magnitude, Technical Report, University of Utah Seismograph Stations, Salt Lake City, Utah, 35 pp. Accessible online at <http://www/seis.utah.edu/Reports/sitla2002b>.
- Arabasz, W. J., S. J. Nava, M. K. McCarter, K. L. Pankow, J. C. Pechmann, J. Ake, and A. McGarr (2004). Coal-mining seismicity and ground-shaking hazard^{3/4}A case study in the Trail Mountain area, Emery County, Utah, *Bull. Seism. Soc. Am.*, submitted.
- Black, B. D., W. R. Lund, and B. H. Mayes (1995). Summary of new information from the South Fork Dry Creek site, Salt Lake County, Utah, in *Environmental and Engineering Geology of the Wasatch Front Region*, W. R. Lund, editor, *Utah Geol. Assoc. Publ.* 24, 11-30.
- Frankel, A., C. Mueller, T. Barnhard, D. Perkins, E. V. Leyendecker, N. Dickman, S. Hanson, and M. Hopper (1996). National Seismic Hazard Maps: Documentation June 1996, *U.S. Geol. Surv. Open-File Rept.* 96-532.
- FEMA (2000). *HAZUS 99 Estimated Annualized Earthquake Losses for the United States*, Federal Emergency Management Agency, *FEMA 366*, Washington, DC, 32 pp.
- Isaacson, A.E. (2002). Utah's economy: Slow growth during 2001, *Utah Economic and Business Review* **62** (11 & 12), 1-15.
- Machette, M. N., S. F. Personius, A. R. Nelson, and D. P. Schwartz (1991). The Wasatch fault zone, Utah—segmentation and history of Holocene earthquakes, *J. Struct. Geol.* **13** (2), 137-149.
- McCalpin, J. P. and C. V. Nelson (2000). Long recurrence records from the Wasatch fault zone, Utah, Final Technical Report, Contract 99HQGR0058, National Earthquake Hazards Reduction Program, U.S. Geological Survey, 61 pp.

- McCalpin, J. P. and S. P. Nishenko (1996). Holocene paleoseismicity, temporal clustering, and probabilities of future large ($M > 7$) earthquakes on the Wasatch fault zone, Utah, *J. Geophys. Res.* **101** (B3), 6233-6253.
- McGarr, A., J. B. Fletcher, and W. J. Arabasz (2004). Seismic hazard to the Joes Valley Dam, central Utah, due to nearby coal-mining-induced earthquakes (abstract), Annual Mtg. of the Eastern Section, Seismological Society of America, *Seismol. Res. Letters* **75**, in press.
- Pankow, K. L. (2003). The anatomy of an earthquake scenario: M7 on the Salt Lake City segment of the Wasatch fault, Utah (abs.): *Geophysical Research Abstracts* **5**, EGS-AGU-EUG Joint Assembly, EAE03-A-00230.
- Pankow, K. L. and J. C. Pechmann, (2004). The SEA99 ground motion predictive relations for extensional tectonic regimes: Revisions and a new peak ground velocity relation, *Bull. Seism. Soc. Am.* **94**, 341–348.
- Pankow, K. L., S. J. Nava, J. C. Pechmann, and W. J. Arabasz (2002). Triggered seismicity in Utah from the November 3, 2002, Denali Fault Earthquake [abs.]: *Eos, Trans. Am. Geophys. Union* **83** (47), Fall Meet. Suppl., S72F-1359, (Late Breaking Session, p. 9).
- Pankow, K. L., W. J. Arabasz, S. J. Nava, and J. C. Pechmann (2003). Triggered seismicity in Utah from the November 3, 2002, Denali Fault earthquake, *Survey Notes* **35** (1) (Utah Geological Survey, Salt Lake City), 11-12.
- QGET Quality Growth Efficiency Tools Work Group (2003). 2003 baseline scenario for the Greater Wasatch Area of Utah, <<http://governor.utah.gov/dea/2003BaselineWEB.pdf>>
- Reaveley, L. D. (2003). Testimony of Lawrence D. Reaveley to the U.S. House of Representatives Committee on Science, Subcommittee on Research, May 8, 2003 <http://www.eeri.org/news/nehrrp/Reaveley_DC_written_testimony.doc>
- Rojahn, C., S. A. King, R. E. Scholl, A. S. Kiremidjian, L. D. Reaveley, and R. R. Wilson (1997). Earthquake damage and loss estimation methodology and data for Salt Lake County, Utah (ATC-36), *Earthquake Spectra* **13** (4), 623-642.
- Sheng, J., G. T. Schuster, K. L. Pankow, J. C. Pechmann, and R. L. Nowack (2003). Coherence-weighted wavepath migration of teleseismic data (abstract), *Eos, Trans. Am. Geophys. Union* **84** (46), Fall Meet. Suppl., Abstract S11E-0344.
- Spudich, P., W. B. Joyner, A. G. Lindh, D. M. Boore, B. M. Margaris, and J. B. Fletcher (1999). SEA99: A revised ground motion prediction relation for use in extensional tectonic regimes, *Bull. Seism. Soc. Am.* **89**, 1156-1170.

REPORTS AND PUBLICATIONS

- Arabasz, W. J. (2003). Lessons for planning or modernizing seismic networks (abstract), *Seismol. Res. Letters* **74** (2), 228.
- Arabasz, W. J., S. J. Nava, M. K. McCarter, K. L. Pankow, J. C. Pechmann, J. Ake, and A. McGarr (2004). Coal-mining seismicity and ground-shaking hazard^{3/4}A case study in the Trail Mountain area, Emery County, Utah, *Bull. Seism. Soc. Am.*, submitted.
- McGarr, A., J. B. Fletcher, and W. J. Arabasz (2004). Seismic hazard to the Joes Valley Dam, central Utah, due to nearby coal-mining-induced earthquakes (abstract), Annual Mtg. of the Eastern Section, Seismological Society of America, *Seismol. Res. Letters* **75**, in press.
- Nava, S. J. (2003). Earthquake activity in the Utah region [summaries and maps of seismicity in the Utah region, published quarterly by the Utah Division of Comprehensive Emergency Management in *Fault Line Forum*].
- Nava, S., W. Arabasz, J. Pechmann, K. Pankow, A. Moeinvaziri, D. Drobeck, and T. Dye (2003). Creating a regional earthquake information system: Practical experience from the Utah regional seismic network (abstract), *Seismol. Res. Letters* **74** (2), 251.
- Pankow, K. L. (2003). The anatomy of an earthquake scenario: M7 on the Salt Lake City segment of the Wasatch fault, Utah, *Geophys. Res. Abstracts* **5**, EGS-AGU-EUG Joint Assembly, Compact Disk, ISSN No. 1029-7006.
- Pankow, K. L. and J. C. Pechmann, (2004). The SEA99 ground motion predictive relations for extensional tectonic regimes: Revisions and a new peak ground velocity relation, *Bull. Seism. Soc. Am.* **94**, 341–348.
- Pankow, K. L., W. J. Arabasz, S. J. Nava, and J. C. Pechmann (2003a). Triggered seismicity in Utah from the November 3, 2002 Denali Fault earthquake, *Survey Notes* (Utah. Geol. Survey) **35** (1), 11–12.
- Pankow, K. L., W. J. Arabasz, S. J. Nava, and J. C. Pechmann (2003b). Utah Regional Seismic Network—Exploring potential EarthScope-ANSS Synergy (abstract), *Proceedings 2003 IRIS/UNAVCO Workshop*, June 19–21, 2003, Fish Camp, California.
- Pankow, K. L., W. J. Arabasz, J. C. Pechmann, and S. J. Nava (2004). Triggered seismicity in Utah from the November 3, 2002, Denali Fault earthquake, *Bull. Seism. Soc. Am.*, submitted.
- Sheng, J., G. T. Schuster, K. L. Pankow, J. C. Pechmann, and R. L. Nowack (2003). Coherence-weighted wavepath migration of teleseismic data (abstract), *Eos, Trans. Am. Geophys. Union* **84** (46), Fall Meet. Suppl., Abstract S11E-0344.
- Velasco, A. A., C. J. Ammon, J. Farrell, and K. Pankow (2004). Rupture directivity of the November 3, 2002 Denali earthquake determined from surface waves, *Bull. Seism. Soc. Am.*, submitted.
- Youngs, R. R., W. J. Arabasz [and multiple authors] (2003). A methodology for probabilistic fault displacement hazard analysis (PFSHA), *Earthquake Spectra* **19**, 191–219.

TABLES AND FIGURES

Table 1
Overview of the University of Utah Regional/Urban Seismic Network
December 2003

Networks Forming Part of Regional Operation:	CODE	Stations/channels
* <i>Utah Region Seismic Network (URSN)</i>	<i>UU</i>	<i>138/371</i>
Yellowstone National Park Seismograph Network (YSN)	WY	23/33

TOTAL Stations/Channels Operated: 161/404

Import data from:	CODE	Stations/channels
Brigham Young University (Idaho) Seismic Network (formerly Ricks College)	RC	1/1
Montana Regional Seismic Network	MB	5/5
Idaho National Engineering and Environmental Laboratory Seismic Network	IE	7/7
Western Great Basin/Eastern Sierra Seismic Network University of Nevada, Reno	NN	6/6
US Bureau of Reclamation Seismic Networks	RE	2/2
US National Seismic Network	US	12/36
US National Strong Motion Program (via EW module getfile; triggered data from instruments in Wasatch Front area)	NP	Variable (.evt and xml files)
US National Strong Motion Program (direct data stream)	NP	4/12
Sandia National Laboratory—Leo Brady Network	LB	1/3
USGS Albuquerque Seismological Laboratory	IU	1/3
Northern Arizona University Seismic Network	AR	3/3
Total Stations/Channels Imported:		42/78

TOTAL Stations/Channels Recorded: 202/482

Export Data To:	Stations/Channels
Brigham Young University (Idaho) Seismic Network (formerly Ricks College)	22/30
Montana Regional Seismic Network	8/8
Idaho National Engineering and Environmental Laboratory Seismic Network	7/7
Northern Arizona University Seismic Network	2/2
US National Seismic Network	Export HPYP messages
US National Seismic Network	18/44
IRIS Data Management Center (via ew2mseed)	167/364
Total Stations/Channels Exported:	224/455

(All real-time data exchange is via Earthworm Import/Export unless otherwise noted)

Table 2
UNIVERSITY OF UTAH COMPLIANCE WITH NEHRP/ANSS PROGRAM OBJECTIVES¹
 (reproduced from University of Utah project proposal to USGS, June 2003)

	Start Date of Utah Compliance	Comments
Task 1: Seismic Network Operations		
1. Monitor regional seismicity and active tectonic structures	1974	Regional telemetered short period network began in 1974 (earlier statewide instrumental monitoring, in 1962); digital recording, in 1981; first broadband installed in 1997; first ANSS strong motion station installed in 2000. Catalog includes > 32,800 earthquakes in the Utah region since 1850.
2. Adhere to ANSS standardized maintenance and operational procedures	Ongoing	Currently use field electronics, sensors, data acquisition hardware and software, routine analysis software, and maintenance/operational procedures commonly accepted by the seismological community, with consistent emphasis on high quality. Will follow standardized maintenance and operational procedures as they are established.
Task 2: Real-time Integration of Regional and National Networks		
1. Use ANSS-approved data exchange protocols	1997	Implemented standard Earthworm import/export modules for routine waveform data exchange with the USNSN and neighboring seismic networks.
2. Adopt ANSS business rules	2002	Implemented Earthworm module ew2mseed for real-time continuous submission of waveform data to the IRIS DMC.
3. Provide strong motion data to NSMP upon request	1998	Adopted CNSS/ANSS authoritative region definitions for submission of hypocenters to composite catalog. Will comply with new business rules and standards as they become available.
4. Adhere to network security standards	Ongoing	Continuously export strong-motion data to IRIS DMC. Automatically receive NSMP .evt and .xml files via Earthworm getfile module for all triggers on NSMP stations located within Wasatch Front, Utah. Will send data as requested to NSMP and to the COSMOS virtual data center. Computers are secured against unwanted intrusion via firewalls and authentication routines. Software and anti-virus patches are kept current. We will comply with ANSS network security standards as they become available.

Table 2 (continued)

	Start Date of Utah Compliance	Comments
Task 3: Access and Distribution of Earthquake Information Products		
1. Distribution of earthquake information:	2002	We send automatic earthquake locations and magnitudes computed by Earthworm to ANSS real-time composite catalog for shocks of M3.0 or larger located within authoritative regions. Messages typically delivered within minutes following completion of location and magnitude computation. Human review and update of automated postings processed within 24 hours of occurrence, often within 30 minutes.
- Contribute real-time earthquake locations and magnitudes to ANSS composite catalog within ten minutes of occurrence		
- Submit reviewed locations and magnitudes within one month of occurrence	1998	All analyst-processed hypocenters for earthquakes located within authoritative region are sent to CNSS/ANSS composite catalog, typically forwarded within several days of occurrence.
- Use QDDS for distribution	2002	We submit QDDS messages for all analyst-processed hypocenters and for M3+ automated solutions located within authoritative regions.
- Run Earthquake-In-The-News listening software	2003	Implemented.
2. Provide public web pages with links to:	2000	Locally implemented USGS RecentEqs software to post events within authoritative regions. Link from our home page to ANSS national RecentEqs Web page.
- RecentEqs		
- Earthquake-In-The-News	2002	Access to password-protected USGS Earthquake-In-the News control pages granted and staff trained in usage.
- Did you feel it?	2002	Link from our Web pages established. Public encouraged to submit reports during media coverage following locally felt earthquakes.
- ShakeMap	2001	Only regional network outside of CA to run automatic ShakeMaps, including direct posting to public Web pages. ShakeMaps are triggered by automatic Earthworm location and magnitude within preset parameters. Have produced ten ShakeMaps to date (M _L 3.0-4.3)
3. Provide annual update of seismic station inventory	2000	Station inventories submitted as requested. Last requested submission in February 2003.
4. Submit digital waveform data and station metadata to a data management center	2000	Have submitted all archived waveform data from UU-seismic network from 1981 through present to IRIS DMC. Earthworm module used to submit UU waveform data in real-time to IRIS DMC BUD system since July 2002. Provide gateway services to forward real-time waveform data to DMC BUD system from INEEL and N. Arizona seismic networks.

Note: 1. Specific dates of compliance routinely documented in annual technical reports submitted to the USGS.

Table 3
Earthquakes in the Utah Region of Magnitude 3.0 and Larger, 2003

DATE	ORIG TIME	LATITUDE	LONGITUDE	DEPTH	MAG	NO.	GAP	DMN	RMS
030103	05:02:12.16	41°16.48'	111°48.12'	11.9	3.6W	47	68	11	0.24
030201	20:37:31.24	41°49.71'	112°12.72'	0.2*	3.2W	37	57	15	0.15
030211	09:00:42.19	38°41.85'	112°15.54'	0.4*	3.3W	22	95	22	0.18
030325	21:11:36.02	36°51.44'	113°00.11'	4.3*	3.0W	7	230	24	0.18
030417	01:04:19.07	39°30.78'	111°54.29'	0.9	4.3W	37	43	8	0.45
030510	17:13:20.84	37°41.78'	113°12.60'	5.7*	3.0W	13	71	23	0.28
030510	17:20:00.15	37°42.62'	113°11.67'	3.0*	3.2W	13	70	23	0.27
030708	02:20:33.77	36°57.22'	111°47.16'	6.6*	3.3W	16	80	45	0.31
030708	02:55:46.84	36°57.39'	111°47.17'	7.0*	3.1W	14	80	45	0.31
030712	01:54:40.04	41°17.14'	111°36.88'	9.2*	3.5W	45	112	22	0.19
031107	06:52:56.02	36°57.20'	111°46.43'	7.2*	3.1W	11	110	44	0.30
031117	23:18:52.15	40°20.93'	111°10.08'	12.6	3.0W	36	149	10	0.19
031129	22:33:09.15	38°26.95'	112°30.12'	3.1*	3.2W	18	82	29	0.24
031212	21:04:13.47	39°32.59'	111°56.27'	0.7*	3.2W	41	86	11	0.25
031226	00:33:06.15	38°59.46'	111°56.11'	3.0*	3.0W	26	73	14	0.20
031227	00:39:24.37	39°38.91'	111°56.99'	1.9*	3.6W	30	87	20	0.23
031227	00:40:41.05	39°38.39'	111°56.79'	1.1*	3.6W	24	96	19	0.22
031227	00:43:23.91	39°38.95'	111°57.42'	1.8*	3.7W	11	133	20	0.18
031227	13:19:00.95	39°38.67'	111°57.46'	2.3*	3.0W	30	98	20	0.22

number of earthquakes = 19

* indicates poor depth control

W indicates Wood-Anderson data used for magnitude calculation

Table 4
Felt Earthquakes in the Utah Region
January 1 – December 31, 2003

Date	Time[†]	Felt Information[‡]	Latitude	Longitude	Magnitude[§]
Jan 2 (MST) Jan 3 (UTC)	22:02 MST 05:02 UTC	<i>CIIM, ShakeMap.</i> Utah. Felt (IV) at Huntsville, Ogden; (III) at Eden, Paradise, Franklin, ID; (II) at Bountiful, Brigham City, Clearfield, Centerville, Croydon, Farmington, Hyde Park, Kaysville, Layton, Logan, Mantua, Morgan, Providence, Richmond, Roy, Salt Lake City, Willard.	41° 16.44'	111° 48.17'	M _L 3.6 M _C 3.9
Feb 1	13:37 MST 20:37 UTC	<i>ShakeMap.</i> Utah. Felt (III) at Clarkston, Fielding, Garland, Plymouth.	41° 49.68'	112° 12.75'	M _L 3.2 M _C 3.3
Feb 11	02:00 MST 09:00 UTC	Utah. Felt (III) at Monroe.	38° 41.85'	112° 15.54'	M _L 3.3 M _C 3.2
April 16 (MDT) April 17 (UTC)	19:04 MDT 01:04 UTC	<i>ShakeMap.</i> Utah. Felt (IV) at Nephi and (II) at Fairview. Also felt at Delta, Ephraim, Levan, Mount Pleasant.	39° 30.77'	111° 54.29'	M _L 4.3 M _C 4.7
July 7 (MDT) July 8 (UTC)	20:55 MDT 02:55 UTC	Arizona. Felt at Page, AZ.	36° 57.39'	111° 47.17'	M _L 3.2 M _C 3.1
July 11 (MDT) July 12 (UTC)	19:54 MDT 01:54 UTC	<i>CIIM, ShakeMap.</i> Utah. Felt (III) at Huntsville, Ogden, Roy. Also felt at Draper, Layton, Salt Lake City, Wellsville	41° 17.14'	111° 36.87'	M _L 3.5 M _C 3.9
Aug 2 (MDT) Aug 3 (UTC)	23:16 MDT 05:16 UTC	Utah. Felt (III) at Cedar City. Also felt at Beryl.	37° 39.80'	113° 16.71'	M _L 2.9 M _C 3.0
Dec 12	14:04 MST 21:04 UTC	<i>CIIM.</i> Utah. Felt (II) at Nephi.	39° 32.59'	111° 56.27'	M _L 3.2 M _C 3.2
Dec 25 (MST) Dec 26 (UTC)	17:33 MST 00:33 UTC	<i>CIIM.</i> Utah. Felt (II) at Salina and Nephi.	38° 59.46'	111° 56.11'	M _L 3.0 M _C 3.0

Table 4 (continued)

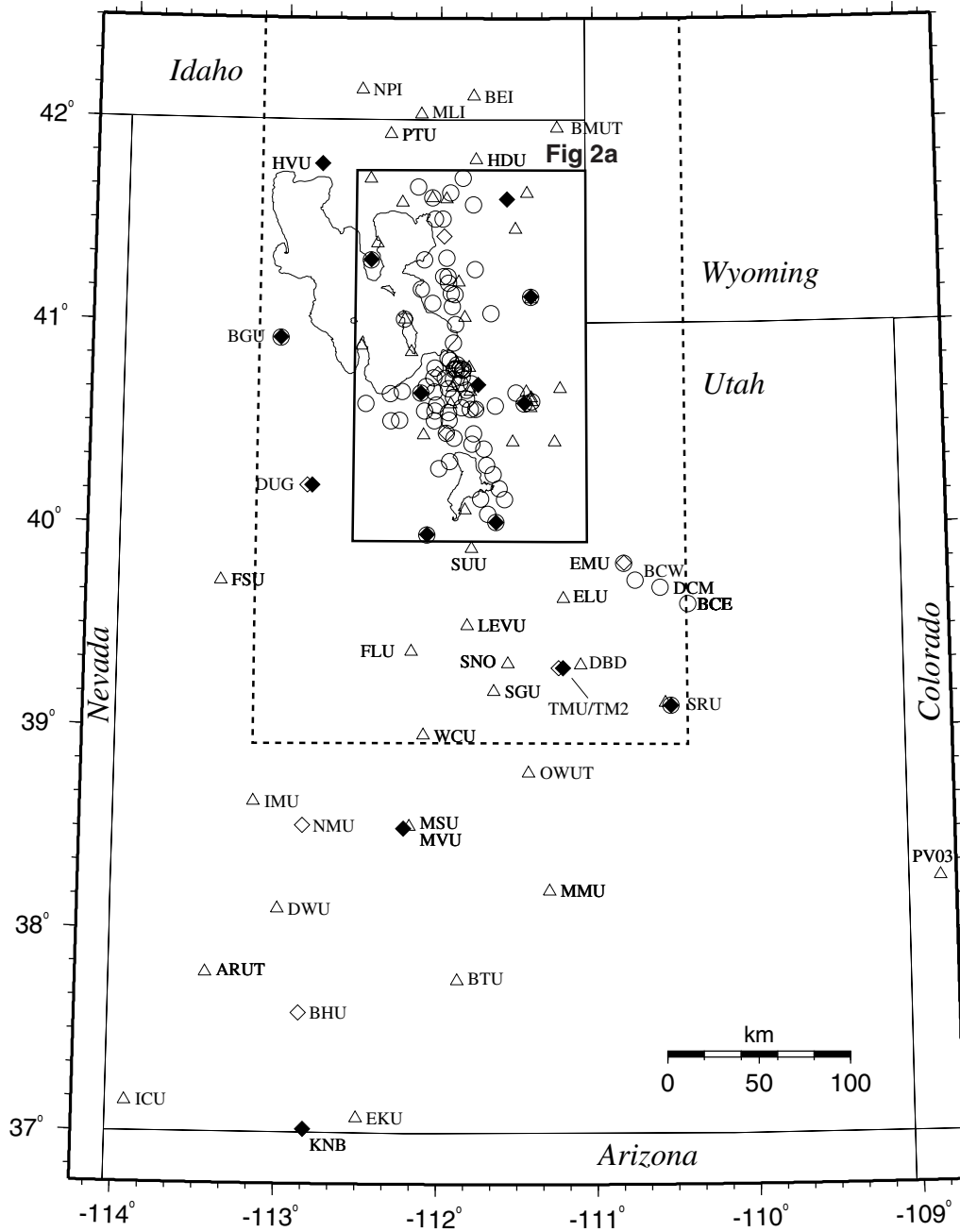
Date	Time[†]	Felt Information[‡]	Latitude	Longitude	Magnitude[§]
Dec 26 (MST) Dec 27 (UTC)	17:39 MST 00:39 UTC	<i>CIIM, ShakeMap</i> . Utah. Felt (III) at Nephi and Ephraim; (II) at Spanish Fork.	39° 38.91'	111° 56.99'	M _L 3.6 M _C 3.8
Dec 26 (MST) Dec 27 (UTC)	17:40 MST 00:40 UTC	<i>CIIM, ShakeMap</i> . Utah. Felt (III) at Nephi.	39° 38.39'	111° 56.79'	M _L 3.6 M _C 4.0
Dec 26 (MST) Dec 27 (UTC)	17:43 MST 00:43 UTC	<i>CIIM, ShakeMap</i> . Utah. Felt (III) at Nephi; (II) at Fairview.	39° 38.95'	111° 57.42'	M _L 3.7 M _C 3.5
Dec 27	06:19 MST 13:19 UTC	<i>CIIM</i> . Utah. Felt (II) at Nephi.	39° 38.67'	111° 57.46'	M _L 3.0 M _C 3.1

[†] Times are listed both as Local Time—Mountain Standard Time (MST) or Mountain Daylight Time (MDT)—and as Universal Coordinated Time (UTC).

[‡] *CIIM* indicates the availability of a Community Internet Intensity Map (<http://pasadena.wr.usgs.gov/shake/imw/archives.html>), compiled by the U.S. Geological Survey (USGS); *ShakeMap* indicates the availability of maps of ground-shaking (<http://www.seis.utah.edu/shake/archive>), produced by the University of Utah Seismograph Stations (UUSS). Roman numerals correspond to the Modified Mercalli intensity scale. Unless otherwise indicated, felt information is from the USGS's (1) PDE Monthly (or) Weekly Listing Files (http://neic.usgs.gov/neis/data_services/ftp_files.html) and/or (2) CIIM reports.

[§] Richter local magnitude (M_L) or coda magnitude (M_C) determined by UUSS. If labeled "NEIC," data are from the National Earthquake Information Center of the USGS.

Utah Regional/Urban Seismic Network December 31, 2003



STATION KEY

- △ = single-component, analog-telemetry, short-period
- ◇ = multi-component, analog-telemetry, short-period
- ◆ = multi-component, digital-telemetry, broadband
- = multi-component, digital-telemetry, strong motion

Bounds of map correspond to standard "Utah Region";
dashed rectangle, traditional "Wasatch Front Area."

Figure 1

Utah Urban Seismic Network December 31, 2003

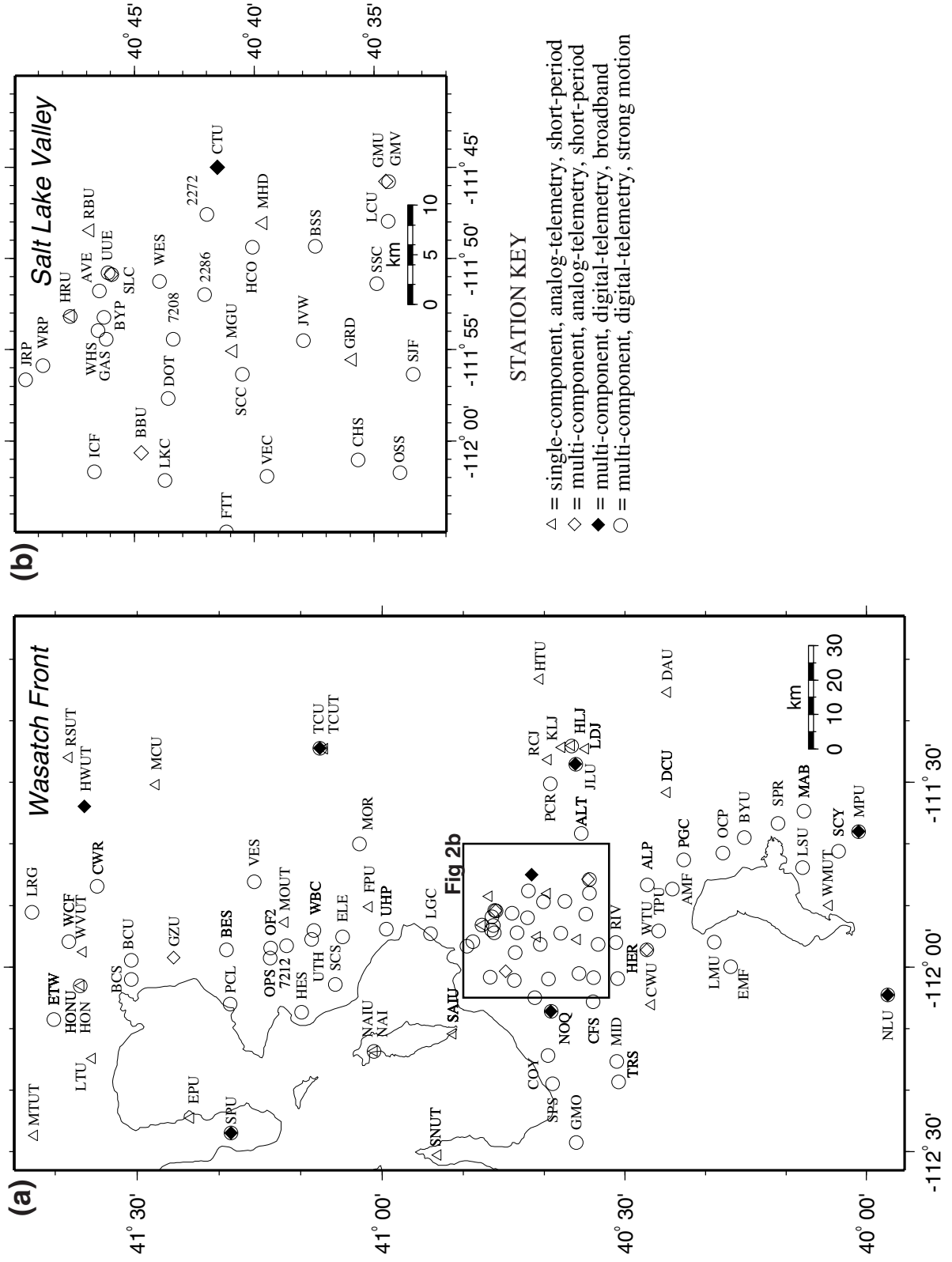


Figure 2

Seismicity of the Utah Region January 1 - December 31, 2003

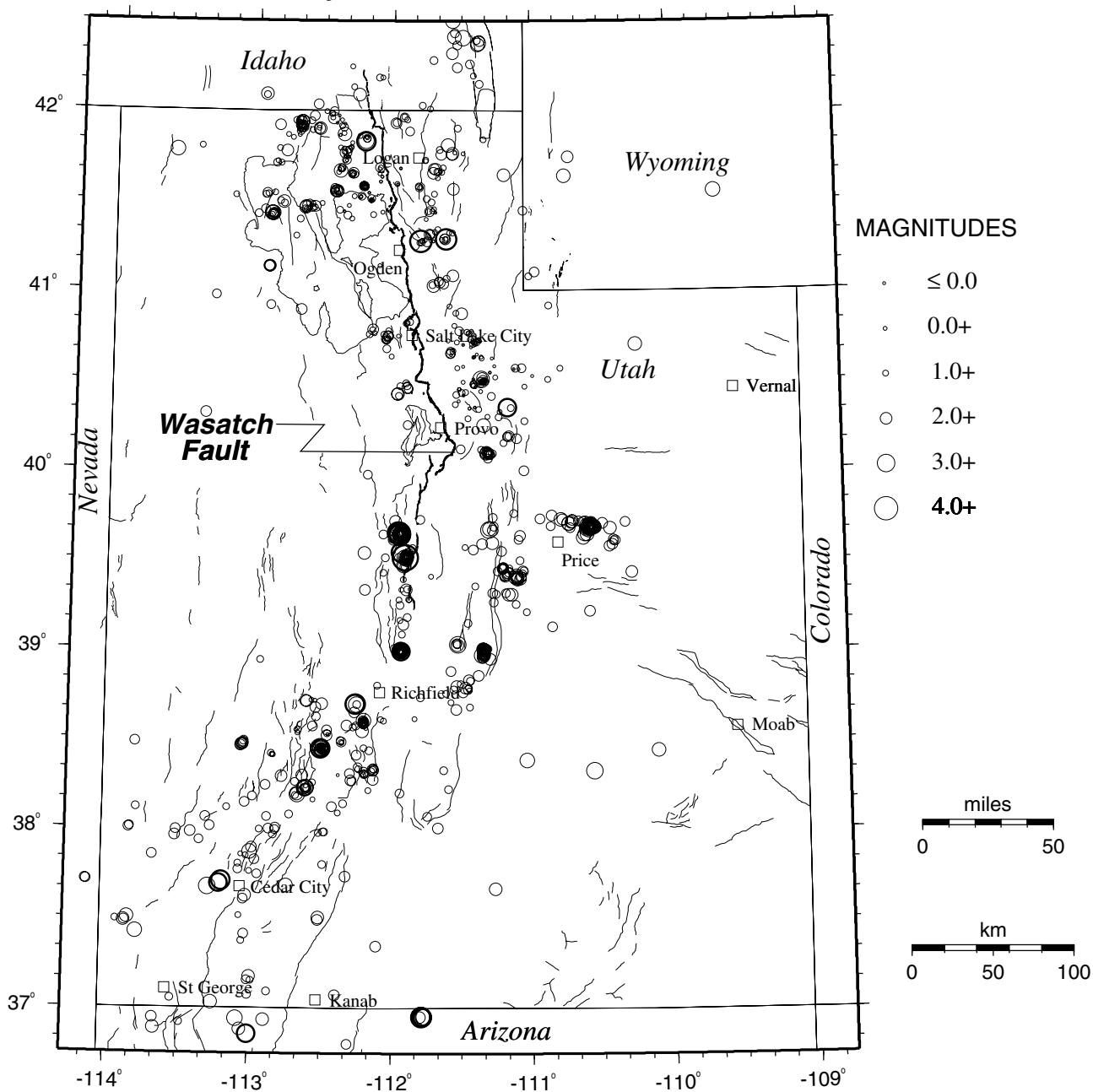


Figure 3. Earthquake epicenters (N=1,084) located by the University of Utah Seismograph Stations, superposed on a map of Quaternary (geologically young) faults compiled by the Utah Geological Survey. The Wasatch fault is shown in bold.

Earthquakes of Magnitude 3.0 and Larger January 1 - December 31, 2003

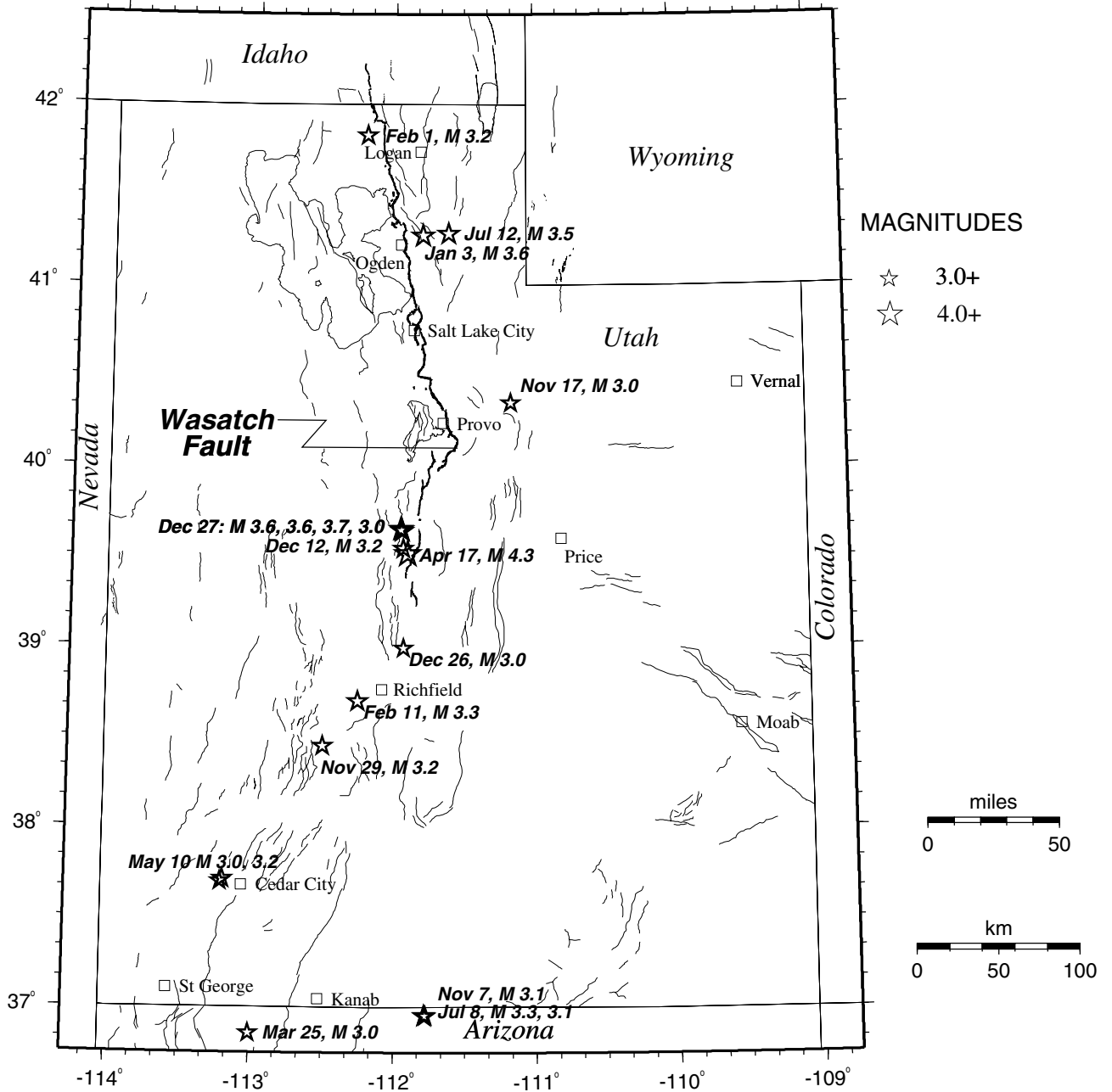


Figure 4. Epicenter map of shocks of magnitude 3.0 and larger in the Utah Region during the period January 1-December 31, 2003 (base map as in Figure 3). Epicenters, keyed to Table 1, are labeled by UTC date and size.

APPENDIX A

Station Information for University of Utah Regional/Urban Seismic Network
December 31, 2003

Table A-1

UNIVERSITY OF UTAH REGIONAL/URBAN SEISMIC NETWORK
Operating Seismograph Stations
December 31, 2003

UURSN Code	Location	SEED Station	SEED Channel	No. of Channels	Network Code	Latitude	Longitude	Elevation (meters)	Sensor	Digitizer	Telemetry	Sponsor
2272	<i>Eastwood Elementary School Salt Lake City, UT</i>	2272	HN[ZEN]	3	NP	40° 41.98'	111° 47.62'	1515	FBA23	Eina	Digital	NSMP
2286	<i>Roosevelt Elementary School Salt Lake City, UT</i>	2286	HN[ZEN]	3	NP	40° 42.08'	111° 52.01'	1314	EpiSensor	K2	Digital	NSMP
7208	<i>SR 201/I-80 Bridge Array, Salt Lake City, UT</i>	7208	EN[ZEN]	3	NP	40° 43.38'	111° 54.43'	1291	EpiSensor	K2	Digital	NSMP
7212	<i>Annex Bldg., Weber State University, Ogden, UT</i>	7212	HN[ZEN]	3	NP	41° 11.75'	111° 56.50'	1422	EpiSensor	K2	Digital	NSMP
AHI	<i>Auburn, ID</i>	AHID	BH[ZEN]	3	US	42° 45.92'	111° 06.02'	1960	*	*	Digital	USGS
ALP	<i>Alpine Fire Station, Alpine, UT</i>	ALP	EN[ZEN]	3	UU	40° 27.26'	111° 46.61'	1510	EpiSensor	K2	Digital	ANSS
ALT	<i>Alta City Offices, Alta, UT</i>	ALT	EN[ZEN]	3	UU	40° 35.42'	111° 38.25'	2635	Applied Mems	ANSS-130	Digital	ANSS
AMF	<i>Tri-Cities Golf Course American Fork, UT</i>	AMF	EN[ZEN]	3	UU	40° 24.11'	111° 47.27'	1445	EpiSensor	K2	Digital	ANSS
ANMO	<i>Albuquerque, NM</i>	ANMO	BH[ZEN]	3	IU	39° 56.77'	106° 27.40'	1740	*	*	Digital	USGS
ARUT	<i>Antelope Range, UT</i>	ARUT	EHZ	1	UU	37° 47.28'	113° 26.42'	1646	L4C	Masscomp	Analog	Utah
AVE	<i>Avenues, Salt Lake City, UT</i>	AVE	EN[ZEN]	3	UU	40° 46.47'	111° 51.83'	1387	Applied Mems	ANSS-130	Digital	ANSS
BBU	<i>Bumble Bee, Salt Lake City, UT</i>	BBU	EH[ZEN]	3	UU	40° 44.73'	112° 00.67'	1291	L4C	Masscomp	Analog	USGS
BCE	<i>Book Cliffs East, UT</i>	BCE	EHZ EN[ZEN]	4	UU	39° 36.79'	110° 24.51'	2666	L4C EpiSensor	K2	Digital	ANSS
BCS	<i>Brigham City Maintenance Shop Brigham City, UT</i>	BCS	EN[ZEN]	3	UU	41° 30.71'	112° 01.98'	1303	EpiSensor	K2	Digital	ANSS
BCU	<i>Brigham City, UT</i>	BCU	EN[ZEN]	3	UU	41° 30.74'	111° 58.93'	1676	EpiSensor	K2	Digital	ANSS
BCW	<i>Book Cliffs West, UT</i>	BCW	EHZ EN[ZEN]	4	UU	39° 43.82'	110° 44.55'	2614	L4C EpiSensor	K2	Digital	ANSS
BEI	<i>Bear River Range, ID</i>	BEI	EHZ	1	UU	42° 07.00'	111° 46.94'	1859	L4C	Masscomp	Analog	USGS
BES	<i>Bates Elementary School Ogden, UT</i>	BES	EN[ZEN]	3	UU	41° 19.10'	111° 57.26'	1455	EpiSensor	K2	Digital	ANSS

UURSN Code	Location	SEED Station	SEED Channel	No. of Channels	Network Code	Latitude	Longitude	Elevation (meters)	Sensor	Digitizer	Telemetry	Sponsor
BGMT	Barton Gulch, MT	BGMT	EHZ	1	MB	45° 14.00'	112° 02.43'	2172	*	*	Analog	MBMT
BGU	Big Grassy Mountain, UT	BGU	EN[ZEN] HH[ZEN]	3 3	UU	40° 55.53'	113° 01.79'	1640	EpiSensor 3ESP	72A-08	Digital	ANSS
BHU	Blowhard Mountain, UT	BHU	EH[ZEN]	3	UU	37° 35.55'	112° 51.42'	3230	S13	Masscomp	Analog	Utah
BMN	Battle Mountain, NM	BMN	BHZ	1	NN	40° 25.89'	117° 13.31'	1594	*	*	Digital	UNR
BMUT	Black Mountain, UT	BMUT	EHZ	1	UU	41° 57.49'	111° 14.05'	2243	S13	Masscomp	Analog	USGS
BON	Boundary Peak, NV	BONR	SHZ	1	NN	37° 57.31'	118° 18.10'	2582	*	*	Digital	UNR
BOZ	Bozeman, MT	BOZ	BH[ZEN]	3	US	45° 38.82'	111° 37.78'	1589	*	*	Digital	USGS
BSS	Butlerville Substation Salt Lake City, UT	BSS	EN[ZEN]	3	UU	40° 37.45'	111° 49.37'	1411	EpiSensor	K2	Digital	ANSS
BTU	Barney Top, UT	BTU	EHZ	1	UU	37° 45.34'	111° 52.46'	3235	S13	Masscomp	Analog	Utah
BW0	Boulder, WY	BW06	BH[ZEN]	3	US	42° 46.00'	109° 33.50'	2224	*	*	Digital	USGS
BYP	Brigham Young Park Salt Lake City, UT	BYP	EN[ZEN]	3	UU	40° 46.26'	111° 53.23'	1323	Applied Mems	ANSS-130	Digital	ANSS
BYU	Brigham Young University Provo, UT	BYU	EN[ZEN]	3	UU	40° 15.17'	111° 38.97'	1421	EpiSensor	K2	Digital	ANSS
BZMT	Bozeman Pass, MT	BZMT	EHZ	1	MB	45° 38.89'	110° 47.80'	1905	*	*	Analog	MBMT
CFS	Copperton Fire Station Copperton, UT	CFS	EN[ZEN]	3	UU	40° 33.96'	112° 05.61'	1654	EpiSensor	K2	Digital	ANSS
CHS	Copper Hills High School, West Jordan, UT	CHS	EN[ZEN]	3	UU	40° 35.68'	112° 01.03'	1460	Applied Mems	ANSS-130	Digital	ANSS
COM	Craters of the Moon, ID	COMI	EHZ	1	IE	43° 27.72'	113° 35.64'	1890	*	*	Digital	INEEL
COY	Coyote Canyon, Tooele Valley, UT	COY	EN[ZEN]	3	UU	40° 39.56'	112° 14.34'	1572	Applied Mems	ANSS-130	Digital	ANSS
CTU	Camp Tracy, UT	CTU	HH[ZEN]	3	UU	40° 41.55'	111° 45.02'	1731	40T	72A-07	Digital	USGS
CWR	Coldwater Ranch, Paradise, UT	CWR	EN[ZEN]	3	UU	41° 34.90'	111° 46.89'	1837	Applied Mems	ANSS-130	Digital	ANSS
CWU	Camp Williams, UT	CWU	EHZ	1	UU	40° 26.75'	112° 06.13'	1945	L4C	Masscomp	Analog	USGS
DAU	Daniels Canyon, UT	DAU	EHZ	1	UU	40° 24.75'	111° 15.35'	2771	S13	Masscomp	Analog	USGS
DBD	Des Bee Dove, UT	DBD	EHZ	1	UU	39° 18.82'	111° 05.55'	2265	L4C	Masscomp	Analog	Utah
DCM	Dugout Coal Mine, UT	DCM	EHZ EN[ZEN]	1 3	UU	39° 41.70'	110° 35.00'	2537	L4C EpiSensor	K2	Digital	Utah
DCU	Deer Creek Reservoir, UT	DCU	EHZ	1	UU	40° 24.82'	111° 31.61'	1829	L4C	Masscomp	Analog	USGS

UURSN Code	Location	SEED Station	SEED Channel	No. of Channels	Network Code	Latitude	Longitude	Elevation (meters)	Sensor	Digitizer	Telemetry	Sponsor
DOT	Utah Dept. of Transportation Region II Offices, Salt Lake City, UT	DOT	EN[ZEN]	3	UU	40° 43.61'	111° 57.65'	1282	Applied Mens	ANSS-130	Digital	ANSS
DUG	Dugway, UT	DUG	BH[ZEN] EH[ZEN] EL[ZEN]	3 6	US UU	40° 11.70'	112° 48.80'	1477	*	*	Digital	USGS
DWU	Dry Willow, UT	DWU	EHZ	1	UU	38° 06.32'	112° 59.85'	2270	S13	Masscomp	Analog	Utah, USGS
ECR	Eagle Creek, ID	ECRI	EHZ	1	IE	43° 03.24'	111° 22.26'	2086	*	Masscomp	Analog	Utah
EKU	East Kanab, UT	EKU	EHZ	1	UU	37° 04.48'	112° 29.81'	1829	S13	Masscomp	Analog	Utah
ELE	East Layton Elementary School, East Layton, UT	ELE	EN[ZEN]	3	UU	41° 04.84'	111° 55.09'	1444	Applied Mens	ANSS-130	Digital	ANSS
ELK	Elko, NV	ELK	BH[ZEN]	3	US	40° 44.69'	115° 14.33'	2210	*	*	Digital	USGS
ELU	Electric Lake, UT	ELU	EHZ	1	UU	39° 38.41'	111° 12.23'	2970	L4C	Masscomp	Analog	Utah
EMF	Eagle Mountain Gas Tap, UT	EMF	EN[ZEN]	3	UU	40° 16.89'	111° 59.92'	1487	Applied Mens	ANSS-130	Digital	ANSS
EMU	Emma Park, UT	EMU	EH[ZEN] ELZ	4	UU	39° 48.84'	110° 48.92'	2268	S13	Masscomp	Analog	USGS
EPU	East Promontory, UT	EPU	EN[ZEN]	3	UU	41° 23.49'	112° 24.53'	1436	FBA23	K2	None	Utah
ETW	Elwood Town Hall, Elwood, UT	ETW	EHZ	1	UU	41° 40.15'	112° 08.53'	1305	L4C	Masscomp	Analog	USGS
FLU	Fool's Peak, UT	FLU	EN[ZEN]	3	UU	41° 40.15'	112° 08.53'	1305	Applied Mens	ANSS-130	Digital	ANSS
FPU	Francis Peak, UT	FPU	EHZ	1	UU	39° 22.69'	112° 10.29'	1951	18300	Masscomp	Analog	USGS
FSU	Fish Springs, UT	FSU	EHZ	1	UU	41° 01.58'	111° 50.21'	2816	L4C	Masscomp	Analog	USGS
FTT	Fire Training Tower, Magna, UT	FTT	EHZ	1	UU	39° 43.35'	113° 23.48'	1487	18300	Masscomp	Analog	Utah
GAS	PacifiCorp Gasification Plant, Salt Lake City, UT	GAS	EN[ZEN]	3	UU	40° 41.16'	112° 04.99'	1381	Applied Mens	ANSS-130	Digital	ANSS
GBI	Big Grassy Butte, ID	GBI	EHZ	1	IE	40° 46.18'	111° 54.41'	1294	Applied Mens	ANSS-130	Digital	ANSS
GCN	Grand Canyon, AZ	GCN	EHZ	1	AR	43° 59.22'	112° 03.78'	1541	*	*	Digital	INEEL
GMO	Grantsville Maintenance Office, Grantsville, UT	GMO	EHZ	1	UU	36° 02.64'	112° 07.68'	2294	*	*	Analog	NAU
GMU	Granite Mountain, UT	GMU	EN[ZEN] ELZ	3 4	UU	40° 36.04'	112° 28.48'	1320	Applied Mens	ANSS-130	Digital	ANSS
GMV	Granite Mountain Vault Sandy, UT	GMV	EHZ	1	UU	40° 34.53'	111° 45.79'	1829	S13	Masscomp	Analog	USGS
GRD	Gardner Farm, UT	GRD	EN[ZEN]	3	UU	40° 34.40'	111° 45.79'	1829	EpiSensor	K2	Digital	ANSS
GRD	Gardner Farm, UT	GRD	EHZ	1	UU	40° 35.93'	111° 55.47'	1323	Ranger	Masscomp	Analog	USGS

UURSN Code	Location	SEED Station	SEED Channel	No. of Channels	Network Code	Latitude	Longitude	Elevation (meters)	Sensor	Digitizer	Telemetry	Sponsor
GRR	Grays Lake, ID	GRR1	EHZ	1	IE	42° 56.28'	111° 25.32'	2207	*	*	Digital	INEEL
GZU	Grizzly Peak, UT	GZU	EH[ZEN] ELZ	4	UU	41° 25.53'	111° 58.50'	2646	S13	Masscomp	Analog	USGS
HCO	Holladay City Offices Holladay, UT	HCO	EN[ZEN]	3	UU	40° 40.07'	111° 49.38'	1362	EpiSensor	K2	Digital	ANSS
HDU	Hyde Park, UT	HDU	EHZ	1	UU	41° 48.18'	111° 45.99'	1807	L4C	Masscomp	Analog	USGS
HER	Herriman Fire Station Herriman, UT	HER	EN[ZEN]	3	UU	40° 30.94'	112° 01.85'	1502	EpiSensor	K2	Digital	ANSS
HES	Hooper Elementary School Hooper, UT	HES	EN[ZEN]	3	UU	41° 09.89'	112° 07.30'	1292	EpiSensor	K2	Digital	ANSS
HHA	Hell's Half Acre, ID	HHAI	EHZ	1	IE	43° 17.70'	112° 22.74'	1371	*	*	Digital	INEEL
HLI	Hailey, ID	HLID	BH[ZEN]	3	US	43° 33.75'	114° 24.83'	1772	*	*	Digital	USGS
HLJ	Hailstone, UT	HLJ	EHZ EN[ZEN]	1 3	UU	40° 36.64'	111° 24.05'	1931	S13 FBA23	Masscomp K2	Analog None	Utah
HON	Honeyville, UT	HON	EN[ZEN]	3	UU	41° 36.97'	112° 03.05'	1528	Applied Mems	ANSS-130	Digital	ANSS
HONU		HONU	EHZ	1					L4C	Masscomp	Analog	USGS
HRU	Hogsback Ridge, UT	HRU	EHZ EN[ZEN]	1 3	UU	40° 47.67'	111° 53.14'	1620	Ranger Applied Mems	Masscomp ANSS-130	Analog Digital	USGS ANSS
HTU	Hoyt, UT	HTU	EHZ	1	UU	40° 40.52'	111° 13.21'	2576	L4C	Masscomp	Analog	USGS
HVU	Hansel Valley, UT	HVU	HH[ZEN]	3	UU	41° 46.78'	112° 46.50'	1609	40T	72A-07	Digital	USGS
HWU	Hardware Ranch, UT	HWUT	BH[ZEN]	3	US	41° 36.41'	111° 33.91'	1830	*	*	Digital	USGS
ICF	International Center Fire Station, Salt Lake City, UT	ICF	EN[ZEN]	3	UU	40° 46.69'	112° 01.72'	1281	EpiSensor	K2	Digital	ANSS
ICU	Indian Springs Canyon, UT	ICU	EHZ	1	UU	37° 08.98'	113° 55.41'	1451	S13	Masscomp	Analog	Utah
IMU	Iron Mountain, UT	IMU	EHZ	1	UU	38° 37.99'	113° 09.50'	1833	L4C	Masscomp	Analog	Utah
IMW	Indian Meadows, WY	IMW	EHZ	1	RC	43° 53.82'	110° 56.34'	2646	*	*	Analog	BYU-I
JLU	Jordanelle, UT	JLU	EN[ZEN] HH[ZEN]	3 3	UU	40° 36.12'	111° 27.00'	2285	EpiSensor 3ESP	72A-08	Digital	ANSS
JRP	Jordan River State Park Salt Lake City, UT	JRP	EN[ZEN]	3	UU	40° 49.54'	111° 56.66'	1284	EpiSensor	K2	Digital	ANSS
JVW	Jordan Valley Water District Well, Murray, UT	JVW	EN[ZEN]	3	UU	40° 37.95'	111° 54.46'	1315	Applied Mems	ANSS-130	Digital	ANSS
KLJ	Keetley, UT	KLJ	EHZ	1	UU	40° 37.85'	111° 24.30'	1992	S13	Masscomp	Analog	Utah
KNB	Kanab, UT	KNB	BH[ZEN]	3	US	37° 01.00'	112° 49.34'	1715	*	*	Digital	LLNL
LCU	Little Cottonwood, UT	LCU	EN[ZEN]	3	UU	40° 34.41'	111° 47.91'	1571	Applied	ANSS-130	Digital	ANSS

UURSN Code	Location	SEED Station	SEED Channel	No. of Channels	Network Code	Latitude	Longitude	Elevation (meters)	Sensor		Digitizer	Telemetry	Sponsor
										Mems			
LDJ	Lady, UT	LDJ	EZH	1	UU	40° 34.89'	111° 24.52'	2217	S13	Masscomp	Analog	Utah	
LEVU	Levan, UT	LEVU	EZH	1	UU	39° 30.39'	111° 48.88'	1996	L4C	Masscomp	Analog	USGS	
LGC	Lakeside Golf Course Bountiful, UT	LGC	EN[ZEN]	3	UU	40° 54.04'	111° 54.51'	1292	EpiSensor	K2	Digital	ANSS	
LKC	Lee Kay Hunter Education Center Magna, UT	LKC	EN[ZEN]	3	UU	40° 43.62'	112° 02.14'	1289	EpiSensor	K2	Digital	ANSS	
LKW	Lake, WY	LKWY	BH[ZEN]	3	US	44° 33.91'	110° 24.00'	2424	*	*	Digital	USGS	
LMU	Lake Mountain, UT	LMU	EN[ZEN]	3	UU	40° 18.91'	111° 55.92'	1593	EpiSensor	K2	Digital	ANSS	
LRG	Logan River Golf Course	LRG	EN[ZEN]	3	UU	41° 42.82'	111° 51.08'	1362	Applied Mems	ANSS-130	Digital	ANSS	
LsU	Lake Shores, UT	LsU	EN[ZEN]	3	UU	40° 07.94'	111° 43.80'	1375	EpiSensor	K2	Digital	ANSS	
LTU	Little Mountain, UT	LTU	EZH	1	UU	41° 35.51'	112° 14.83'	1585	L4C	Masscomp	Analog	USGS	
MAB	Mapleton Ambulance Building Mapleton, UT	MAB	EN[ZEN]	3	UU	40° 07.85'	111° 34.67'	1440	EpiSensor	K2	Digital	ANSS	
MCID	Moose Creek, ID	MCID	EZH	1	WY	44° 11.45'	111° 11.03'	2137	L4C	Masscomp	Analog	USGS	
MCU	Monte Cristo Peak, UT	MCU	EZH	1	UU	41° 27.70'	111° 30.45'	2664	18300	Masscomp	Analog	USGS	
MGU	Meadow Brook Golf Course Salt Lake City, UT	MGU	EZH	1	UU	40° 40.89'	111° 55.09'	1291	Ranger	Masscomp	Analog	USGS	
MHD	Mile High Drive, UT	MHD	EZH	1	UU	40° 39.64'	111° 48.05'	1597	Ranger	Masscomp	Analog	USGS	
MID	Middle Canyon, UT	MID	EN[ZEN]	3	UU	40° 31.04'	112° 15.28'	1722	Applied Mems	ANSS-130	Digital	ANSS	
MLI	Malad Range, ID	MLI	EZH	1	UU	42° 01.61'	112° 07.53'	1896	L4C	Masscomp	Analog	USGS	
MMU	Miners Mountain, UT	MMU	EZH	1	UU	38° 11.57'	111° 17.66'	2387	S13	Masscomp	Analog	Utah	
MOMT	Montida, MT	MOMT	EZH	1	MB	44° 35.60'	112° 23.66'	2220	*	*	Analog	MBMT	
MOR	Morgan, UT	MOR	EN[ZEN]	3	UU	41° 02.77'	111° 39.94'	1633	Applied Mems	ANSS-130	None	ANSS	
MOUT	Mount Ogdan, UT	MOUT	EZH	1	UU	41° 11.94'	111° 52.73'	2743	S13	Masscomp	Analog	USGS	
MPU	Maple Canyon, UT	MPU	EN[ZEN]	3	UU	40° 00.93'	111° 38.00'	1909	EpiSensor	K2	Digital	ANSS	
MSU	Marysvale, UT	MSU	HH[ZEN]	3	UU	38° 30.74'	112° 10.63'	2105	40T	72A-07	Digital	USGS	
MTLO	Mt. Logan, AZ	MTL	EZH	1	AR	36° 21.18'	113° 11.94'	2418	18300	Masscomp	Analog	Utah	
MTUT	Morton Thiokol, UT	MTUT	EZH	1	UU	41° 42.55'	112° 27.28'	1373	*	*	Analog	NAU	
MVU	Marysvale, UT	MVU	BH[ZEN]	3	LB	38° 30.22'	112° 12.74'	2240	L4C	Masscomp	Analog	USGS	
NAI	North Antelope Island, UT	NAI	EN[ZEN]	3	UU	41° 00.97'	112° 13.68'	1472	*	*	Digital	Sandia	
NAIU		NAIU	EZH	1	UU				EpiSensor L4C	K2	Digital	ANSS	

UURSN Code	Location	SEED Station	SEED Channel	No. of Channels	Network Code	Latitude	Longitude	Elevation (meters)	Sensor	Digitizer	Telemetry	Sponsor
NLU	North Lily Mine, UT	NLU	EN[ZEN] HH[ZEN]	3 3	UU	39° 57.29'	112° 04.50'	2036	Episensor 3ESP	72A-08	Digital	ANSS
NMU	North Mineral Mountain, UT	NMU	EH[ZEN] ELZ	4	UU	38° 30.99'	112° 51.00'	1853	S13	Masscomp	Analog	Utah
NOQ	North Oquirrh Mountains, UT	NOQ	EN[ZEN] HH[ZEN]	3 3	UU	40° 39.17'	112° 07.13'	1622	EpiSensor 40T	K2 72A-07	Digital Digital	ANSS USGS
NPI	North Pocatello, ID	NPI	EHZ	1	UU	42° 08.84'	112° 31.10'	1640	L4C	Masscomp	Analog	USGS
OCF	Orem City Park, Orem, UT	OCF	EN[ZEN]	3	UU	40° 17.87'	111° 41.44'	1464	EpiSensor	K2	Digital	ANSS
OF2	Ogden Fire Station #2 Ogden, UT	OF2	EN[ZEN]	3	UU	41° 13.70'	111° 56.92'	1358	EpiSensor	K2	Digital	ANSS
OPS	Ogden Public Safety Building, Ogden, UT	OPS	EN[ZEN]	3	UU	41° 13.72'	111° 58.54'	1317	Applied Mems	ANSS-130	None	ANSS
OSS	Oquirrh Sub Station, UT	OSS	EN[ZEN]	3	UU	40° 33.77'	112° 01.61'	1503	Applied Mems	ANSS-130	Digital	ANSS
OWUT	Old Woman Plateau, UT	OWUT	EHZ	1	UU	38° 46.80'	111° 25.42'	2568	L4C	Masscomp	Analog	Utah
P03	Wild Steer, Paradox Basin, CO	PV03	EHZ	1	RE	38° 15.26'	108° 50.88'	1975	*	*	Analog	USBR
P15	Potato Mountain Paradox Basin, CO	PV15	EHZ	1	RE	38° 20.51'	108° 28.86'	2280	*	*	Analog	USBR
PCL	Plain City Landfill Plain City, UT	PCL	EN[ZEN]	3	UU	41° 18.60'	112° 06.00'	1290	Applied Mems	ANSS-130	Digital	ANSS
PCR	Park City Recreation Center Park City, UT	PCR	EN[ZEN]	3	UU	40° 39.25'	111° 30.19'	2100	EpiSensor	K2	Digital	ANSS
PGAZ	Page, AZ	PGA	EHZ	1	AR	36° 54.34'	111° 16.86'	1272	*	*	Analog	NAU
PGC	Pleasant Grove Creek, UT	PGC	EN[ZEN]	3	UU	40° 22.71'	111° 42.62'	1707	EpiSensor	K2	Digital	ANSS
PRN	Pahroc, Range, NV	PRN	SHZ	1	NN	37° 24.40'	115° 03.05'	1402	*	*	Digital	UNR
PTI	Pocatello, ID	PTI	EHZ	1	IE	42° 52.20'	112° 22.21'	1670	*	*	Digital	INEEL
PTU	Portage, UT	PTU	EHZ	1	UU	41° 55.76'	112° 19.48'	2192	L4C	Masscomp	Analog	USGS
QLMT	Earthquake Lake, MT	QLMT	EHZ	1	MB	44° 49.84'	111° 25.80'	2064	*	*	Analog	MBMT
RBU	Red Butte Canyon, UT	RBU	EHZ	1	UU	40° 46.85'	111° 48.50'	1676	L4C	Masscomp	Analog	USGS
RCJ	Ross Creek, UT	RCJ	EHZ	1	UU	40° 39.51'	111° 26.36'	2090	S13	Masscomp	Analog	Utah
RIV	Public Works Building Riverton, UT	RIV	EN[ZEN]	3	UU	40° 31.16'	111° 56.05'	1347	EpiSensor	K2	Digital	ANSS
RSUT	Red Spur, UT	RSUT	EHZ	1	UU	41° 38.31'	111° 25.90'	2682	S13	Masscomp	Analog	USGS
SAIU	South Antelope Island, UT	SAIU	EHZ	1	UU	40° 51.29'	112° 10.89'	1384	L4C	Masscomp	Analog	USGS
SCC	Salt Lake Community College Salt Lake City, UT	SCC	EN[ZEN]	3	UU	40° 40.49'	111° 56.37'	1306	EpiSensor	K2	Digital	ANSS

UURSN Code	Location	SEED Station	SEED Channel	No. of Channels	Network Code	Latitude	Longitude	Elevation (meters)	Sensor	Digitizer	Telemetry	Sponsor
SCS	Syracuse City Cemetery Shop Syracuse, UT	SCS	EN[ZEN]	3	UU	41° 05.73'	112° 02.81'	1321	EpiSensor	K2	Digital	ANSS
SCY	Salem City Yard, Salem, UT	SCY	EN[ZEN]	3	UU	40° 03.47'	111° 41.14'	1386	Applied Mems	ANSS-130	Digital	ANSS
SGU	Sterling, UT	SGU	EHZ	1	UU	39° 10.94'	111° 38.68'	2357	18300	Masscomp	Analog	USGS
SHP	Sheep Range, NV	SHP	EHZ	1	NN	36° 30.33'	115° 09.61'	1590	*	*	Digital	UNR
SJF	South Jordan Fire Station, South Jordan, UT	SJF	EN[ZEN]	3	UU	40° 33.37'	111° 56.34'	1356	Applied Mems	ANSS-130	Digital	ANSS
SLC	University of Utah WBB Bldg Salt Lake City, UT	SLC	EL[EN] EN[ZEN]	2 3	UU	40° 45.97'	111° 50.86'	1436	WA Sim FBA23	Masscomp Masscomp	Hardwired	USGS
SNO	Snow College, UT	SNO	EHZ	1	UU	39° 19.18'	111° 32.33'	2503	Ranger	Masscomp	Analog	Utah
SNUT	Stanbury North, UT	SNUT	EHZ	1	UU	40° 53.10'	112° 30.52'	1652	18300	Masscomp	Analog	USGS
SPR	Wildlife Resource Center Springville, UT	SPR	EN[ZEN]	3	UU	40° 10.94'	111° 36.71'	1379	EpiSensor	K2	Digital	ANSS
SPS	Stansbury Park Sewage Lagoon Stansbury Park, UT	SPS	EN[ZEN]	3	UU	40° 38.97'	112° 18.95'	1293	Applied Mems	ANSS-130	Digital	ANSS
SPU	South Promontory Point, UT	SPU	EN[ZEN] HH[ZEN]	3 3	UU	41° 18.52'	112° 26.95'	2086	EpiSensor 3ESP	72A-08	Digital	ANSS
SRU	San Rafael Swell, UT	SRU	EHZ HH[ZEN] EN[ZEN]	1 6	UU	39° 06.65'	110° 31.43'	1804	S13 3T EpiSensor	Masscomp 72A-08	Analog Digital	Utah
SSC	Sandy Senior Center Sandy, UT	SSC	EN[ZEN]	3	UU	40° 34.89'	111° 51.35'	1414	EpiSensor	K2	Digital	ANSS
SUU	Santaquin Canyon, UT	SUU	EHZ	1	UU	39° 53.29'	111° 47.45'	2024	18300	Masscomp	Analog	USGS
TCU	Toone Canyon, UT	TCU	EN[ZEN] HH[ZEN]	3 3	UU	41° 07.04'	111° 24.47'	2269	EpiSensor 3ESP	72A-08	Digital	ANSS
TCUT	Toone Canyon, UT	TCUT	EHZ	1	UU	41° 07.07'	111° 24.51'	2320	L4C	Masscomp	Analog	USGS
TMI	Taylor Mountain, ID	TMI	EHZ	1	IE	43° 18.30'	111° 55.08'	2179	*	*	Digital	INEEL
TMU	Trail Mountain, UT	TMU	HH[ZEN]	3	UU	39° 17.79'	111° 12.49'	2731	40T	72A-08	Digital	Utah
TM2		TM2	EH[ZEN]	3	UU				S13			
TPMT	Tepee Creek, MT	TPMT	EHZ	1	MB	44° 43.79'	111° 39.94'	2518	*	*	Analog	MBMT
TPNV	Topopah Spring, NV	TPNV	BH[ZEN]	3	US	36° 56.93'	116° 14.97'	1600	*	*	Digital	USGS
TPU	Thanksgiving Point, Lehi, UT	TPU	EN[ZEN]	3	UU	40° 25.81'	111° 54.13'	1383	EpiSensor	K2	Digital	ANSS
TRC	Troy Canyon, NV	TRC	BHZ	1	NN	38° 20.98'	115° 35.11'	1815	*	*	Digital	UNR
TRS	Tooele County Radio Shop, Tooele, UT	TRS	EN[ZEN]	3	UU	40° 30.83'	112° 18.63'	1568	EpiSensor	K2	Digital	ANSS

UURSN Code	Location	SEED Station	SEED Channel	No. of Channels	Network Code	Latitude	Longitude	Elevation (meters)	Sensor	Digitizer	Telemetry	Sponsor
TUC	Tucson, AZ	TUC	BH[ZEN]	3	US	32° 18.58'	110° 47.05'	906	*	*	Digital	USGS
UHP	Utah Highway Patrol Farmington, UT	UHP	EN[ZEN]	3	UU	40° 59.47'	111° 53.88'	1295	EpiSensor	K2	Digital	ANSS
UTH	Uintah Town Hall, Uintah, UT	UTH	EN[ZEN]	3	UU	41° 08.65'	111° 55.52'	1389	EpiSensor	K2	Digital	ANSS
UUE	University of Utah EMCB Bldg. Salt Lake City, UT	UUE	EN[ZEN]	3	UU	40° 46.09'	111° 50.77'	1449	EpiSensor	K2	Digital	ANSS
VEC	Valley Emergency Communications Center West Valley City, UT	VEC	EN[ZEN]	3	UU	40° 39.21'	112° 01.95'	1480	EpiSensor	K2	Digital	ANSS
VES	Valley Elementary School, Huntsville, UT	VES	EN[ZEN]	3	UU	41° 15.72'	111° 46.20'	1501	Applied Mens	ANSS-130	Digital	ANSS
WBC	Weber Canyon, UT	WBC	EN[ZEN]	3	UU	41° 08.38'	111° 54.05'	1602	EpiSensor	K2	Digital	ANSS
WCF	Wellsville Fire Station, Wellsville, UT	WCF	EN[ZEN]	3	UU	41° 38.37'	111° 55.94'	1387	Applied Mens	ANSS-130	Digital	ANSS
WCN	Washoe, NV	WCN	HHZ	1	NN	39° 18.10'	119° 45.38'	1500	*	*	Digital	UNR
WCU	Willow Creek, UT	WCU	EHZ	1	UU	38° 57.88'	112° 05.44'	2673	18300	Masscomp	Analog	USGS
WES	Westminster College Salt Lake City, UT	WES	EN[ZEN]	3	UU	40° 43.97'	111° 51.26'	1341	EpiSensor	K2	Digital	ANSS
WHS	West High School	WHS	EN[ZEN]	3	UU	40° 46.51'	111° 53.93'	1301	EpiSensor	K2	Digital	ANSS
WMUT	West Mountain, UT	WMUT	EHZ	1	UU	40° 04.60'	111° 50.00'	1981	L4C	Masscomp	Analog	USGS
WRP	Water Reclamation Plant Salt Lake City, UT	WRP	EN[ZEN]	3	UU	40° 48.82'	111° 55.87'	1286	Applied Mens	ANSS-130	Digital	ANSS
WTU	Western Traverse Mountains, UT	WTU	EH[ZEN] ELZ EN[ZEN]	4 3	UU	40° 27.29'	111° 57.21'	1552	S13 Applied Mens	Masscomp ANSS-130	Analog Digital	USGS ANSS
WUAZ	Wupatki, AZ	WUAZ	BH[ZEN]	3	US	35° 31.01'	111° 22.43'	1592	*	*	Digital	USGS
WVUT	Wellsville, UT	WVUT	EHZ	1	UU	41° 36.61'	111° 57.55'	1828	L4C	Masscomp	Analog	USGS
YCJ	Canyon Junction (YNP), WY	YCJ	EHZ	1	WY	44° 44.48'	110° 29.83'	2426	L4C	Masscomp	Analog	USGS
YDC	Denny Creek, MT	YDC	EHZ	1	WY	44° 42.51'	111° 14.60'	2025	L4C	Masscomp	Analog	USGS
YFT	Old Faithful (YNP), WY	YFT	HH[ZEN]	3	WY	44° 27.05'	110° 50.24'	2292	40T	72A-07	Digital	USGS
YGC	Graying Creek, MT	YGC	EHZ	1	WY	44° 47.77'	111° 06.45'	2075	L4C	Masscomp	Analog	USGS
YHB	Horse Butte, MT	YHB	EHZ	1	WY	44° 45.07'	111° 11.71'	2157	L4C	Masscomp	Analog	USGS
YHH	Holmes Hill (YNP), WY	YHH	EH[ZEN]	3	WY	44° 47.30'	110° 51.03'	2717	S13	Masscomp	Analog	USGS
YJC	Joseph's Coat (YNP), WY	YJC	EHZ	1	WY	44° 45.33'	110° 20.95'	2684	S13	Masscomp	Analog	USGS

UURSN Code	Location	SEED Station	SEED Channel	No. of Channels	Network Code	Latitude	Longitude	Elevation (meters)	Sensor	Digitizer	Telemetry	Sponsor
YLA	Lake Butte (YNP), WY	YLA	EHZ	1	WY	44° 30.76'	110° 16.12'	2580	L4C	Masscomp	Analog	USGS
YLT	Little Thumb Creek (YNP), WY	YLT	EHZ	1	WY	44° 26.25'	110° 35.28'	2439	L4C	Masscomp	Analog	USGS
YMC	Maple Creek (YNP), WY	YMC	EHZ	1	WY	44° 45.53'	111° 00.41'	2073	L4C	Masscomp	Analog	USGS
YML	Mary Lake (YNP), WY	YML	EHZ	1	WY	44° 36.20'	110° 38.63'	2653	L4C	Masscomp	Analog	USGS
YMP	Mirror Plateau (YNP), WY	YMP	EH[ZEN]	3	WY	44° 44.38'	110° 09.40'	2774	S13	Masscomp	Analog	USGS
YMR	Madison River (YNP), WY	YMR	HH[ZEN]	3	WY	44° 40.12'	110° 57.90'	2149	40T	72A-07	Digital	USGS
YMS	Mount Sheridan (YNP), WY	YMS	EHZ	1	WY	44° 15.84'	110° 31.67'	3106	L4C	Masscomp	Analog	USGS
YMV	Mammoth Vault (YNP), WY	YMV	EHZ	1	WY	44° 58.42'	110° 41.33'	1829	L4C	Masscomp	Analog	USGS
YNR	Norris Junction (YNP), WY	YNR	HH[ZEN]	3	WY	44° 42.93'	110° 40.75'	2336	40T	RT-130	Digital	USGS
YPC	Pelican Cone (YNP), WY	YPC	EHZ	1	WY	44° 38.88'	110° 11.55'	2932	L4C	Masscomp	Analog	USGS
YPM	Purple Mountain (YNP), WY	YPM	EHZ	1	WY	44° 39.43'	110° 52.12'	2582	L4C	Masscomp	Analog	USGS
YPP	Pitchstone Plateau (YNP), WY	YPP	EHZ	1	WY	44° 16.26'	110° 48.27'	2707	S13	Masscomp	Analog	USGS
YSB	Soda Butte (YNP), WY	YSB	EHZ	1	WY	44° 53.04'	110° 09.06'	2072	L4C	Masscomp	Analog	USGS
YTP	The Promontory (YNP), WY	YTP	EHZ	1	WY	44° 23.51'	110° 17.10'	2384	L4	Masscomp	Analog	USGS
YWB	West Boundary (YNP), WY	YWB	EHZ	1	WY	44° 36.35'	111° 06.05'	2310	L4C	Masscomp	Analog	USGS

* Indicates station operated by another agency and recorded as part of University of Utah regional seismic network

Network Statistics: 482 data channels from 202 stations were being recorded at the end of this report period

EXPLANATION OF TABLE

UURSN Code: Station code used in routine processing. Due to processing software limitations, the station code may not be the station code used by the original operator. For multi-component stations, the vertical, east-west, and north-south high gain (low gain) components are identified by an appended Z(V), E(L), and N(M), respectively.

Location: General description of station location. YNP = Yellowstone National Park.

SEED Station: The SEED (Standard for the Exchange of Earthquake Data) station code used by the original operator.

SEED Channel: The SEED format uses three letters to name seismic channels. See <<http://www.iris.washington.edu/manuals/SEED_appA.html>> for information about the SEED channel naming convention. Relevant sections are reproduced below. In the SEED convention, each letter describes one aspect of the instrumentation and its digitization. The first letter specifies the general sampling rate and the response band of the instrument. Band codes used in this table include:

Band Code	Band Type	Sample Rate	Corner Period
E	Extremely short period	= 80 Hertz	< 10 seconds
H	High broadband	= 80 Hertz	= 10 seconds
B	Broadband	= 10 to < 80 Hertz	=10 seconds
S	Short period	= 10 to < 80 Hertz	< 10 seconds

The second letter specifies the family to which the sensor belongs. Sensor families used in this table are:

Instrument Code	Description
H	High gain seismometer
L	Low gain seismometer
N	Accelerometer

The third letter specifies the physical configuration of the members of a multiple axis instrument package. Channel orientations used in this table are:

Z E N Traditional (Vertical, East-West, North-South)

Number of Channels: Total number of waveform channels recorded.

Network Code: The FDSN (Federation of Digital Seismographic Networks) registered network code. See <<<http://www.iris.washington.edu/FDSN/networks.txt>>> for information about registered seismograph network codes. Network codes referenced in this table:

Network Code	Network name; Network operator or responsible organization
AR	Northern Arizona Seismic Network, Northern Arizona University
LB	Leo Brady Network; Sandia National Laboratory
IE	Idaho National Engineering and Environmental Laboratory

IU	IRIS/USGS Network; USGS Albuquerque Seismological Laboratory
MB	Montana Regional Seismic Network; Montana Bureau of Mines and Geology
NN	Western Great Basin; University of Nevada, Reno
NP	National Strong Motion Program; U.S. Geological Survey
RC	Formerly Ricks College Network; Ricks College, Idaho; now BYU-Idaho
RE	U.S. Bureau of Reclamation Seismic Networks; U.S. Bureau of Reclamation, Denver Federal Center
UU	University of Utah Regional Network; University of Utah
US	US National Network; USGS National Earthquake Information Center
WY	Yellowstone Wyoming Seismic Network; University of Utah

Latitude, Longitude : Sensor location in degrees and decimal minutes; North latitude, West longitude.

Elevation: Sensor altitude in meters above sea level.

Sensor Description

L4, L4C	Mark Products short-period seismometer
S13, 18300	Geotech S13 or 18300 short-period seismometer
Ranger	Kinometrics Ranger short-period seismometer
40T	Guralp CMG-40T broadband seismometer
3T	Guralp CMG-3T broadband seismometer
3ESP	Guralp CMG-3ESP broadband seismometer
FBA23	Kinometrics accelerometer
EpiSensor	Kinometrics accelerometer
Applied Mems	Applied Mems accelerometer
WA Sim	Wood-Anderson displacement seismometer (electronically simulated)

Digitizer Description

Masscomp	Concurrent Computer Corporation (formerly Masscomp) 7200C computer(with 12-bit digitizer)
K2	Kinometric s Altus Series K2 (19-bit resolution field digitizer)
Etna	Kinometrics Altus Series Etna (19-bit resolution field digitizer)
72A-07	Refraction Technology (REF TEK) model 72A-07 (24-bit field digitizer)
72A-08	Refraction Technology (REF TEK) model 72A-08 (24-bit field digitizer)
ANSS-130	Refraction Technology (REF TEK) model 130-ANSS/02 (24-bit resolution field digitizer)
RT-130	Refraction Technology (REF TEK) model RT-130 (24-bit resolution field digitizer)

Telemetry Description

Analog	Data transmission is analog along part of the transmission pathway
Digital	Data are converted to digital form at the station site
Hardwired	Direct physical cable connection to computer recording system
None	On-site recording system

Sponsor (or Operator for stations marked by * in preceding columns)

USGS	U.S. Geological Survey
Utah	State of Utah
ANSS	Advanced National Seismic System
INEEL	Idaho National Engineering and Environmental Laboratory
USBR	U.S. Bureau of Reclamation
LLNL	Lawrence Livermore National Laboratory
Sandia	Sandia National Laboratory
BYU-I	Brigham Young University, Idaho (formerly Ricks College)
MBMT	Montana Bureau of Mines and Geology
NSMP	National Strong Motion Program, U.S. Geological Survey
UNR	University of Nevada, Reno

NETWORK CHANGES DURING OCTOBER 1–DECEMBER 31 (Italicized rows in Table)*

October 8, 2003	Begin continuous recording of stations LCU and OSS
October 15, 2003	Begin on-site triggered recording of station MOR components EN[ZEN]
October 27, 2003	Begin on-site triggered recording of station EMF components EN[ZEN]
October 31, 2003	Begin continuous recording of new broadband digital telemetry station at YNR
November 6, 2003	Begin continuous recording of stations PCL and EMF
November 7, 2003	Begin continuous recording of station SPS
November 11, 2003	Begin on-site triggered recording of station COY components EN[ZEN]
November 24, 2003	Begin continuous recording of station CWR
November 25, 2003	Begin continuous recording of station COY

* Italicized rows for stations not noted among the network changes have updated locations based on GPS surveying and provided by field engineering staff (December 31, 2003). The MBMT station QLMT is an exception, as this station was moved to a slightly different location.

Note: MBMT station GCMT was mistakenly included in previous station tables beginning in 2002.

APPENDIX B

Triggered Seismicity in Utah from the November 3, 2002, Denali Fault Earthquake

Kris L. Pankow, Walter J. Arabasz, James C. Pechmann, and Susan J. Nava¹
University of Utah Seismograph Stations
Dept. of Geology and Geophysics
University of Utah
135 South 1460 East Rm 705 WBB
Salt Lake City, UT 84112-0111

¹Present Address: ENSCO, Inc., Melbourne, FL

Preprint of manuscript submitted to the
Bulletin of the Seismological Society of America
January 2004

Triggered Seismicity in Utah from the November 3, 2002, Denali Fault Earthquake

Kris. L. Pankow, Walter. J. Arabasz, James. C. Pechmann, and Susan. J. Nava

Abstract

Immediately following the arrival of the surface waves from the M_w 7.9 Denali Fault, Alaska, earthquake on November 3, 2002, the University of Utah regional seismic network recorded an abrupt increase in local microseismicity throughout most of Utah's main seismic belt. We examined this seismicity increase in the context of the regional background seismicity using a catalog of 2,651 earthquakes from January 1, 2000 to June 30, 2003. Statistical analyses of this catalog above spatially-varying magnitudes of completeness ranging from 1.2 to 1.7 allow us to reject with >95% confidence the null hypothesis that the observed increases were due to random occurrence. The elevated seismicity was most intense during the first 24 hours (>10 times the average prior rate) but continued above background level for 25 days (at the 95% confidence level) in most areas. We conclude that the increased seismicity was triggered by the Denali Fault earthquake, which occurred more than 3000 km from the study region. High peak dynamic stresses of 0.12 MPa to 0.35 MPa that occurred during the passage of the Love waves are consistent with the interpretation of triggering. The peak dynamic stresses were estimated by measuring peak vector velocities at 43 recording sites, 37 of which were relatively new strong-motion stations of the Advanced National Seismic System.

The triggered seismicity ranged in magnitude (M_c and/or M_L) from less than 0 to 3.2 and was widely distributed across the state, primarily in seismically active regions. In contrast to many previously-published observations of remotely-triggered seismicity, the majority of the triggered earthquakes did not occur near Quaternary volcanic vents or in areas of magma-related

geothermal activity. In several areas the triggered seismicity was spatially clustered (>5 earthquakes each separated by < 5 km). Double-difference relative relocations for the earthquakes in three of these clusters indicate that most, but not all, of the triggered events were spatially separated from source zones of prior seismicity during 2000-2003. Focal mechanisms for the two largest triggered events have northeast- to northwest-trending tension axes, which are unusual for the region where they occurred. The temporal decay of the triggered activity was similar to that of Utah aftershock sequences and can be described by the modified Omori's law with a p -value of 0.6 to 0.7. The frequency-magnitude distribution of the triggered earthquakes is also similar to that of Utah aftershocks, and for the study area as a whole can be described by the Gutenberg-Richter relation with a b -value of 0.81 ± 0.16 . These similarities between the triggered seismicity and Utah aftershock sequences suggest the possibility that the causative mechanism could be the same for both.

Introduction

In 1992, following the M_w 7.3 Landers, California, earthquake, the first unambiguous observations were made of an earthquake triggering smaller earthquakes at distances of up to 1300 km (Hill *et al.*, 1993; Bodin and Gomberg, 1994; Anderson *et al.*, 1994). At the time, this was a remarkable observation because aftershocks ordinarily occur at distances of up to one or two rupture lengths from the mainshock rupture, which for the Landers earthquake is 70 to 140 km (Hill *et al.*, 1993). Later, in 1999, remotely-triggered seismicity was detected following both the M_w 7.1 Hector Mine, California, earthquake (Gomberg *et al.*, 2001; Hough and Kanomori, 2002; Glowacka *et al.*, 2002) and the M_w 7.4 Izmit, Turkey earthquake (Brodsky *et al.*, 2000). In the above three cases, the triggered seismicity was recorded by modern seismic networks and

recognized shortly thereafter. In light of these observations, earthquake catalogs have been scoured to search for past instances of remotely-triggered seismicity. Such studies have revealed that the 1811 and 1812 $M_w \geq 7$ New Madrid earthquakes and the 1906 M_w 7.8 San Francisco earthquake triggered seismicity at distances of two or more main shock rupture lengths, which in these cases is hundreds of kilometers (Hough, 2001; Hough *et al.*, 2003; Meltzner and Wald, 2003). At The Geysers geothermal field in California, it appears that increases in seismicity following distant earthquakes occur regularly (Stark and Davis, 1996).

Arguably the most spectacular documented case of remotely-triggered earthquakes occurred following the November 3, 2002 M_w 7.9 Denali fault, earthquake (DFE; Fig. 1). This earthquake, which was located in southern Alaska, triggered earthquakes more than 3000 km away throughout much of the western continental U. S. (Gomberg *et al.*, 2004; Husen *et al.*, 2004; Husker and Brodsky, 2004; Prejean *et al.*, 2004). The triggered seismicity following the Landers and Hector Mine earthquakes seemed to occur preferentially in regions with recent (≤ 1 million years old) volcanic activity or in regions of magma-related geothermal fluid flow (Hill *et al.*, 1993; Gomberg *et al.*, 2001; Glowacka *et al.*, 2002). This is not the case with the DFE triggering. Although the most productive region of DFE-triggered seismicity was in and near the Yellowstone caldera (Husen *et al.*, 2004), locations of seismicity increases following the DFE are not clearly correlated with areas of recent volcanics or magma-related geothermal activity (Gomberg *et al.*, 2004). The triggered seismicity in the Utah region is a good example of this lack of correlation, as will be shown in this paper.

Utah is situated astride the eastern boundary of the Basin and Range province and is a seismically active area. The historical seismicity is characterized by diffuse, small- to moderate-size ($M \leq 6.6$), normal, oblique-normal, and strike-slip earthquakes concentrated within the

Intermountain Seismic Belt (ISB)—a band of seismicity extending from Montana to Arizona (Smith and Arabasz, 1991; Arabasz *et al.*, 1992). The region also has the potential for large ($6.5 \leq M \leq 7.5$) earthquakes on major normal faults including the ~380-km long Wasatch fault. However, in the time-period of instrumental recording, the Wasatch fault appears almost quiescent (Smith and Arabasz, 1991; Arabasz *et al.*, 1992). The ISB in Utah is characterized by relatively high heat flow (Morgan and Gosnold, 1989) and E-W to ESE-WNW extension (Arabasz and Juliander, 1986; Bjarnson and Pechmann, 1989; Zoback, 1989). There are numerous Quaternary volcanic vents in Utah—the most recent $< 660 \pm 170$ years old (Valastro *et al.*, 1972)—located primarily in the southwestern part of the state (Fig. 2). There are also numerous hot springs throughout the state. However, these hot springs are not associated with magma bodies but are instead related to ground water moving from depth to the surface along major faults (Ehlers and Chapman, 1999).

The purpose of this paper is to carefully document the observations indicating that the DFE triggered increased seismicity throughout the Utah region. We also compare the spatial and temporal characteristics of the triggered earthquakes to those of aftershocks and other earthquakes in this region. We conclude by discussing our observations in the context of previously proposed triggering mechanisms. The most significant aspects of this study are that: (1) the triggering occurred at distances greater than 3000 km, (2) unlike most places where triggered seismicity has been documented, the triggered seismicity in Utah was widespread and not preferentially located near volcanic source regions, and (3) data from the University of Utah regional seismic network enable us to rigorously quantify the statistical significance, frequency-magnitude distribution, temporal decay rate, and duration of the triggered seismicity.

Waveform Analysis

The DFE produced 340 km of surface rupture along three faults (Susitna Glacier, Denali, and Totschunda) in southern Alaska (Eberhart-Phillips *et al.*, 2003). The composite mechanism was dextral strike-slip (Harvard centroid moment tensor) and the earthquake ruptured with strong directivity to the southeast (Eberhart-Phillips *et al.*, 2003; Velasco *et al.*, 2004). The state of Utah is located within 10° of the great circle path of directivity from the DFE (Fig. 1). Even though Utah is more than 3000 km (9 rupture lengths) from the DFE epicenter, the surface waves from this event caused a majority of stations located in Utah and recorded by the University of Utah Seismograph Stations (UUSS) regional network to clip: nearly all UUSS high-gain, analog telemetry, short period instruments and most of the horizontal component broadband digital telemetry instruments operated by UUSS and the U.S. Geological Survey in Utah.

Although most of the broadband instruments were clipped by the surface waves of the DFE, the DFE was well-recorded by the strong-motion stations of the Advanced National Seismic System (ANSS). Using these recordings, we were able to estimate the peak dynamic stress (PDS) at the surface generated by the passage of the surface waves at 43 recording sites (37 of which were relatively new ANSS strong-motion stations). These stations are located from 39° N to 42° N and 110.5° W to 113° W. Following the method of Hill *et al.* (1993), the PDS calculations were done by converting the acceleration records to velocity in the passband 0.02 to 0.25 Hz and then calculating a peak vector velocity. In almost all cases this peak corresponds in time to the passage of ~15-second period Love waves. The PDS is estimated by multiplying the peak vector velocity by μ/β , where μ is the shear modulus (33,000 MPa) and β is the shear velocity (3300 m/s). The PDS values in Utah from the DFE range from 0.12 MPa to 0.35 MPa with an average of 0.23 MPa. Following the 1992 Landers and 1999 Hector Mine, California

earthquakes, PDS values (calculated using either peak vector velocities or peak horizontal velocities) ranged from 0.1 MPa – 4.5 MPa in regions of triggering (Gomberg *et al.*, 2001). In Greece, a region also characterized by neither active volcanism nor geothermal activity, the average PDS (calculated using peak horizontal velocities) following the Izmit, Turkey earthquake was 0.18 MPa (Brodsky *et al.*, 2000). Thus the PDS values estimated in Utah following the DFE are consistent with other measurements of PDS where triggered seismicity has occurred.

The evidence most suggestive that the DFE triggered earthquakes in Utah is the abrupt increase in seismicity following the passage of the surface waves. Figure 3 shows 1-Hz highpass filtered vertical-component broadband recordings from three northern Utah stations beginning an hour before the arrival of the DFE seismic waves and ending 2.7 hours after. On these seismograms it can be seen that no local earthquakes were recorded in the hour preceding the arrival of the P waves from the DFE (P-wave arrival shown in Fig. 3a). However, after the passage of the surface waves (approximate in time to Fig. 3b) many local earthquakes were recorded at these stations. The local events appear as spikes in the long-time window. Expanded time sections for sample events are shown in Figure 3c-f. On the three records shown, there are > 10 spikes (local events) in the first hour following the DFE body waves (3400-7000 sec). Small local events continued at an enhanced rate for the remainder of the time period shown. By examining the broadband records, we determined that the onset of the increased seismicity began with the passage of the Love waves. The first locatable earthquake appears in the seismogram as a high frequency signal on the shoulder of 15- to 20-sec period Love waves (Fig. 4). This first triggered earthquake (M_L 2.1) occurred ~20 km east of Salt Lake City, Utah.

Earthquake Catalog

Compilation

For a more detailed study, we used a catalog of earthquakes in the Utah region for the time period January 1, 2000, through June 30, 2003. The time period spanned by this catalog is long enough to enable the calculation of meaningful seismicity rate statistics before and after the DFE but short enough that the changes in the network detection threshold during this time should be minimal. The vast majority of the 2,651 earthquakes in this catalog are from routine processing of UUSS regional seismic network data. However, as described later, we made a major effort to improve the completeness of the catalog during the first few hours after the DFE when the DFE surface waves interfered with the normal UUSS data processing. Quarry blasts have been removed from the catalog based on location, time of day, and information provided by the quarry operators. We have also removed all seismic events from areas in east-central Utah dominated by mining-related seismicity (see Arabasz *et al.*, 1997).

The routine network data processing during the time period of interest utilized data from time windows containing potential seismic events identified by the triggering algorithm of Johnson (1979). P- and S-wave arrival times were picked for local seismic events found in these time windows and used to compute hypocentral locations with a modified version of the computer program Hypoinverse (Klein, 1978) and a set of three region-specific velocity models (see Nava *et al.*, 1990). If possible, local magnitude (M_L) was computed from maximum peak-to-peak amplitudes on paper or synthetic Wood-Anderson seismograms—the latter created primarily from UUSS and USNSN broadband digital telemetry data. Coda magnitude (M_c), a calibrated estimate of M_L , was computed for most of the earthquakes using gain-corrected measurements of seismic signal durations on short-period, vertical-component velocity sensors

(Pechmann *et al.*, 2001; Arabasz *et al.*, 2003). The preferred magnitude is M_L when M_L values from two or more stations are available to be averaged. Magnitudes were determined for 99.5% of the events. For further details on UUSS data acquisition and processing see Nava *et al.* (1990) and Arabasz *et al.* (2002, 2003).

The catalog produced by the routine data processing was incomplete for the first 3.75 hours following the arrival of seismic waves from the DFE in Utah because (1) the large, long-period body and surface waves from the DFE obscured local earthquake signals and interfered with the event triggering algorithm, and (2) the large number and widespread distribution of the triggered local earthquakes made it difficult to sort out the P and S arrivals from different events. In order to locate more of the triggered earthquakes which occurred in the Utah region during this time period, we retrieved continuous waveform data from seismic stations in the region for the time period Nov. 3, 22:16 UTC to Nov. 4, 02:00 UTC. We highpass filtered this data at 1 Hz and then played it back through the Earthworm V6.0 automatic earthquake location system (see <http://gldbrick.cr.usgs.gov/ew-doc/>) to obtain a list of possible local earthquakes. For each of the 44 events identified by Earthworm that was not already in the catalog, an analyst interactively picked arrival times on highpass-filtered data and attempted to locate the event. As a result of these efforts, we were able to add 22 events (including five of $M \geq 1.5$) to the Utah region earthquake catalog in addition to the 16 events that were already in the catalog for this time period.

To prevent surface waves from interfering with M_L determinations for earthquakes during the first four hours after the DFE, we highpass filtered the synthetic Wood-Anderson records using a frequency-domain cosine taper with an amplitude of 0.0 at 0.4 Hz and 1.0 at 0.8 Hz. Tests indicate that this filtering has a negligible effect on M_L determinations for earthquakes in

the size range for which we applied it, $M_L \leq 2.6$. All of the M_C determinations for earthquakes during the first 17 hours after the DFE were done on records filtered with a 3-pole, 1-pass, 1-30 Hz Butterworth bandpass filter. This filtering was necessary because the signal duration measurements used to calculate M_C are made with the aid of UUSS-developed software which fits an equation to the latter part of the seismic record where the amplitude decays with time. This automated duration measurement procedure does not give accurate results for local earthquakes superimposed on large, long-period surface waves.

Initial Observations

An obvious increase in local seismicity began with the arrival of surface waves from the DFE. Figures 2, 5, 6, and 7 illustrate this seismicity rate increase in four different ways. Figure 5 shows the spatiotemporal distribution of seismicity in the Utah region during the 3.5-year time period included in the catalog. The earthquake epicenters (Fig. 5a) are concentrated within the northerly-trending Intermountain Seismic Belt (e.g., Smith and Arabasz, 1991). In the space-time plot (Fig. 5b), a vertical alignment of earthquakes immediately following the DFE reflects near-simultaneous seismicity over a 500-km north-south extent of the seismic belt, extending from north of the Utah border to at least latitude 37.7° on the south. The occurrence of such a widespread concentration of seismicity over such a narrow time window is a unique observation. Figure 6 shows the temporal distribution of seismicity in the Utah region during the 3.5-year time period included in the catalog. Note the abrupt increase in seismicity following the arrival of surface waves from the DFE. During the first four hours, 39 earthquakes ($M \leq 2.6$) occurred, and a total of 65 shocks (none larger than $M 2.6$) occurred during the first 24 hours. Such a daily rate is more than an order of magnitude greater than the pre-DFE rate of 1.9 events/day for the catalog and is particularly notable in the absence of a moderate-to-large local main shock.

Figure 7 gives a third useful perspective, focusing on Utah's Wasatch Front area (Fig. 8, Region II), where seismographic coverage in the state is most dense. The magnitude-time plot shows a marked contrast in seismicity before and after the DFE. The increase in seismicity rate after the DFE is accompanied by larger magnitude earthquakes, consistent with a greater sample size of earthquakes with a typical exponential size distribution (see Anderson *et al.*, 1994). Figure 7 further shows that what we will identify as triggered earthquakes involved not only immediate occurrences on a time scale of hours following the DFE but also delayed occurrences ($M \leq 3.2$) on a time scale of days. To first order the seismicity came in bursts: a strong burst in the first few hours to a day followed by bursts around days 5, 11, and 14. Note that there were no large DFE aftershocks ($M \geq 7$) during the time frame of Figure 7 which could have triggered these bursts. Figure 2 shows the spatial distribution of the seismicity in the 14 days preceding and following the DFE. This figure again shows the widespread distribution of triggered seismicity in the region. However, it also shows that in the 14 days following the DFE many of the earthquakes were spatially clustered. Further figure 2 demonstrates that there is no correlation between the epicenters of the triggered events and locations of regional Quaternary volcanic vents.

Statistical Analyses of Increased Seismicity

In order to analyze the statistical significance and other characteristics of the increased seismicity following the DFE, we began with a scrutiny of our earthquake catalog for homogeneity and completeness. Key steps included (1) "declustering" the catalog (i.e., decomposing it into main and secondary events), (2) analyzing the catalog for evidence of changes in reporting quality as a function of time, and (3) determining the magnitude of

complete reporting as a function of space and time. To decluster the catalog, we used a modified version of Reasenberg's (1985) algorithm with a generic Utah aftershock model (Arabasz and Hill, 1994, 1996). We explored adjusting parameters in the algorithm, evaluating outcomes by visually inspecting space-time plots of the decomposed catalog and by examining identified clusters for appropriate linkage of secondary events in space and time (e.g., Savage and dePolo, 1993). Ultimately, we achieved satisfactory results using declustering parameters nearly identical to those used by Reasenberg (1985) for California seismicity. For the magnitudes of completeness that we adopted (discussed presently), resulting counts of independent main shocks were fairly insensitive to changes in declustering parameters.

We evaluated the homogeneity of magnitude reporting with time using the GENAS tool in the software package *ZMAP*, v.6 (Wiemer, 2001, and references therein). Processing a declustered version of the catalog ($M \geq 0.0$) for the entire Utah region, we found no inhomogeneities in magnitude reporting. Although 60 strong-motion and 5 broadband/strong motion digital telemetry stations were incrementally added to Utah's real-time seismic network in the Wasatch Front area during the catalog period as part of an ANSS initiative (Arabasz *et al.*, 2003), the set of stations employed in the network triggering algorithm did not change greatly.

In order to determine the minimum magnitude of complete recording, M_{comp} , as a function of both space and time, we followed the methodology of Wiemer and Wyss (2000, 2003), again using *ZMAP*. We note that the high-quality catalog used in this study differs from a western United States catalog, 1995–1999, analyzed by Wiemer and Wyss (2000), based on which they reported M_{comp} for parts of Utah. For our catalog, we estimated M_{comp} from the nearest 150 earthquakes to nodes of a grid spaced 10 km apart (mean sampling radii ~40–45 km), requiring a minimum of 75 earthquakes $\geq M_{\text{comp}}$. We used the *ZMAP* option that estimates

M_{comp} based on the "best" results from three calculations involving goodness of fit to a power law and maximum curvature of the frequency-magnitude distribution (FMD). Both clustered and declustered versions of the catalog were analyzed, and we generated and examined FMDs for selected spatial samples of seismicity throughout the region to ensure that false minima were not distorting results. Based on iterative analyses that were guided by the distribution of seismic stations and seismicity in the catalog region, we defined three polygons shown in Figure 8 within which we have confidence that the indicated M_{comp} is reasonably uniform both spatially and temporally. We use these polygons and corresponding values of M_{comp} shown in Figure 8 to investigate the significance, duration, decay rate, and FMDs of the increased seismicity following the DFE.

Figure 9 shows the cumulative number of independent main shocks in Region II ($M \geq 1.5$) and their daily rate as a function of time. The linearity of the cumulative plot reflects both the homogeneity and effective declustering of the derivative catalog. Both plots show increased seismicity following the DFE. The average rate increased by a factor of 22 from 0.32 events/day before the DFE to 7 events/day during the first 24 hrs following the DFE. The corresponding rate increases for independent main shocks above the completeness thresholds in Regions I and III are factors of 16 and 43, respectively.

Binomial-distribution Analysis

The significance of a change in average seismicity rate between two time intervals in a specified area is commonly measured using the β -statistic (Matthews and Reasenber, 1988; Reasenber and Simpson, 1992; see also Gomberg *et al.*, 2003). Before describing β -statistic

methods and our results, we first describe an independent approach we took to reject the null hypothesis that the increased seismicity following the DFE was due to stationary random occurrence. We do this because we are mindful that the absolute significance level of β relies on underlying statistical assumptions and because of the need for caution in interpreting the significance of extrema in β for short time intervals (Matthews and Reasenber, 1988; Gomberg *et al.*, 2003). Consider a time interval of duration \mathbf{d} (in integer days) following some known time T of a causative event, such as a main shock or the passage of surface waves from a large teleseism, after which a seismicity increase is observed. We seek to determine the statistical significance of the seismicity increase during the time $T + \mathbf{d}$ with respect to its complement (the rest of the catalog, both before and after) and also to determine that value of \mathbf{d} beyond which seismicity returns to the "background" level of its complement. Assuming that earthquakes follow a binomial process, we can use the binomial distribution to represent the probability of random occurrence of independent earthquakes following the DFE (e.g., Ang and Tang, 1975):

$$P [X = k] = \binom{n}{k} p^k (1 - p)^{n-k} \quad (1)$$

where X is the number of successes, k , in n repeated Bernoulli trials, each with probability p of success. We define a "success" to be the occurrence of N or more earthquakes per day, and we count successes during n successive integer days $\leq \mathbf{d}$. For independent main shocks of $M \geq 1.5$ in Region II, Figure 10a shows values of k for $N = 1$, that is, for one or more earthquakes per day as a function of n days (1 to 50) after the arrival of surface waves from the DFE. As expected during a period of above-average seismicity, k increases with n more sharply during the first several days (Fig. 10a). For the observed values of k and n , the parameter P_{pred} (Fig. 10b) is the predicted value of $P [X = k]$ from equation (1). Figure 10b shows that the predicted probability

of the observed k successes between about day 7 and day 25 is less than 0.05, the significance level α . The value of P_{pred} is larger than 0.05 for small n , in part, because of an early hiatus in triggered seismicity (Fig. 7). We use the point at which P_{pred} rises above 0.05 to define the duration d of anomalous seismicity and a return to background level. To check this result using an empirical method, which does not depend on an assumed probability distribution, for each observed pair of k and d we computed the corresponding relative frequency of k or more successes in all possible strings of d consecutive days in the catalog complement. We define this quantity as P_{obs} and note that, for conservatism, we computed it for k or more occurrences rather than exactly k . P_{obs} (Fig. 10c) validates the significance of P_{pred} . Figures 10b and 10c confirm that the seismicity following the DFE was anomalous and significant at $\alpha < 0.05$. These figures also show that the increased seismicity was anomalous at the 95% confidence level for a duration of approximately 25 days, after which time it returned to background level for independent main shocks of $M \geq 1.5$ in Region II. A similar analysis for independent main shocks of $M \geq 1.7$ in Region I indicated a duration of 44 days for increased seismicity at $\alpha < 0.05$. This longer duration for the more extensive seismic belt appears to be real and reflects the fact that most of the events between days 25 and 44 occurred in SW Utah outside the bounds of Region II (see Figure 8). Data for $M \geq 1.2$ in Region III were too sparse for reliable analysis.

β -statistics

Returning to β -statistics, we follow Reasenber and Simpson (1992) to compare the rate r_a during a later period of duration t_a with the rate r_b during an earlier period of duration t_b , where

$r_a = n_a/t_a$, $r_b = n_b/t_b$, and n_a , n_b are the numbers of earthquakes occurring in the respective intervals. The β -statistic is then expressed as

$$\beta(n_a, n_b, t_a, t_b) = [n_a - E(n_a)] / [\text{var}(n_a)]^{1/2} \quad (2)$$

where var denotes variance and $E(n_a) = r_b t_a$ is the expected value of n_a under the null hypothesis of stationary random occurrence. Further following Reasenber and Simpson (1992): (1) t_a and t_b are normalized so that $t_a + t_b = 1$; (2) secondary events (aftershocks and foreshocks) are removed from the earthquake catalog to avoid biased comparisons; (3) $\text{var}(n_a) = n_b t_a$, assuming a binomial process; and (4) critical values for β estimated from its asymptotic (Gaussian) distribution are: 1.96 for significance level $\alpha = 0.05$ and 2.57 for $\alpha = 0.01$. Table 1 summarizes values of β computed for $t_a = 1$ day and $t_a = 25$ days following the DFE, compared to $t_b = 1037$ days in the pre-DFE catalog. For the three cases of independent main shocks in Regions I, II, and III, whether for t_a of one day or 25 days, values of β under the above assumptions all exceed 2.57 and thus indicate anomalous seismicity increases with a significance level $\alpha < 0.01$.

The β -statistic was originally defined by Matthews and Reasenber (1988) to measure differences in seismicity rate in a sequence of earthquakes between some interval of duration \mathbf{d} and its complement, calculated for all possible values of t (interval end time) and \mathbf{d} . We computed and contoured values of $\beta(t, \mathbf{d})$, following Matthews and Reasenber (1988), for the entire 3.5 year catalog of independent main shocks in Region II ($M \geq 1.5$) using uniform grid spacings of 7, 14, 21, and 28 days. As might be expected from the seismicity (Fig. 9), the contour plots of $\beta(t, \mathbf{d})$ we produced are relatively featureless except for a few extrema in β . In such an application, one-sided critical values of β may be adopted from Reasenber and Matthews (1988, Table 3) as 4.04 for $\alpha = 0.05$, and 4.44 for $\alpha = 0.01$. However, extrema in β may be less significant than these values suggest if the underlying stochastic process is not

Poisson (P. A. Reasenber, personal communication, 2003). The β -analyses identified a seismicity decrease ($|\beta| < 3.0$) in late 2000 and a significant increase following the DFE, consistent with the sharp increase in seismicity observed in Figure 9. For a grid spacing of 7 days, $\beta = 6.2$ for a 7-day period ending November 8, 2002, five days after the DFE. For a 14-day grid spacing, $\beta = 4.2$ for a 14-day period also ending on November 8. Thus, extrema in β (albeit for short intervals) corresponding to the post-DFE seismicity were objectively recognized by calculating β for all possible values of t and d in the catalog for the stated grid spacings. Based on our independent binomial-distribution analyses, reinforced by these varied β -statistic results, we reject with $> 95\%$ confidence the null hypothesis that the observed increased seismicity in Utah following the DFE was due to random occurrence.

We reviewed the timing of 25 other teleseisms of $M_w \geq 7.0$ that occurred during the period of our special-study catalog (Jan. 1, 2000–June 30, 2003) and found no evidence of other instances of remotely-triggered local seismicity comparable to that following the DFE, as apparent in Figure 5b. Because some triggered seismicity conceivably may involve a delay of days after the passage of a dynamic stress pulse, as observed in this study, and perhaps have a subtle manifestation, we recognize that a suitable experiment has to be devised for systematically discriminating such seismicity. We leave that experiment for future work.

Comparisons with Background Seismicity

Spatial Distribution

As already mentioned, one of the most notable features of the triggered seismicity is its spatial extent. Microseismicity dramatically increased over a 500-km-long section of the ISB in Utah following the DFE. The majority of this activity occurred in seismically active regions.

However, unlike many previously-documented cases of triggered seismicity (see Hill et al., 1992), there is no correlation between the triggered event locations and the locations of Quaternary volcanic vents (Fig. 2). A second notable feature is that a large number of the triggered earthquakes occurred in spatial clusters. In this section, we present results from a detailed analysis of each of these spatial clusters.

We define a spatial cluster as a group of five or more earthquakes with interevent spacings of < 5 km. A catalog sort of seismicity 14 days post-DFE included seven such spatial clusters (Fig. 2). These clusters are widespread throughout the region, as are the rest of the triggered events. To get precise relative locations for the triggered seismicity relative to the background seismicity, we applied a double-difference relocation technique (Waldhauser and Ellsworth, 2000) using analyst-picked arrival times from the UUSS network. For three of the seven clusters, this algorithm produced stable results. In the other four cases, there were either too few earthquakes or too few nearby stations to adequately relocate the triggered seismicity.

Figure 11a shows the relocated epicenters for clusters A, C, and F. In map view, the triggered seismicity appears even more tightly clustered than originally thought. In clusters C and F, which include some background seismicity, the majority of the triggered events are spatially separated from the background seismicity. Cluster A is particularly interesting because it occurred in a region of no prior seismicity near the northern terminus of the Wasatch fault (Fig. 2), where the catalog contains no prior seismicity. Because the epicentral locations of these earthquakes are 2–3 km east of the west-dipping Wasatch fault, these earthquakes probably did not occur on the Wasatch fault. This burst of seismicity occurred on day 14 towards the end of the triggering period.

Of the seven clusters identified, clusters A, D, and E are in regions of little or no prior seismicity in the catalog (Fig. 12). In these clusters the seismicity occurred in a short time period and then abruptly ceased. The seismicity in cluster C also appears to have terminated with the end of the triggered seismicity, even though there were several prior background earthquakes. In the other clusters characterized by frequent background earthquakes (clusters B, F, and G), the seismicity persists throughout the catalog-time period. In fact, a larger regional event (M_L 3.6) occurred in cluster B on January 3, 2003, shortly after the return to background seismicity rates.

Omori-like Decay Rate and b-Values

In aggregate, the seismicity triggered by the DFE in Utah displayed an aftershock-like decay rate (Figs. 6 and 7). The added complexity of localized space-time clustering resulted in a composite appearance (Fig. 7) similar to that commonly observed within aftershock sequences having secondary "offspring" sequences (e.g., Utsu *et al.*, 1995; Guo and Ogata, 1997). Our intent here is two-fold: to demonstrate that the triggered seismicity can be modeled as an aftershock sequence and to compare the decay rate of triggered seismicity quantitatively to that of aftershocks in the same region. Given the large spatial extent of the triggered seismicity compared to what might be modeled in a localized aftershock sequence, we choose simply to model its overall decay rate using the modified Omori law (Utsu, 1961, Kisslinger and Jones, 1991):

$$n(t) = k / (t + c)^p \quad (3)$$

where $n(t)$ is the number of events per unit time at time t , and k , c , and p are constants specific to the sequence. Our particular interest is in the relative value of the parameter p , which measures the exponential rate of decay of seismic activity (with larger p implying a faster decay rate). We

set aside discussion of k , a measure of the productivity or total number of events in the sequence, and c , an adjustment term that reflects incomplete detection in the earliest part of the sequence and also avoids a singularity at $t = 0$. Model parameters were computed using maximum-likelihood techniques implemented in *ZMAP* and incorporating Reasenberg's (1994) ASPAR software (see Wiemer, 2001, and references therein). We modeled triggered seismicity using both the raw (clustered) catalog and the declustered catalog. The motivation for considering results from the latter is that the declustered triggered seismicity may be more analogous to aftershocks caused by a simple point process and hence be better represented by the modified Omori law.

Table 1 lists p -values computed for Regions I, II, and III for the indicated values of M_{comp} and for both clustered and declustered earthquakes during the 25-day period following the arrival of surface waves from the DFE. Figure 12 illustrates results for the modified-Omori-law modeling of decay rate for *all* earthquakes located in the Wasatch Front area (Region II) during the same 25-day period (seismicity in Fig. 12 can be directly compared with that in Fig. 7 for the 25-day post-DFE period). In Figure 12, we assume reasonably homogeneous reporting down to smaller magnitudes (i.e., the reporting of a constant proportion of events as a function of size), as opposed to using the M_{comp} threshold of 1.5. The magnitude distribution for the sampled earthquakes (inset, Fig. 11) peaks slightly above magnitude 1. The p -value of 0.65 ± 0.04 shown in Figure 11 approximates the average of the six p -values listed in Table 1, which range from 0.53 to 0.75, and is a fair representation of the overall regionwide temporal decay of triggered seismicity in Utah following the DFE. For comparison, Arabasz and Hill (1994) determined a mean p -value of 0.80 ± 0.13 (1 std. dev; median = 0.75) for 11 aftershock sequences in Utah following main shocks of M_L 4.5 to 6.0, 1975–1992. For 62 aftershock sequences in California,

1933–1987, Reasenber and Jones (1989; see also Kisslinger and Jones, 1991) reported a mean p -value of 1.07 ± 0.03 (median = 1.08), indicating a faster decay rate on average than for aftershocks in the Utah region. We recognize that p -values may vary in space and time within individual aftershock sequences (e.g., Wiemer *et al.*, 2002); so the p -values reported here (Table 1, Fig. 11) clearly represent overall averages. From our p -value analyses, we conclude that the triggered seismicity in Utah can be modeled successfully with the modified Omori law. The p -value for the Wasatch Front area (Region II) decay rate is approximately 0.6–0.7 (Fig. 11), slightly lower than but comparable to a mean value of 0.80 (median = 0.75) determined for 11 aftershock sequences in Utah.

To further compare the triggered seismicity with background seismicity and aftershocks in the same region, we investigated FMDs in terms of the well known Gutenberg-Richter relationship: $\log_{10}N = a - bM$, where N is the cumulative number of earthquakes of magnitude M or larger, and a and b constants. Here, our emphasis is on comparing values of b , the slope of the linear-log FMD, which describes the relative proportion of earthquakes as a function of size. All b -values were determined using the maximum-likelihood procedure of Weichert (1980) for a doubly-truncated exponential. Because samples of declustered triggered seismicity were too sparse for analysis, we consistently used the clustered catalog to compare triggered and background seismicity. Table 1 lists b -values computed for Regions I, II, and III for the indicated values of M_{comp} , both for (1) background seismicity during a 1037-day period preceding the DFE and (2) triggered seismicity during the 25-day period following the DFE. The b -values for the background seismicity range from 0.77 to 0.91. The available b -values for the triggered seismicity in Regions I and II (Table 1, 0–25 days) are 0.81 ± 0.04 and 0.60 ± 0.13 , respectively. These values are lower than those for the corresponding background seismicity by

0.10 and 0.17, respectively. For the 11 Utah aftershock sequences referred to above, Arabasz and Hill (1994) determined b -values (also from clustered seismicity and using the Weichert algorithm) ranging from 0.53 to 1.40, with a mean of 0.83 ± 0.22 (1 std. dev.; median = 0.87). The b -values for the DFE-triggered seismicity fall within about one standard deviation of the mean b -value for these aftershock sequences.

We evaluated the statistical significance of the differences in b -value between the triggered and background seismicity using two tests described by Wiemer and Wyss (1997). One test, following Utsu (see Wiemer and Wyss, 1997, equation 2), calculates the probability that two FMDs come from the same population, based on their respective b -values and sample sizes. The other test uses a Monte Carlo technique, implemented in *ZMAP*, to evaluate the uncertainty of b -value as a function of sample size. For Region II, the Utsu test gives a probability of 0.06 that the b -values for the triggered and background seismicity come from the same population, and the Monte Carlo test indicates that the b -value for the triggered seismicity is in the lower 5% tail of the expected distribution for sampling the background seismicity with a sample size of 59. For Region I, however, both tests indicate that the b -values for triggered and background seismicity are not different at a level of significance < 0.2 . Thus there is mixed evidence whether the b -value for seismicity triggered by the DFE is significantly different from, and perhaps lower than, background seismicity.

Focal Mechanisms

We were able to determine focal mechanisms from P-wave first motions for the two largest triggered earthquakes in Utah: an M_L 3.2 event which occurred on Nov. 8 in Cluster F

(Figs. 2 and 13b) and an M_L 3.0 event which occurred on Nov. 9 in Cluster E (Figs. 2 and 13c). We attempted to determine focal mechanisms for the next two largest events in each cluster ($2.3 \leq M_L \leq 2.8$). However, there was not enough first motion data for these smaller earthquakes to reliably constrain the focal mechanisms. For comparison purposes, we also determined focal mechanisms for (1) a 1992 M_L 4.3 event in Cluster F (Fig. 13a) and (2) the two largest earthquakes triggered near Cedar City, Utah, by the 1992 Landers, California, earthquake (Fig. 13d,e; see Hill *et al.*, 1993). The focal mechanisms were done using velocity models and procedures described in Bjarnason and Pechmann (1989) with one modification. For the earthquakes in Cluster F, we used the Southern Wasatch Plateau velocity model of Pechmann *et al.* (1992) because this model gives a much better fit to the travel-time data and more realistic focal depths.

The focal mechanism for the M_L 3.2 earthquake in Cluster F shows dominantly strike-slip faulting on a poorly-constrained NW- or NE-striking plane (Fig. 13b). All of the first motions for the M_L 3.0 earthquake in Cluster E are compressional (Fig. 13c). Nevertheless, the focal mechanism for this event is reasonably well constrained and indicates normal faulting on a N- or S-dipping plane. The contours on the focal sphere plots in Figure 13 outline orientations of the tension axes for solutions with the minimum number of readings in error (solid contours) and up to one good or two lesser-quality readings in error (dashed). Based on these contours, the focal mechanism tension axes for the two largest Denali-triggered events are constrained to trend between NE-SW and NW-SE. These axes are notably different from the average tension axis direction for earthquakes in this area, which is E-W to ESE-WNW (Arabasz and Julander, 1986; Bjarnason and Pechmann, 1989). The first motion data that we compiled for the smaller events during 2002 in clusters E and F indicate that the focal mechanisms for the events in each cluster

are variable. Therefore, it is difficult to judge the significance of the unusual tension axis orientations for the largest events.

The focal mechanism for the 1992 M_L 4.3 event in Cluster F shows dominantly strike-slip faulting on a NW- or NE-striking plane, with an ESE-WNW- to ENE-WSW-trending tension axis that is reasonably close to the average regional trend (Fig. 13a). Of the two focal mechanisms for the 1992 Landers-triggered earthquakes (Fig. 13d, e), only the second is well constrained. This focal mechanism shows normal faulting on a W- or SE-dipping plane and has a SE-NW-trending tension axis, which is fairly close to the average regional trend. Therefore, in contrast to the focal mechanisms for the Denali-triggered earthquakes, the focal mechanisms for the Landers-triggered earthquakes do not appear to have any unusual properties. Note, however, that because of the difference in the directions of the Landers and Denali earthquakes from Utah (SW versus NW), the orientations of the dynamic stresses from these earthquakes probably had different orientations.

Implications for Triggering Mechanisms

Although evidence that large earthquakes trigger remote seismicity is conclusive, the mechanism remains elusive. Anderson *et al.* (1994) found some similarities between Landers-triggered seismicity and aftershock sequences. For the seismicity triggered in Utah following the DFE, we found that both the temporal decay and the FMD are similar to those of Utah aftershock sequences. These similarities between triggered seismicity and aftershocks suggest the possibility that the causative mechanism could be the same for both. A dynamic stress pulse associated with the passage of surface waves is a possible candidate for initiating both remotely triggered seismicity (see Hill *et al.*, 1993 and Gomberg *et al.*, 2001) and aftershocks (see Kilb,

2002; Kilb *et al.*, 2002; Gomberg *et al.*, 2003). However, since dynamic stress change can only cause instantaneous failures (Gomberg, 2001; Belardinelli *et al.*, 2003), and the time lag between the surface waves and remotely triggered earthquakes can range from seconds to days, the properties of the dynamic stress pulse—magnitude (Gomberg *et al.*, 2001) and spectral content (Anderson *et al.*, 1994; Vosin, 2002; Brodsky, 2003)—must somehow modify the properties of the fault or immediate environs such that failure is induced or time to failure is accelerated. Proposed mechanisms resulting from a dynamic stress pulse include: unclamping of the fault caused by oscillations normal to the fault surface (Brune *et al.*, 1993), changes in pore fluid pressure or (Hill *et al.*, 1993), rate-and-state dependent friction (Dietrich, 1994), non-linear friction (Voisin, 2002), or subcritical crack growth (Das and Scholz, 1981).

From our analysis of triggered seismicity in Utah following the DFE, we are unable to determine a mechanism. However, we can conclude, as have other studies, that the triggering mechanism is somehow related to an elevated dynamic stress pulse. If this conclusion is correct, then our results imply that the dynamic stress pulse must cause changes that persist for at least 25 days. A complete model should also account for secondary bursts of activity and spatial clustering of events. We found no correlation with Quaternary volcanic vents. Thus, the mechanism apparently does not require conditions which are unique to areas of active volcanism. However, the mechanism should be able to explain why volcanic regions associated with active geothermal fluid flow are more often triggered and have a higher productivity of triggered earthquakes than more typical continental crust. For example, the DFE triggered 250 locatable events in Yellowstone in the first 24 hours (Husen *et al.*, 2004) compared to 65 locatable events in the Utah region during the same time interval.

. We cannot rule out mechanisms related to pore fluid pressure changes because we know that: (1) ground water flows along regional normal faults forming hot springs (Ehlers and Chapman, 1999) and (2) the DFE seismic energy disturbed the ground water table in at least one well located at the north end of the Great Salt Lake (Mark Danner, personal communication, 2002). With the available data we also cannot rule out any of the other aforementioned mechanisms.

Conclusions

With greater than 95% confidence, we conclude that the increase in earthquake activity following the passage of the surface waves from the DFE did not occur randomly. Elevated rates were highest immediately following the DFE and subsequently decreased with time in a manner similar to that of Utah aftershock sequences. The rates declined to background levels (at the 95% confidence level) in most areas after 25 days. The triggered earthquakes were all small ($M \leq 3.2$) and had a frequency-magnitude distribution comparable to that of Utah aftershocks. Because of the timing of the seismicity rate increase and the high peak dynamic stresses of 0.12 to 0.35 MPa generated by the DFE surface waves, we conclude that the increased earthquake activity was most likely triggered by some mechanism associated with or ancillary to the dynamic stress pulses associated with the surface waves. The similarities between the DFE-triggered seismicity and Utah aftershock sequences suggest that aftershocks might also be triggered by dynamic stresses, as some have hypothesized (e.g. Kilb, 2002; Kilb *et al.*, 2002; Gomberg *et al.*, 2003).

The triggered seismicity was widespread throughout the ISB in Utah, occurred generally within seismically active areas, and tended to spatially cluster. There is no correlation between the

locations of the triggered earthquakes and Quaternary volcanic vents. Relative relocations for the earthquakes in three of the spatial clusters show that the epicenters of most, but not all, of the triggered events were spatially separated from those of prior seismicity during 2000-2003. Comparisons of first-motion focal mechanisms from the two largest triggered earthquakes to focal mechanisms of other Utah region earthquakes tentatively suggest the possibility of a least-principal-stress-axis rotation associated with these triggered events. Remotely triggered seismicity in the Utah earthquake catalog appears to be rare. Whether instances go unrecognized because of incomplete detection or masking during the time period of hours following earthquakes with large surface waves is left for future work.

Acknowledgements

This study was aided by discussions with Stephan Husen, and Johanna Edwards. We appreciate the careful work of our analysts, Paul Roberson and Fabia Terra, in processing very complicated data. We thank Mike Hagerty for providing the program *myhp* and Paul Reasenber for providing the program *betatime2000*. We also thank Salah Mehanee for coding the binomial distribution analysis. We appreciate the water-well data provided by Mark Danner of the U. S. Geological Survey, Utah District Office. Figures 1 and 2 were generated using the Generic Mapping Tool (Wessel and Smith, 1995). This work was supported by the U. S. Geological Survey under award number 01HQAG0014 and by the State of Utah.

References

- Anderson, J. G., J. N. Brune, J. N. Louie, Y. Zeng, M. Savage, G. Yu, Q. Chen, and D. dePolo (1994). Seismicity in the Western Great Basin apparently triggered by the Landers, California, earthquake, 28 June 1992, *Bull. Seis. Soc. Am.* **84**, 863-891.
- Ang, A. H-S and W. H. Tang (1975). *Probability Concepts in Engineering Planning and Design, Volume I—Basic Principles*, John Wiley and Sons, Inc., New York, 409 pp.
- Arabasz, W. J., and D. R. Julander (1986). Geometry of seismically active faults and crustal deformation within the Basin and Range -Colorado Plateau transition, in *Cenozoic Tectonics of the Basin and Range Province: A Perspective on Processes and Kinematics of an Extensional Origin*, L. Mayer (Editor), *Geol. Soc. Am. Special Paper 208*, 43-74.
- Arabasz, W. J., J. C. Pechmann, and E.D. Brown (1992). Observational seismology and the evaluation of earthquake hazards and risk in the Wasatch front area, Utah, in *Assessment of Regional Earthquake Hazards and Risk Along the Wasatch Front, Utah*, P.L. Gori and W.W. Hays (Editors), *U.S. Geol. Surv. Profess. Paper 1500-A-J*, D1-D36.
- Arabasz, W. J. and S. J. Hill (1994). Aftershock temporal behavior and earthquake clustering in the Utah region, in Smith, R. B., W. J. Arabasz, J. C. Pechmann, and C. M. Meertens, Seismicity, ground motion, and crustal deformation—Wasatch Front, Utah, and adjacent Intermountain Seismic Belt, *Technical Report*, U.S. Geol. Surv. Grant No. 1434-93-G-2348, University of Utah, Salt Lake City, Utah, Attachment No. 2, 31 pp.
- Arabasz, W. J. and S. J. Hill (1996). Applying Reasenberg's cluster-analysis algorithm to regional earthquake catalogs outside California (abstract), *Seism. Res. Lett.* **67** (2), 30.
- Arabasz, W. J., S. J. Nava, and W. T. Phelps (1997). Mining seismicity in the Wasatch Plateau and Book Cliffs coal mining districts, Utah, USA, in *Rockbursts and Seismicity in Mines*, S. J. Gibowicz and S. Lasocki (Editors), A. A. Balkema, Rotterdam, 111-116.

- Arabasz, W. J., S. J. Nava, M. K. McCarter, and K. L. Pankow (2002). Ground-motion recording and analysis of mining-induced seismicity in the Trail Mountain area, Emery County, Utah, Technical Report, University of Utah Seismograph Stations, Salt Lake City, Utah, 162 pp. Accessible online at <http://www.seis.utah.edu/Reports/sitla2002a> .
- Arabasz, W. J., R. B. Smith, S. J. Nava, J. C. Pechmann, and K. L. Pankow (2003). Urban and regional seismic monitoring—Wasatch Front Area, Utah, and adjacent Intermountain Seismic Belt, Annual Technical Report (January 1–December 31, 2002), U.S. Geological Survey Cooperative Agreement No. 01HQAG0014, 57 pp. Accessible online at <http://www.seis.utah.edu/Reports/usgs2003a/index.shtml>.
- Belardinelli, M. E., A. Bizzarri, M. Cocco (2003). Earthquake triggering by static and dynamic stress changes, *J. Geophys. Res.*, **108**, doi:10.1029/2002JB001779.
- Bjarnason, I. T. and J. C. Pechmann (1989). Contemporary tectonics of the Wasatch fault region, Utah, from earthquake focal mechanisms, *Bull. Seis. Soc. Am.* **79**, 731-755.
- Blackett, R. E. and S. Wakefield (2002). Geothermal resources of Utah, *Utah Geol. Surv., Open-File Rept. 397*, CD-ROM, ISBN 1-55791-677-2.
- Bodin, P. and J. Gomberg (1994). Triggered seismicity and deformation between the Landers, California, and Little Skull Mountain, Nevada, earthquakes, *Bull. Seis. Soc. Am.* **84**, 835-843.
- Brodsky, E. E., V. Karakostas, and H. Kanomori (2000). A new observation of dynamically triggered regional seismicity: Earthquakes in Greece following the August, 1999 Izmit, Turkey earthquake, *Geophys. Res. Lett.* **27**, 2741-2744.
- Brune, J. N., S. Brown, and P. Johnson (1993). Rupture mechanism and interface separation in foam rubber models of earthquakes: A possible solution to the heat flow paradox and the paradox of large overthrusts, *Tectonophysics*, **218**, 59-67.

- Das, S. and C. H. Scholz (1981). Theory of time-dependent rupture in the Earth, *J. Geophys. Res.*, **86**, 6039-6051.
- Dietrich, J. (1994). A constitutive law for rate of earthquake production and its application to earthquake clustering, *J. Geophys. Res.*, **99**, 2601-2618.
- Eberhart-Phillips, D, P. J. Haeussler, J. T. Feymueller, A. D. Frankel, C. M. Rubin, P. Craw, N. A. Ratchkovski, G. Anderson, G.A. Carver, A. J. Crone, T. E. Dawson, H. Fletcher, R. Hanson, E. L. Harp, R. A. Harris, D. P. Hill, S. Hreinsdóttir, R. W. Jibson, L. M. Jones, R. Kayen, D. K. Keefer, C. F. Larsen, S. C. Moran, S. F. Personius, G. Plafker, B. Sherrod, K. Sieh, N. Sitar, W. K. Wallace (2003). The 2002 Denali fault earthquake, Alaska: A large magnitude, slip-partioned event, *Science* **300**, 1113-1118.
- Ehlers, T. A. and D. S. Chapman (1999). Normal fault thermal regimes: conductive and hydrothermal heat transfer surrounding the Wasatch fault, Utah, *Tectonophysics* **312**, 217-234.
- Glowacka, E., F. A. Nava, G. D. de Cossío, V. Wong, and F. Farafán (2002). Fault slip, seismicity, and deformation in Mexicali Valley, Baja California, Mexico, after the M 7.1 1999 Hector Mine earthquake, *Bull. Seis. Soc. Am.* **92**, 1290-1299.
- Gomberg, J. (2001). The failure of earthquake failure models, *J. Geophys. Res.*, **106**, 16,253-16,263.
- Gomberg, J., P. A. Reasenberg, P. Bodin, and R. A. Harris (2001). Earthquake triggering by seismic waves following the Landers and Hector Mine earthquakes, *Nature* **411**, 462-466.
- Gomberg, J. , P. Bodin, and P. A. Reasenberg (2003). Observing earthquakes triggered in the near field by dynamic deformations, *Bull. Seism. Soc. Am.* **93**, 118–138.

- Gomberg, J., P. Bodin, K. Larson, and H. Draggert (2004). The fundamental process of earthquake nucleation by transient deformations revealed by the M7.9 Denali, Alaska earthquake, submitted to *Nature*.
- Guo, A. and Y. Ogata (1997). Statistical relations between the parameters of aftershocks in time, space, and magnitude, *J. Geophys. Res.* **102**, 2857-2873.
- Hill, D. P., P. A. Reasonberg, A. Michael, W. J. Arabasz, G. Beroza, J. N. brune, D. Brumbaugh, R. Castro, S. Davis, D. dePolo, W. L. Ellsworth, J. Gomberg, S. Harmsen, L. House, S. M. Jackson, M. Johnston, L. Jones, R. Keller, S. Malone, L. Munguia, S. Nava, J. C. Pechmann, A. Sanford, R. W. Simpson, R. S. Smith, M. Stark, M. Stickney, A. Vidal, S. Walter, V. Wong, and J. Zollweg (1993). Seismicity in the western United States remotely triggered by the M 7.4 Landers, California, earthquake of June 28, 1992, *Science* **260**, 1617-1623.
- Hough, S. E. (2001). Triggered earthquakes and the 1811 – 1812 New Madrid, central U. S. earthquake sequence, *Bull. Seis. Soc. Am.* **91**, 1574-1581.
- Hough, S. E. and H. Kanamori (2002). Source properties of earthquakes near the Salton Sea triggered by the 16 October 1999 M 7.1 Hector Mine, California, earthquake, *Bull. Seis. Soc. Am.* **92**, 1281-1289.
- Hough, S. E., L. Seeber, and J. G. Armbruster (2003). Intraplate triggered earthquakes: Observations and interpretations, *Bull. Seis. Soc. Am.* **93**, 2212-2221.
- Husen, S. S. Wismer, and R. Smith (2004). Remotely triggered seismicity in the Yellowstone National Park Region by the 2002 $M_w=7.9$ Denali Fault earthquake, Alaska, submitted to *Bull. Seism Soc. Am.*
- Husker, A. and E. E. Brodsky (2004). Dynamically triggered seismicity in Idaho and western Montana: The necessary geology, submitted.

- Johnson, C. J. (1979). I, CEDAR-An approach to the computer automation of short-period local seismic networks, II, Seismotectonics of the Imperial Valley of southern California, *Ph.D. Thesis*, California Institute of Technology, Pasadena, California. 332 pp.
- Kilb, D. (2002). A strong correlation between induced peak dynamic Coulomb stress change from the 1992 M7.3 Landers, California, earthquake and the hypocenter of the 1999 M7.1 Hector Mine, California earthquake, *J. Geophys. Res.*, **107**, doi:10.1029/2001JB00678.
- Kilb, D., J. Gomberg, and P. Bodin (2002). Aftershock triggering by complete Coulomb stress changes, *J. Geophys. Res.*, **107**, doi:10.1029/2001JB00202.
- Kisslinger, C. and L. M. Jones (1991). Properties of aftershock sequences in southern California, *J. Geophys. Res.*, **96**, 11,947-11,958.
- Klein, F. W. (1978). Hypocenter location program HYPOINVERSE, *U. S. Geol. Surv., Open-File Rept. 78-694*, 113 pp.
- Matthews, M. V., and P. A. Reasenber (1988). Statistical methods for investigating quiescence and other temporal seismicity patterns, *Pure and Appl. Geophys.* **126**, 357–372.
- Meltzner, A. J. and D. J. Wald (2003). Aftershocks and triggered events of the great 1906 California, earthquakes, *Bull. Seis. Soc. Am.* **93**, 2160-2186.
- Morgan, P. and W. D. Gosnold (1989). Heat flow and thermal regimes in the continental United States, in *Geophysical framework of the continental United States*, L. C. Pakiser and W. D. Mooney (Editors), *Geological Society of America Memoir 172*, 493-522.
- Nava, S. J., J. C. Pechmann, W. J. Arabasz, E. D. Brown, L. L. Hall, P. J. Oehmich, E. McPherson, and J. K. Whipp (1990). *Earthquake Catalog for the Utah Region, January 1, 1986 to December 31, 1988*, Special Publication, University of Utah Seismograph Stations, Salt Lake City, Utah, 96 pp.

- Pechmann, J.C., S.J. Nava, and W.J. Arabasz (1992). Seismological analysis of four recent moderate (ML 4.8 to 5.4) earthquakes in Utah, *Utah Geological Survey, Contract Rept. 92-1*, 107 pp.
- Pechmann, J. C., J. C. Bernier, S. J. Nava, F. M. Terra, and W. J. Arabasz (2001). Correction of systematic time-dependent coda-magnitude errors in the Utah and Yellowstone National Park region earthquake catalogs, 1981-2001, *Eos. Trans. Am. Geophys. Union* **82**, no. 47, Fall Meet. Suppl., Abstract S11B-0572.
- Prejean, S., D. Hill, E. Brodsky, S. Hough, M. Johnston, S. Malone, D. Oppenheimer, M. Pitt, and K. Richards-Dinger (2004). Remotely triggered seismicity on the United States west coast following the M 7.9 Denali fault earthquake, submitted to *Bull. Seis. Soc. Am.*
- Reasenber, P. (1985). Second-order moment of central California seismicity, 1969–1982, *J. Geophys. Res.* **90**, 5479-5495.
- Reasenber, P. (1994). Computer programs ASPAR, GESAS and ENAS and APROB for the statistical modeling of aftershock sequences and estimation of aftershock hazard, *U.S. Geol. Surv. Open-File Rept. 94-221*, Menlo Park, California, 29 pp.
- Reasenber, P. A. and L. M. Jones (1989). Earthquake hazard after a mainshock in California, *Science* **243**, 1173-1176.
- Reasenber, P. A. and R. W. Simpson (1992). Response of regional seismicity to the static stress change produced by the Loma Prieta earthquake, *Science* **255**, 1687-1690.
- Savage, M. K. and D. M. dePolo (1993). Foreshock probabilities in the Western Great-Basin Eastern Sierra Nevada, *Bull. Seis. Soc. Am.*, **83**, 1910-1938.
- Smith, R. B. and W. J. Arabasz (1991). Seismicity of the Intermountain seismic belt, in *Neotectonics of North America*, D. B. Slemmons, E. R. Engdahl, M. D. Zoback, and D. D. Blackwell, Editors, *Geol. Soc. Am. Decade Map Vol. 1*, 185-228.

- Stark, M. A. and S. D. Davis (1996). Remotely triggered microearthquakes at The Geysers geothermal field, CA, *Geophys. Res. Lett.* **23**, 945-948.
- Utsu, T. (1961). Statistical study on the occurrence of aftershocks, *Geophys. Mag.* **30**, 521–605.
- Utsu, T., Y. Ogata, and R. S. Matsu'ura (1995). The centenary of the Omori formula for a decay law of the aftershock activity, *J. Phys. Earth* **43**, 1–33.
- Valastro, S., Jr., E. M. Davis, and Ag.G. Varela (1972) University of Texas at Austin Radiocarbon dates IX. *Radiocarbon*, **14**, 461-485.
- Velasco, A., C. Ammon, J. Farrell, and K. L. Pankow (2004). Rupture directivity and its effects of the November 3, 2002 Denali (M=7.9) fault earthquake, submitted to *Bull. Seism. Soc. Am.*
- Vosin, C. (2002). Dynamic triggering of earthquakes: The nonlinear slip-dependent friction case, *J. Geophys. Res.*, **107**, doi:10.1029/2001JB001121.
- Waldhauser, F. and W. L. Ellsworth (2000). A double-difference earthquake location algorithm: Method and application to the northern Hayward fault, California, *Bull. Seis. Soc. Am.* **90**, 1353-1368.
- Weichert, D. H. (1980). Estimation of the earthquake recurrence parameters for unequal observation periods for different magnitudes, *Bull. Seism. Soc. Am.* **70**, 1337–1436.
- Wessel, P. and W. H. F. Smith (1995). New version of the Generic Mapping Tools released. *EOS* **76**, 329.
- Whitcomb, J. H. (1973). The 1971 San Fernando earthquake series focal mechanisms and tectonics, *Ph.D. Thesis (Part II)*, California Institute of Technology, Pasadena, California.
- Wiemer, S. (2001). A software package to analyze seismicity: *ZMAP*, *Seism. Res. Lett.* **72** (2), 373–382.

- Wiemer, S. and M. Wyss (1997). Mapping the frequency-magnitude distribution in asperities: An improved technique to calculate recurrence times?, *J. Geophys. Res.* **102**, 15,115–15,128.
- Wiemer, S. and M. Wyss (2000). Minimum magnitude of completeness in earthquake catalogs: Examples from Alaska, the western United States, and Japan, *Bull. Seism. Soc. Am.* **90**, 859–869.
- Wiemer, S. and M. Wyss (2003). Reply to "Comment on 'Minimum magnitude of completeness in earthquake catalogs: Examples from Alaska, the western United States, and Japan,' by Stefan Wiemer and Max Wyss, " by Paul A. Rydelek and I. S. Sacks, *Bull. Seism. Soc. Am.* **93**, 1868–1871.
- Wiemer, S., M. Gerstenberger, and E. Hauksson (2002). Properties of the aftershock sequence of the 1999 M_w 7.1 Hector Mine earthquake: Implications for aftershock hazard, *Bull. Seism. Soc. Am.* **92**, 1227–1240.
- Zoback, M. L. (1989). State of stress and modern deformation of the northern Basin and Range Province, *J. Geophys. Res.* **94**, 7105-7128

Table 1
Statistical and Seismicity Parameters¹

Region	Period (days) ²	Num. > M_{comp}	b	b -value	p -value
I ($M_{\text{comp}} = 1.7$)	pre-DFE	559 (382)	NA	0.91±0.04	NA
	0–1	9 (6)	(9.28)	-----	-----
	0–25	54 (22)	(4.27)	0.81±0.16	0.53±0.09 (0.59±0.14)
II ($M_{\text{comp}} = 1.5$)	pre-DFE	523 (337)	NA	0.77±0.04	NA
	0–1	10 (7)	(11.7)	-----	-----
	0–25	59 (19)	(3.86)	0.60±0.13	0.53±0.09 (0.70±0.14)
III ($M_{\text{comp}} = 1.2$)	pre-DFE	247 (169)	NA	0.79±0.06	NA
	0–1	11 (7)	(16.9)	-----	-----
	0–25	27 (16)	(5.98)	-----	0.73±0.11 (0.75±0.15)

1. Values in parentheses based on "declustered" catalog; all others, on raw catalog with clustering
2. pre-DFE catalog = 1037 days; 0–1 and 0–25 indicate days after arrival of DFE surface waves
3. Values of b and p are maximum-likelihood estimates \pm standard error of estimation

Figure Captions

Figure 1. Transverse Mercator projection depicting the Harvard centroid moment tensor (<http://www.seismology.harvard.edu/CMTsearch.html>), great circle extension (solid line) of the rupture direction and $\pm 10^\circ$ from the rupture direction (dashed lines). Utah is within 10° of the peak directivity along the rupture direction.

Figure 2. Comparison of seismicity in Utah immediately before and after the DFE. Diamonds in the right panel are epicenters of earthquakes occurring during the first 24 hours following the DFE surface waves. Circles represent the remainder of the epicenters during the indicated time periods. Crosses show locations of Quaternary volcanic vents (Blackett and Wakefield, 2002). Clusters A-G are keyed to Figure 11.

Figure 3. Seismograms of 1-Hz high-pass filtered vertical broadband data for ~ 1 hour before and ~ 2.7 hours after the arrival of the body waves from the DFE in Utah. The high frequency spikes correspond to local tectonic earthquakes. For the record from station HVU, 30-second windows have been enlarged to show (a) the DFE body waves, (b) a local event overprinted on DFE surface waves, and (c-f) local tectonic earthquakes. All three records are from stations in northern Utah.

Figure 4. (a) Broadband seismograms of the Denali Fault Earthquake from station CTU in northern Utah. L and R denote the Love and Rayleigh waves, respectively. The shaded box highlights the first triggered earthquake in Utah. Note that its arrival is coincident with the Love

waves. (b) Enlarged vertical-component waveforms from the shaded box in (a). The M_L 2.1 earthquake shown was located 13 km northeast of the station at 11 km depth.

Figure 5. All earthquakes in the Utah region, excluding mining-related seismicity, January 1, 2000–June 30, 2003. (a) Epicenter map with rectangular bounds corresponding to the catalog domain; state boundary of Utah shown for reference. (b) Space-time diagram for seismicity included in (a). Earthquakes are plotted as a function of origin time and latitude, projected along the line A–A'. Arrow marks the time of the Denali fault earthquake (DFE) and temporally related seismicity in Utah.

Figure 6. Number of earthquakes per calendar day (UTC) versus time in the 3.5-year earthquake catalog depicted in Figure 5. Upward arrow marks the time of the Denali fault earthquake (DFE); downward arrows, the times of earthquakes of magnitude (M_L) 4.0 or larger in the catalog.

Figure 7. Plot of earthquake magnitude versus time showing the relative rate and size distribution of seismicity in Utah's Wasatch Front area 30 days before and after the Denali fault earthquake (DFE), set at time 0. The sample includes all earthquakes located within Region II on Figure 8 during the specified time window.

Figure 8. Map of three domains of differing magnitudes of completeness, M_{comp} , used for statistical analyses. Seismicity and base map as in Figure 5a. Values of M_{comp} are indicated on

the right side of the figure. Note that Region I encompasses Region II, which in turn encompasses Region III.

Figure 9. Independent main shocks of $M=1.5$ in the Wasatch Front area (Region II, Fig. 8) during the 3.5-year period, January 1, 2000–June 30, 2003. (a) Cumulative number plot with arrow indicating the time of the Denali fault earthquake (DFE). (b) Stick plot of number of earthquakes per day (binned in calendar days, UTC) for the same period.

Figure 10. Composite plot showing results of a binomial-distribution analysis for independent main shocks of $M \geq 1.5$ located within Region II (Fig. 8) during a 50-day period following the Denali fault earthquake (DFE). Corresponding values of k , P_{pred} , and P_{obs} (see text) are plotted as a function of time. Arrows indicate crossings of a probability level of 0.05, taken to represent the end of an anomalous period of increased seismicity following the DFE and a return to background level.

Figure 11. Magnitude vs. time plots for the spatial clusters identified on Figure 2. Each sample is for the time period Jan. 1, 2000 to June 30, 2003. (a) Includes an epicenter map where the seismicity in the cluster has been relocated using a double-difference procedure (Waldhauser and Ellsworth, 2000). The bold crosses are triggered events and the gray crosses are background events. The cross dimensions show an estimate of the 2 std. dev. error.

Figure 12. Temporal decay of triggered seismicity in the Wasatch Front area following the Denali fault earthquake (DFE) and modeled with the modified Omori law. The time after

triggering (horizontal axis) is measured from November 3, 2002, 22:29:00.0. This composite plot includes all earthquakes located in Region II (Fig. 8) within 25 days of the DFE. The magnitude distribution for the sample is shown in the inset.

Figure 13. Focal mechanisms for the following earthquakes: (a) M_L 4.3, Cluster F, 10 years before the DFE; (b) M_L 3.2, Cluster F, 4.6 days after the DFE; (c) M_L 3.0, Cluster E, 5.4 days after the DFE; (d) M_c 4.2 near Cedar City, Utah, 0.55 days after the 1992 M 7.3 Landers, California, earthquake; (e) M_c 4.0 near Cedar City, Utah, 0.58 days after the Landers earthquake. The mechanisms are labeled with the earthquake origin time (UTC), date, magnitude (M), and depth (H). P-wave first motions are plotted on a lower-hemisphere projection, with compressions and dilatations shown as solid and open circles, respectively. Smaller circles indicate readings of lower confidence. The triangles show slip vectors and compression (P) and tension (T) axes. The contours show the uncertainty limits on the T-axis orientations as determined by the computer program FOCPLT (Whitcomb, 1973), assuming no additional stations in error (solid lines) and up to one good or two lesser-quality readings in error (dashed lines).

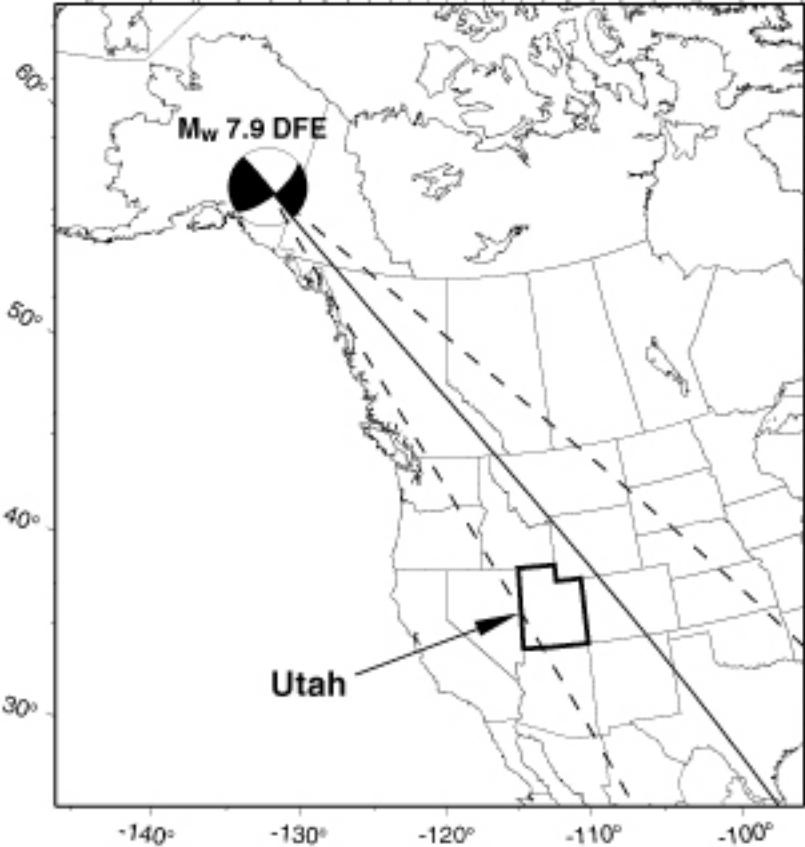


Fig. 1

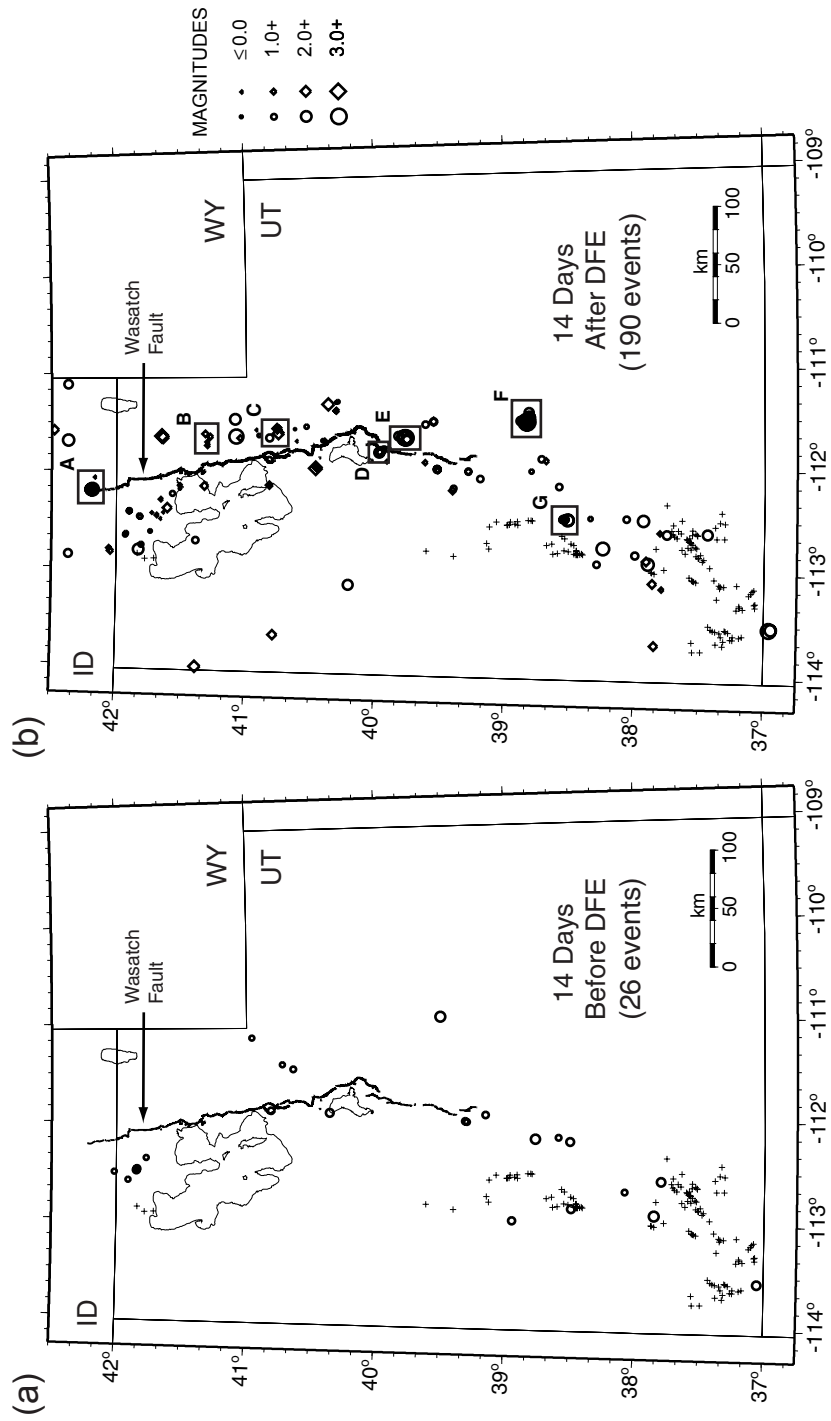


Fig. 2

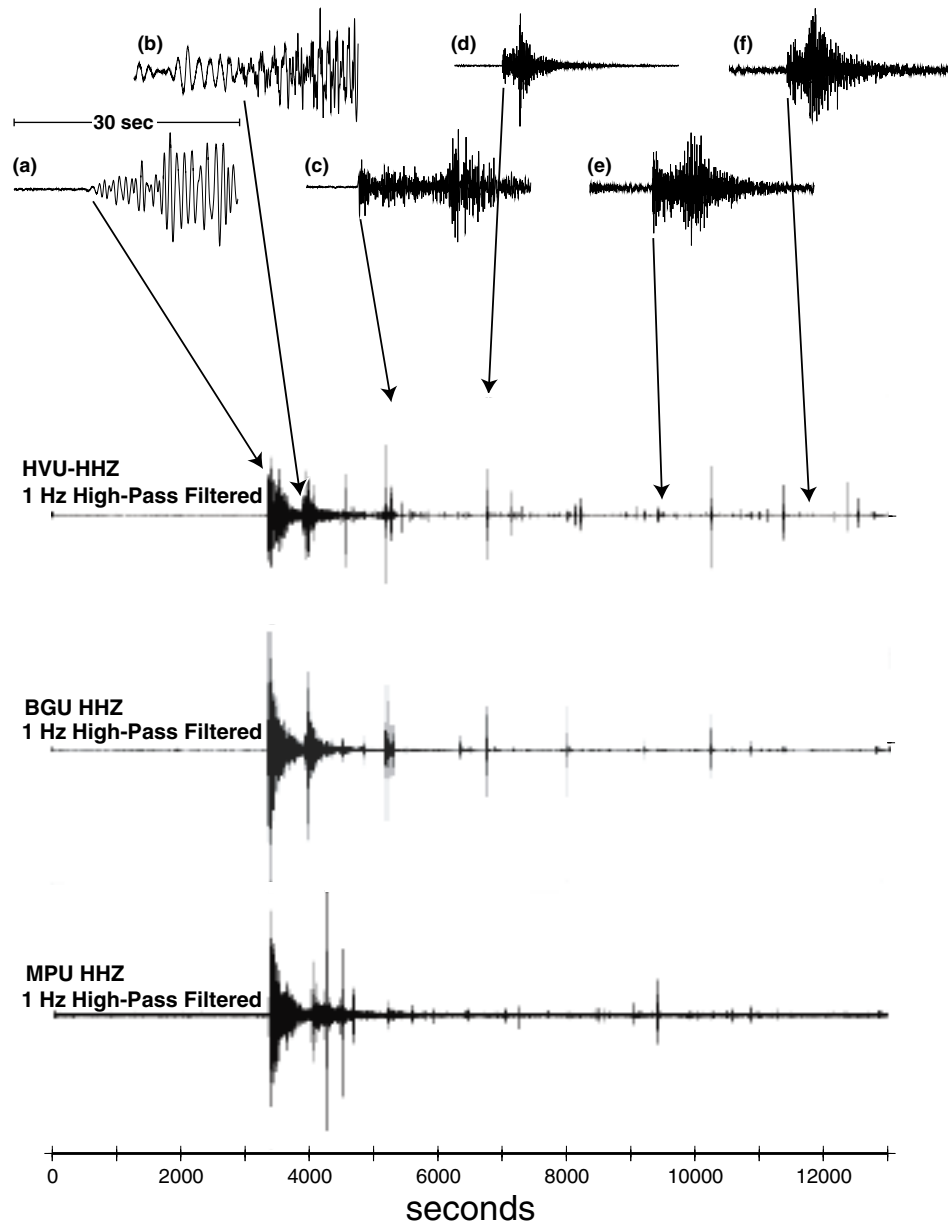


Fig. 3

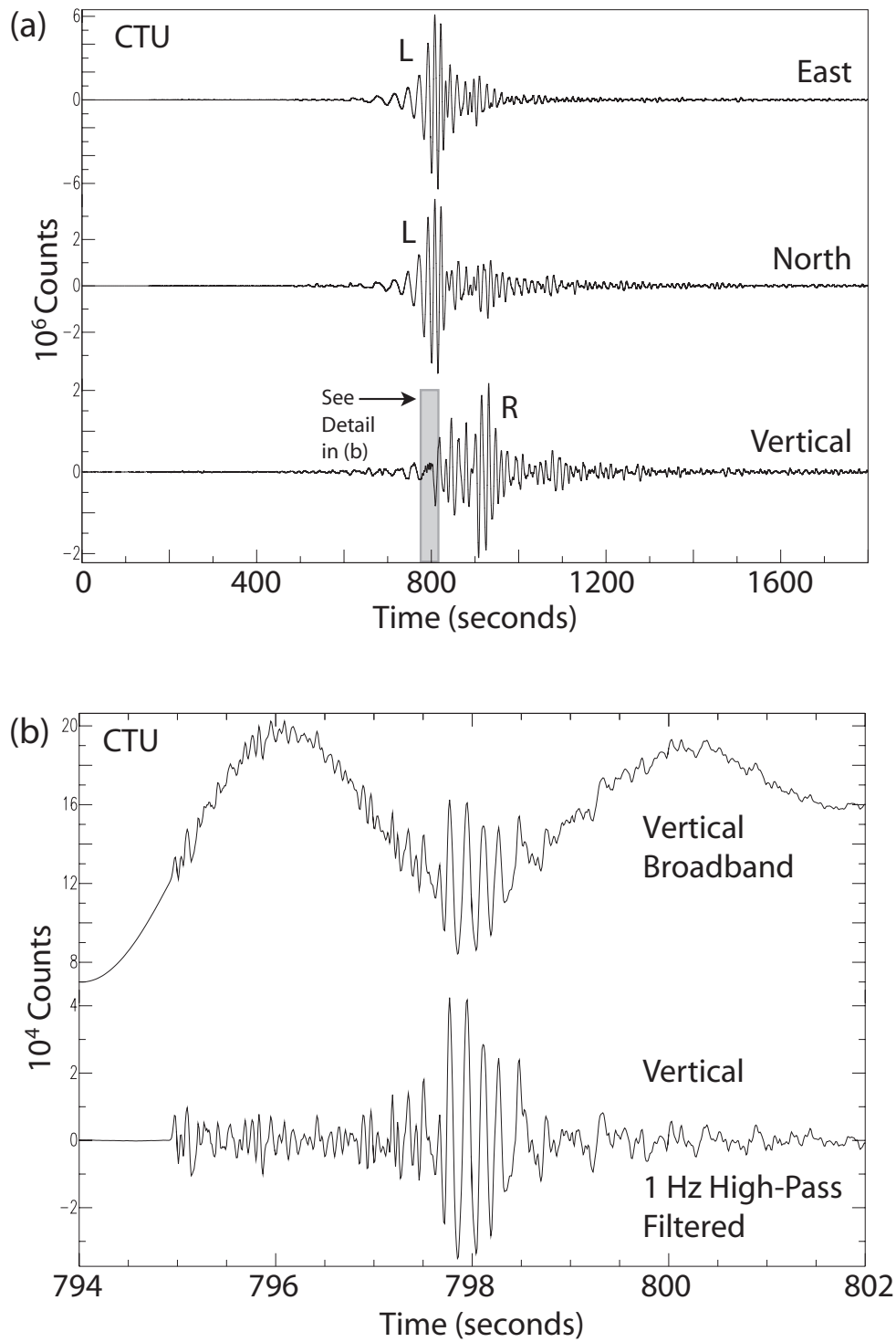


Fig. 4

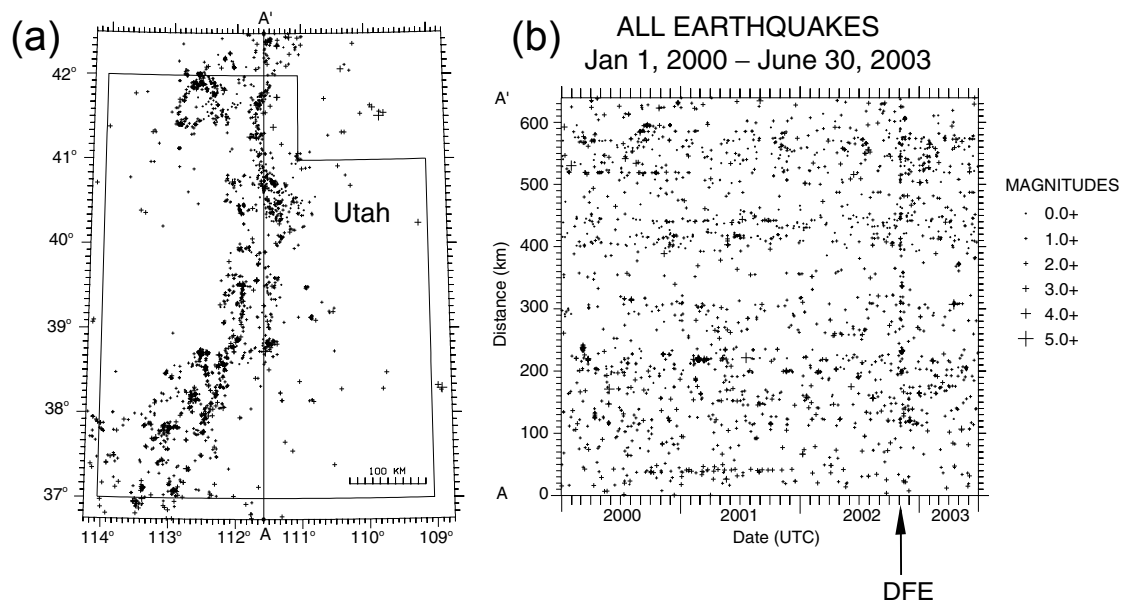


Fig. 5

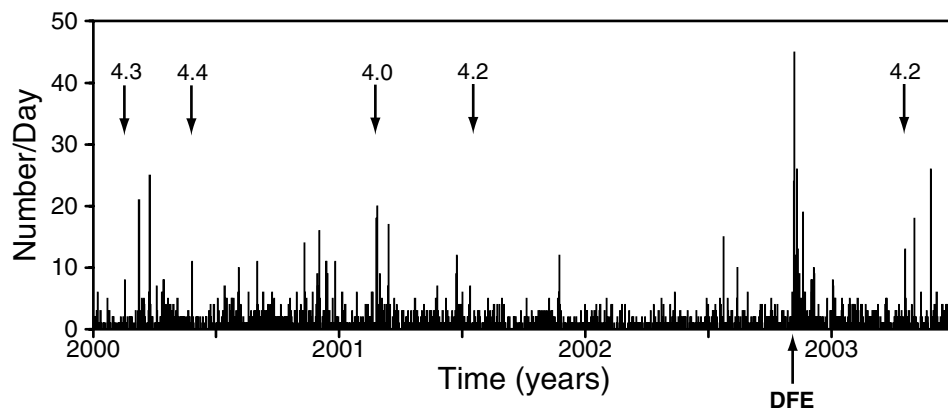


Fig. 6

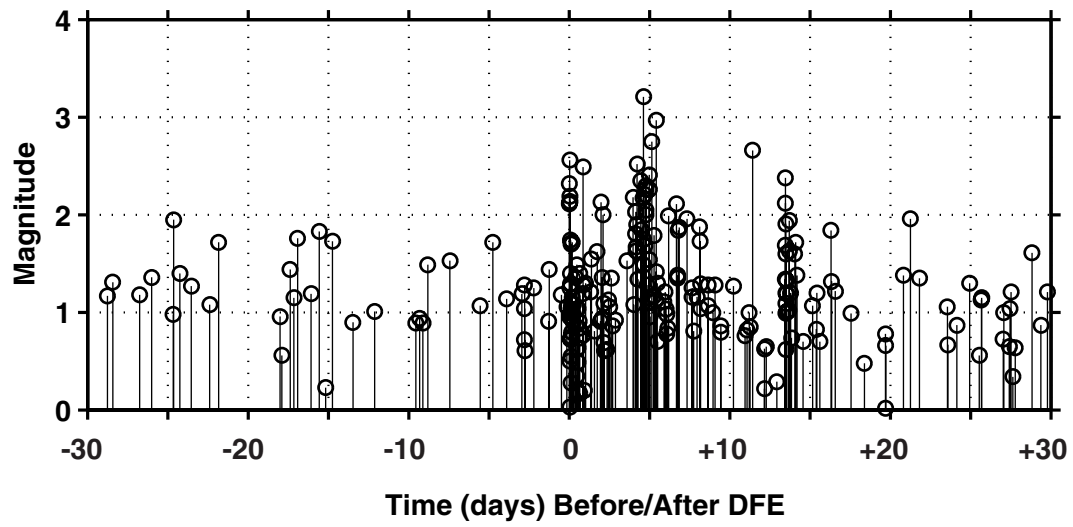


Fig. 7

Regions of Different Mcomp
for Statistical Analyses

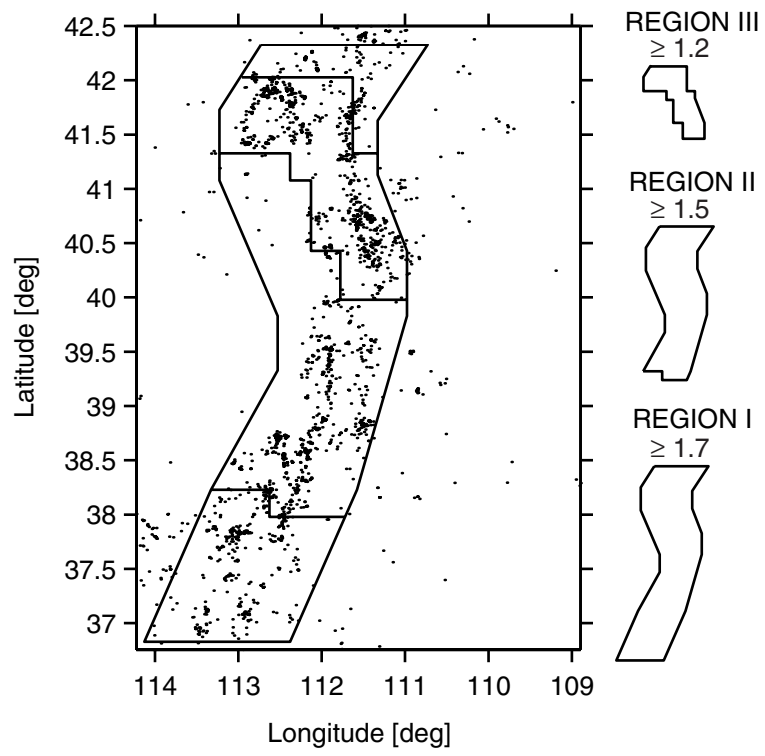


Fig. 8

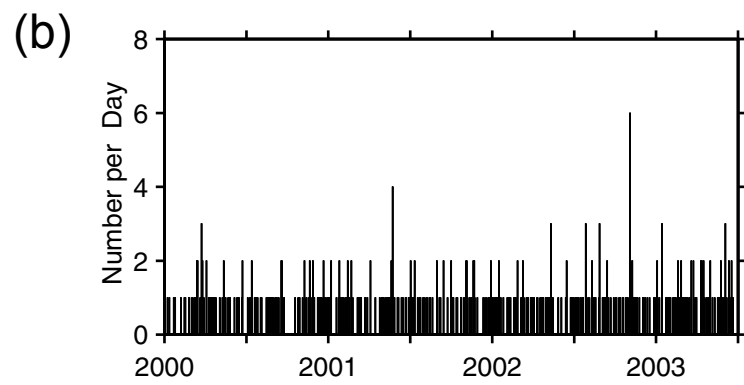
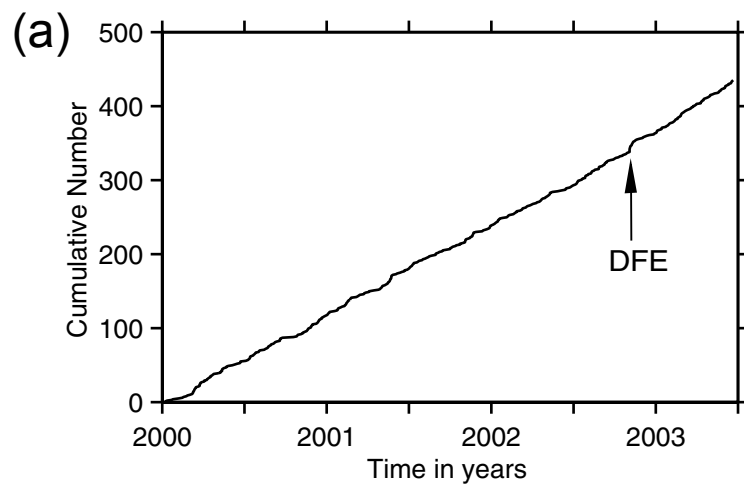


Fig. 9

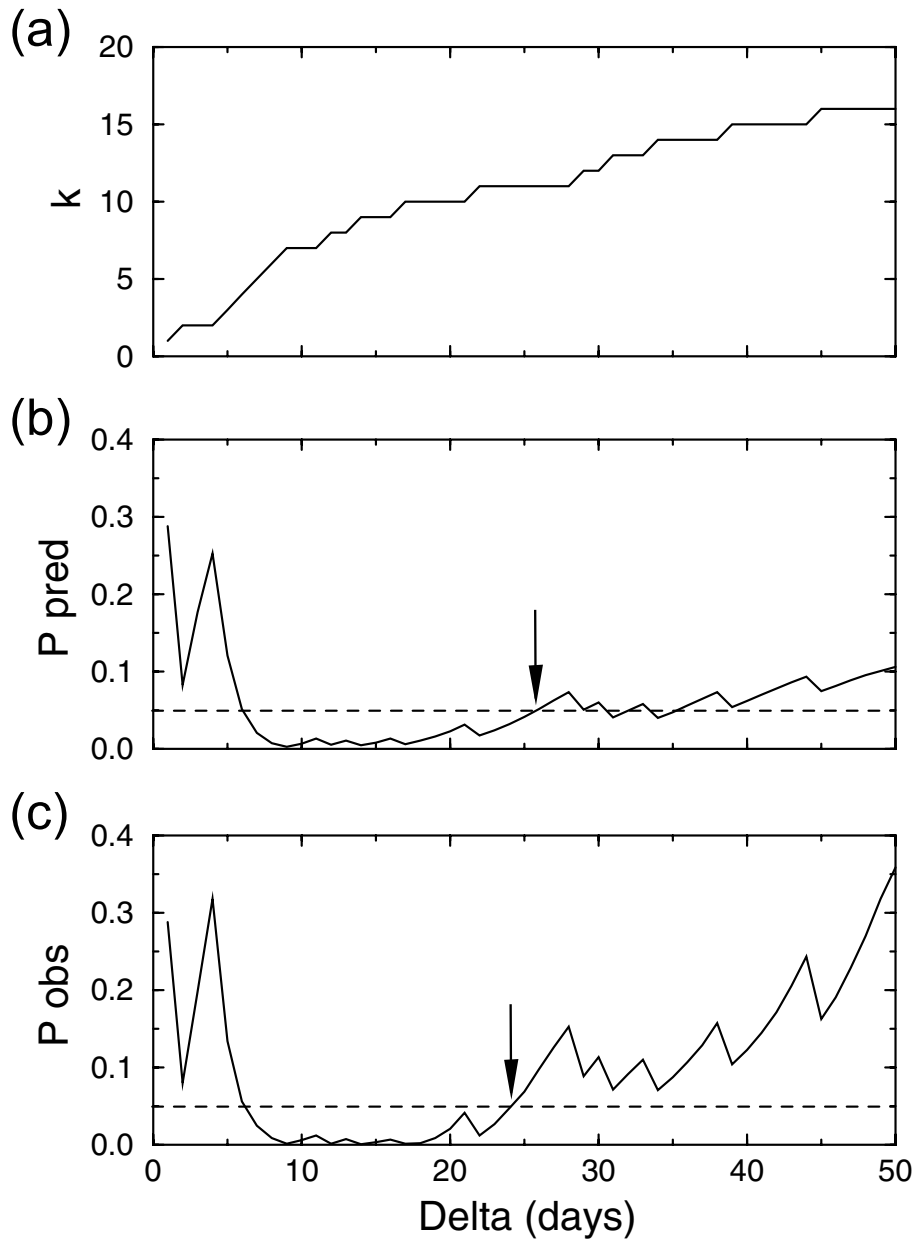
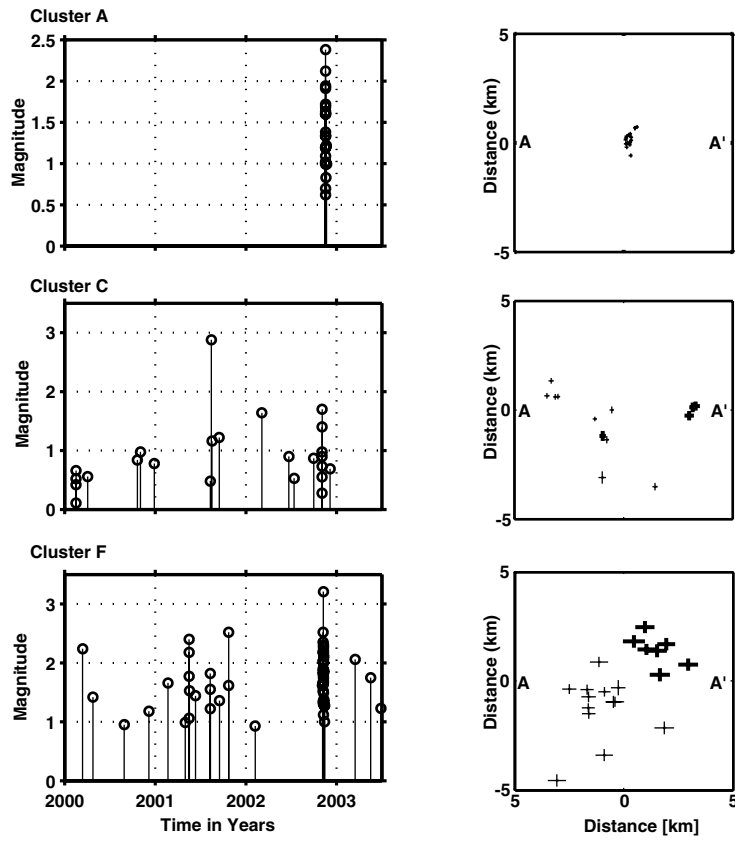


Fig. 10

(a)



(b)

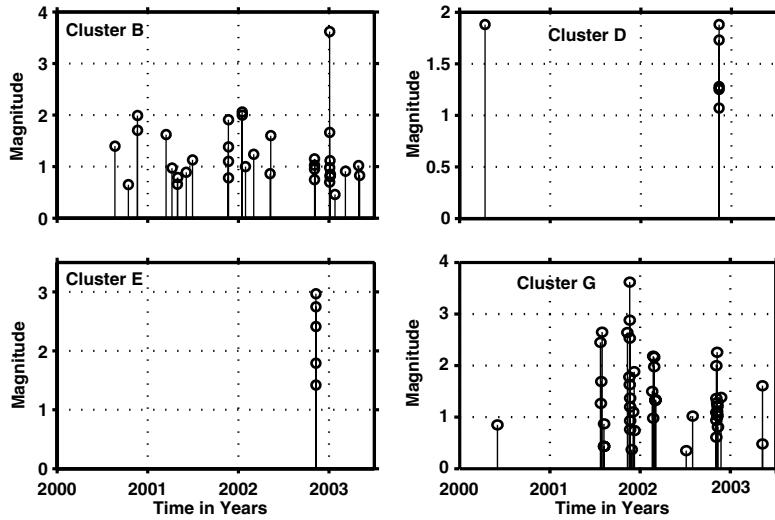


Fig. 11

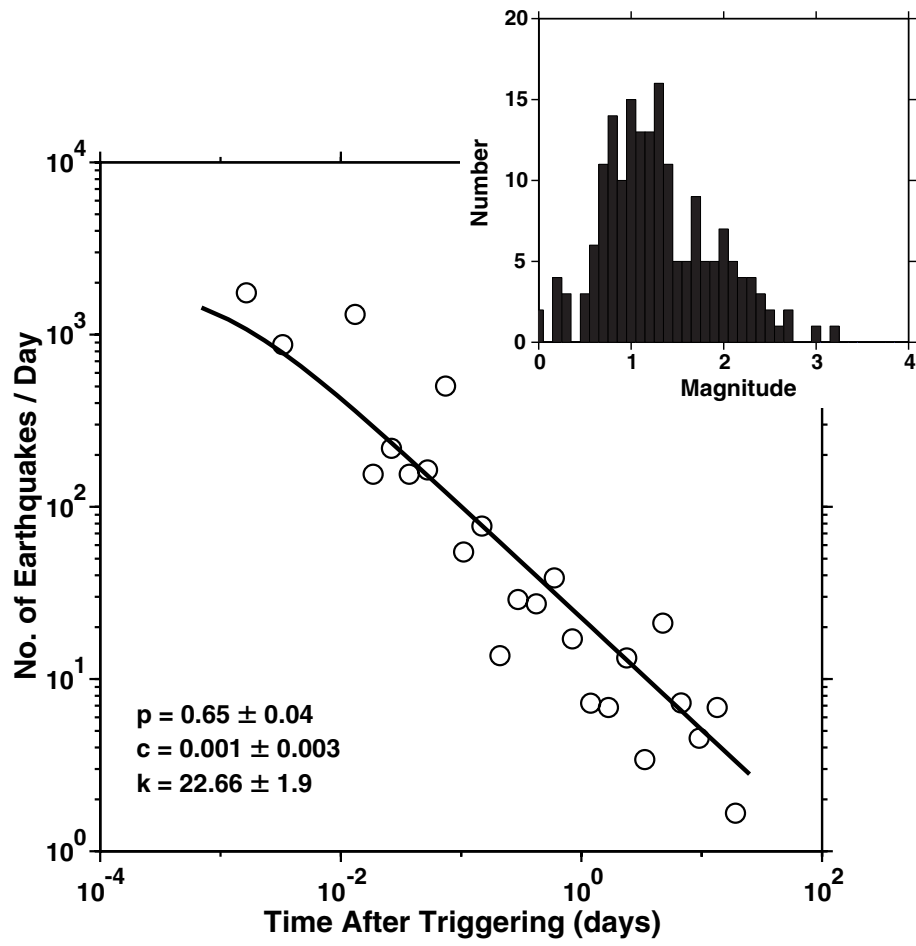


Fig. 12

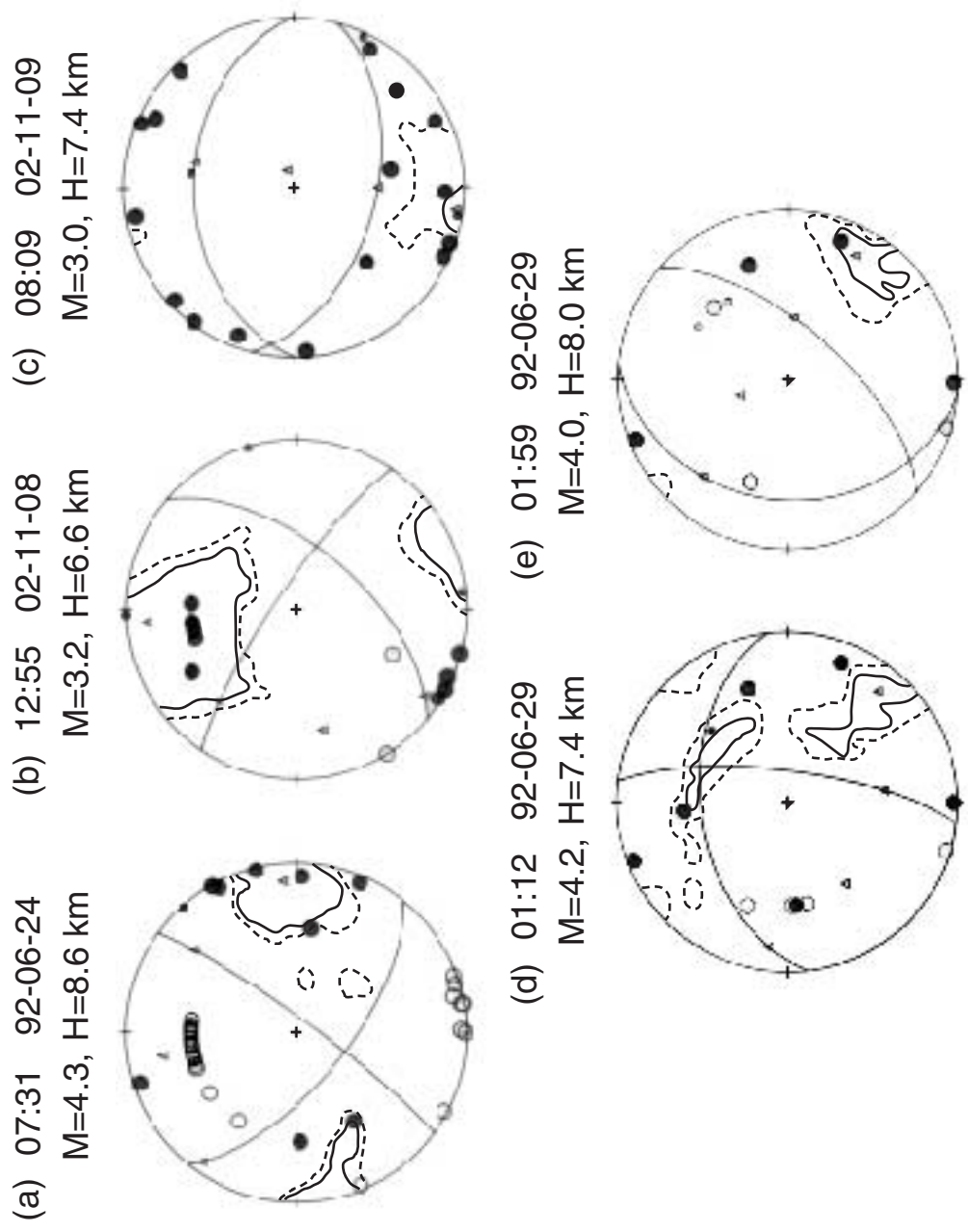


Fig. 13

DISTRIBUTION OF ANNUAL TECHNICAL REPORT

	<u>Number of Copies</u>
Dr. John D. Unger	1 unbound
Project Officer and Manager	5 copies
U.S. Geological Survey External Research	
12201 Sunrise Valley Drive, MS 905A	Abstract & Non-technical Summary
Reston, Virginia 20192	1 electronic copy
Dr. Walter J. Arabasz	1
Principal Investigator	
Dr. Robert B. Smith	1
Co-Principal Investigator	
Dr. James C. Pechmann	1
Co-Investigator	
Susan J. Nava	1
Co-Investigator	
Dr. Kristine L. Pankow	1
Co-Investigator	
Office of Sponsored Projects	1
University of Utah	
[summary only]	
File Copies	2
Administrative Assistant	
University of Utah Seismograph Stations	